REMOVAL OF DIVALENT CATIONS FROM MARCELLUS SHALE FLOWBACK WATER THROUGH CHEMICAL PRECIPITATION

by

Meng Li

B.S. in Environmental Engineering, Hebei University of Technology, 2009

Submitted to the Graduate Faculty of

Swanson School of Engineering in partial fulfillment

of the requirements for the degree of

Master of Science

University of Pittsburgh

2011

UNIVERSITY OF PITTSBURGH

SWANSON SCHOOL OF ENGINEERING

This thesis was presented

by

Meng Li

It was defended on

July 5, 2011

and approved by

Radisav D. Vidic, Professor, Department of Civil and Environmental Engineering

Willie F. Harper, Associate Professor, Department of Civil and Environmental Engineering

Jason D. Monnell, Research Assistant Professor, Department of Civil and Environmental Engineering

Thesis Advisor: Radisav D. Vidic, Professor, Department of Civil and Environmental Engineering

REMOVAL OF DIVALENT CATIONS FROM MARCELLUS SHALE FLOWBACK WATER THROUGH CHEMICAL PRECIPITATION

Meng Li, M.S.

University of Pittsburgh, 2011

Flowback water from natural gas extraction in Marcellus Shale contains very high concentrations of inorganic salts (mostly chlorides) and organic chemicals. Due to its adverse impact to the human health and environment, proper disposal of flowback is required. Reuse or reinjection of flowback water for the development of subsequent wells is one of the most sustainable management methods. However, the reuse of flowback water requires the removal of scale-forming cations, namely barium, strontium, and calcium. Barium and strontium can be chemically precipitated as sulfates, while calcium is best removed as carbonate.

This study focused on both fundamental and practical aspects of chemical precipitation in Marcellus Shale flowback water by the addition of sulfate and carbonate. Thermodynamic equilibrium programs (MINEQL+ & PhreeqcI) based on ion association theory (Davis equation and "WATEQ" Debye-Hückel equation) and ion interaction theory (Pitzer equations) were utilized to predict and interpret experimental results and understand the impact of ionic strength on chemical reactions of interest.

A treatability study of flowback water conducted with sulfate addition indicated that celestite ($SrSO_4$) precipitation is a much slower than barite ($BaSO_4$) precipitation. The degree of sulfate supersaturation had a positive impact while ionic strength and presence of other divalent cations had negative impacts on the kinetics of barite and celestite precipitation. The presence of

organics did not show any impact on the precipitation kinetics. Chemical equilibrium in this complex water system can be predicted reasonably well using the Pitzer model.

This study also documented that carbonate is a good precipitation reagent for calcium and strontium removal. Addition of carbonate without any pH adjustment (pH = 8) accomplished better removal of strontium than when the pH was increased to 10 to aid in calcium removal. The three models tested in this study failed to accurately predict barium and strontium equilibrium when carbonate was added to the solution, while calcium equilibrium was predicted fairly well with the Pitzer model.

Keywords: Marcellus Shale, Flowback water, High ionic strength, Chemical precipitation, MINEQL+, PhreeqcI, Pitzer equations, Chemical equilibrium models, Kinetics

TABLE OF CONTENTS

LIST OF TABLES

LIST OF FIGURES

ACKNOWLEDGMENTS

I wish to express my sincere gratitude to my supervisor, Dr. Radisav D. Vidic, for his support and direction of this master program. I am highly impressed by his remarkable insight into research and enthusiastic work attitude. I will never forget his advice and kindness to me. I would like to give my sincere thanks to Dr. Elise Barbot who gives me the unreserved help not only with my research but also with my thinking. I will always remember her for giving me the most-needed and timely aid when I was down. In addition, I appreciate Dr.Jason D. Monnell for his great support on my lab work.

I am very grateful to my colleagues and friends, Heng Li, Sean Shih, Juan Peng, for their help with daily work, study, and life. I would like to send my thanks to my parents and girlfriend, Jingjing Guo for their love and support.

1.0 INTRODUCTION

Continental shale gas reservoir developments are a growing source of natural gas to meet the energy needs of the United States. The Marcellus Shale of the Appalachian Basin has recently been estimated to contain 262-500 Tcf (trillion cubic feet) of natural gas reserves and is one of the largest underdeveloped reservoirs of shale gas in the US (Engelder and Lash, 2008; Milici and Swezey, 2006). The Marcellus Shale underlies most of Northern and Western Pennsylvania, including about 70% of the state (de Witt et al., 1993). The recoverable volume of gas from the Marcellus formation is difficult to predict and estimates vary over several orders of magnitude. However, the resource certainly represents many years of natural gas needs for the eastern U.S. (Pletcher, 2008). Recent advances in horizontal drilling and multi-stage hydraulic fracturing technology have enabled development of highly productive gas wells in Marcellus Shale (Harper, 2008).

Hydraulic fracturing or "hydrofracing" is the cornerstone technology, which has enabled the economical recovery of natural gas from Marcellus Shale. It involves the introduction of fracturing fluid with high enough pressure to fracture the shale formation and increase its permeability for economical quantity and rates of gas recovery. The fracturing fluid is mostly freshwater withdrawn from local streams, amended with chemical additives that include; 1) viscosity modifiers to optimize flow characteristics, 2) biocides to inhibit biological growth, 3) proppant material used to hold open the fractures, such as well-sorted sand and spheres

composed of ceramic or Bauxite, 4) corrosion inhibitors to protect the well casing, and 5) surfactants (Economides, et al. 1998). A single well hydrofracture in the Marcellus may require 2 – 5 million gallons of fracturing fluid (Rogers, 2008) of which 10-40% may be returned to the surface as "flowback" or "produced" water (Harper, 2008).

The flowback from hydrofracturing includes inorganic salts, metals, and organics from the target geologic formation and it exhibits vastly different chemistry than the original fracturing fluid. Once brought to the surface, flowback must be managed in accordance with federal, state, and local environmental regulations, which depend on the chemistry of the water. Although a variety of produced water management options are available for the developers of our natural gas resources, they are severely limited by the unusually concentrated chemical constituents and high-volume flow observed in flowback from Marcellus Shale gas development. Given the mounting concerns over proper treatment and disposal of low-quality produced water and the potential for the depletion of valuable groundwater resources, an ideal solution for flowback water management would minimize the need to dispose of flowback water while simultaneously minimizing necessary withdrawals of fresh water through reuse of the flowback water on site.

Natural gas developers pay a great deal of money to purchase fresh water, transport fresh water to a site, transport contaminated produced water to a disposal/treatment site where they also pay for its disposal. As a result, a variety of technologies have been offered for recycling flowback water for reuse in hydraulic fracturing. This solution reduces the cost of natural gas production, especially in areas where fresh water is scarce and/or disposal costs are high.

Typical flowback water from Marcellus hydrofracturing contains, in addition to the hydrofracturing fluid amendments, greatly elevated total dissolved solids (TDS), hydrocarbons,

metals, and potentially naturally occurring radioactive material such as radium (Hill et al., 2004). These constituents preclude reuse, reinjection, and direct discharge onto land or into receiving streams. The TDS from Marcellus is high enough to be particularly problematic because it is not amenable to reinjection because of high concentrations of Ba and Sr and the potential for calcite precipitation in the injection well.

It is well known that Ba and Sr can be removed from solution through precipitation as sulfates salts while Ca can be precipitated as carbonate salts. However, it is not known whether the kinetics and equilibrium predictions that are typically available for fairly dilute solutions would still be applicable under the conditions of extremely high ionic strength that is typical of Marcellus Shale flowback water. This study was designed to evaluate the applicability of several chemical equilibrium models to predict the behavior of solutions that are representative of Marcellus Shale flowback water. In addition, the feasibility of using abandoned mine drainage (AMD) as a source of sulfate and carbonate for the precipitation of Ba, Sr and Ca was investigated both in terms of fundamental and practical aspects as a potential inexpensive way to achieve necessary flowback water treatment prior to reuse.

1.1 OBJECTIVES

The present research focuses on the sulfate and carbonate precipitation reactions in both synthetic and actual flowback water under the conditions that are relevant in practical applications. The overall objectives of this work include:

1) Investigate the influence of sulfate and carbonate on the removal of target cations in flowback water with a wide range of ionic strengths.

2) Evaluate the potential of chemical equilibrium models based on Davis equation, "WATEQ" Debye-Hückel equation, and Pitzer equations to predict the solution behavior in a highly concentrated multi-component medium.

1.2 APPROACH

In this study, the interests were focused on the use of sulfate and carbonate (caustic if necessary) to simulate the function of Abandoned Mine Drainage (AMD) water for reducing target ions (Ba, Sr, and Ca). These ionic metals can be converted to insoluble forms, such as sulfate and carbonate salts, with corresponding precipitation reagents. Synthetic and actual flowback water from three well sites were selected for their wide range of ionic strength and varying concentrations of target ions. These waters prepared as synthetic or actual flowback water were then mixed with different doses of precipitant(s). These mixtures were sampled and analyzed over time to profile the kinetics and equilibrium of the constituents of interests. In addition, efforts were made towards using chemical equilibrium programs based on ion-association theory and ion-interaction theory to predict the reactions in these flowback waters. Comparisons between the experimental results and calculations were performed to show the evidence for their application limits and help to interpret the kinetics and equilibria in these mixtures.

2.0 THEORITICAL REVIEW

In this part of work, a fundamental introduction with respect to precipitation is given. Chemical precipitation is the most commonly used technology to convert dissolved ionic metals into insoluble forms in wastewater treatment. Although this process has already been elaborated in details in many textbooks and other publications, it is still worthwhile to present here the basic concepts, calculations, and models utilized in this study.

2.1 ACTIVITY COEFFICIENT MODELS

2.1.1 Mineral solubility product

A mineral can be formed in the aqueous system through a chemical reaction between ionic metals and corresponding reagents, like sulfate or carbonate. The reaction can be written as

$$MX_{(s)} \leftrightarrows M^{2+} + X^{2-} \quad (1)$$

Where $MX_{(s)}$ = the mineral in a solid phase, $M^{2+} =$ the ionic metal, $X^{2-} =$ the precipitating reagents.

Eq.(1) describes the fate of a mineral in a solution: dissolution and precipitation. If the reaction goes to the right, it means that solid is dissolved. If the reaction goes to the left, it means

that solid is precipitated. This depends on which side would generate more energy. The equilibrium can be determined mathematically by two different algorithms (Kolik, 2002): One is called Law of Mass-Action (LMA); the other is called Gibbs Free Energy Minimization (GFEM). Although they are based on different theories, they are both functionally equivalent (Van and Storey, 1970; Smith and Missen, 1982). In this study, LMA is used because of its many advantages. The most important reasons include: 1) it's simple in theory; 2) less thermodynamic data required; 3) and utilized in chemical equilibrium programs selected for this study.

Based on the law of mass-action, the chemical equilibrium can be expressed as

$$K_{sp} = \frac{[M^{2+}][X^{2-}]}{[MX]} \quad (2)$$

Where K_{sp} = thermodynamic equilibrium constant (solubility product constant).

Molar concentration is generally used in the expression of equilibrium constants of reactions, since the estimation of equilibrium constants is based on quantity change of reacting species and the law of mass balance. However, the molarity can only be used in a very dilute aqueous system, ignoring any interaction between species in the system. For more concentrated solutions, such as Marcellus Shale flowback water, it is necessary to use activity instead of molarity since the high ionic strength of this water reduces the ability of all molecules present in solution to freely participate in chemical reactions.

Activity is a measure of the "effective concentration" of a species in a mixture:

$$\alpha_i = \gamma_i \cdot m_i \quad (3)$$

Where α_i = the activity of species i, γ_i = the activity coefficient, m_i = the molarity of species i.

Thus, the Eq. (2) can be then expressed as

$$K_{sp} = \frac{\alpha_M \cdot \alpha_X}{\alpha_{MX}} = (\gamma_M \cdot m_M)(\gamma_X \cdot m_X) \quad (4)$$

Because α_{MX} is equal to one for solid phase.

2.1.2 Activity coefficient

An activity of an ion is typically lower than its concentration simply because it will interact with other ions (so-called ion-pair formation) and thus reduce its activity. Activity coefficient measures deviation in activity of a species in a mixture from ideal system and it is based on the ionic strength of a solution. The ionic strength, μ, can be calculated as follows:

$$\mu = \frac{1}{2}\sum(C_i Z_i^2) \quad (5)$$

Where C_i = concentration of ionic species i and Z_i = charge of species i.

For the thermodynamic calculations in the concentrated solution, the activity coefficient is difficult to determine because not a single equation cold be versatile enough to estimate activity coefficients at all conditions. Several equations are derived in the literature based on ion-association theory (Church and Wolgemuth, 1972) or/and ion-interaction theory (namely Pitzer equations, Plummer et al., 1988, Pitzer, 1991; Clegg and Whitfield, 1991; and Kühn et al., 2002) to calculate the activity coefficient of a certain species in solutions with different ionic strength. Each equation can be applied to a certain range of ionic strength, and the selection of equations will impact the results of activity coefficient calculation.

2.1.2.1 Ion-association model

Ion-association is the reaction of forming a distinct species from ions carrying opposite charge. DEBYE-HÜCKEL limiting-law equation is derived from this theory assuming that long-range electrostatic interactions between ions in the solution are the only source of non-ideality. They

used statistical mechanics to evaluate the charge distribution around a specific ion (O' Dowd et al., 2000). Several other equations basically inferred from this equation but with some corrections for higher ionic strength. These equations are listed in Table 1.

Table 1. Summary of activity coefficient equations based on ion-association model.

Activity Coefficient model	Equations	Ranges/Molality	Sources
DEBYE-HÜCKEL limiting-law equation	$\log(\gamma_i) = -A \cdot Z_i^2 \cdot \sqrt{\mu}$	$\mu < 0.005$	Debye & Hückel, 1923
Extended DEBYE-HÜCKEL equation	$\log(\gamma_i) = \frac{-A \cdot Z_i^2 \cdot \sqrt{\mu}}{1 + B \cdot a_i \cdot \sqrt{\mu}}$	$\mu < 0.01$	Hückel, 1925
GÜNTELBERG equation	$\log(\gamma_i) = -0.5 \cdot Z_i^2 \frac{\sqrt{\mu}}{1 + 1.4\sqrt{\mu}}$	$\mu < 0.01$	Güntelberg, 1926
Davis equation	$\log(\gamma_i) = -A \cdot Z_i^2 \left(\frac{\sqrt{\mu}}{1 + \sqrt{\mu}} - 0.2\mu \right)$	$\mu < 0.5$	Davies, 1962
WATEQ DEBYE-HÜCKEL equation	$\log(\gamma_i) = \frac{-A \cdot Z_i^2 \cdot \sqrt{\mu}}{1 + B \cdot a_i \cdot \sqrt{\mu}} + b_i \cdot \mu$	$\mu < 1$	Truesdell and Jones, 1974

For all equations in Table 1, a_i and b_i are ion-specific parameters determined by the ion size. The values of a_i and b_i for different ions are listed in Table 2. It should be noted that the constant of 0.2 in Davis equation is an empirical number and often replaced by 0.3 (Zhu & Anderson, 2003). In the MINEQL+ calculations, this constant is changed to 0.24. These numbers are determined based on mean salt activity coefficient data. Generally, Davis equation is used for calculating the activity coefficient for charged species. For an uncharged species, the first terms of WATEQ DEBYE-HÜCKEL equation is zero which makes the equation become $\log \gamma_i = b_i \cdot \mu$.

Table 2. Ion-specific parameters a_i and b_i (after Parkhurst et al., 1980 and Truesdell and Jones,1974)

Ion	a_i [Å]	b_i [Å]	Ion	a_i [Å]	b_i [Å]
H^+	4.78	0.24	Fe^{2+}	5.08	0.16
Li^+	4.76	0.20	Co^{2+}	6.17	0.22
Na^+	4.32	0.06	Ni^{2+}	5.51	0.22
K^+	3.71	0.01	Zn^{2+}	4.87	0.24
Cs^{2+}	1.81	0.01	Cd^{2+}	5.80	0.10
Mg^{2+}	5.46	0.22	Pb^{2+}	4.80	0.01
Ca^{2+}	4.86	0.15	OH^-	10.65	0.21
Sr^{2+}	5.48	0.11	F^-	3.46	0.08
Ba^{2+}	4.55	0.09	Cl^-	3.71	0.01
Al^{3+}	6.65	0.19	ClO_4^-	5.30	0.08
Mn^{2+}	7.04	0.22	SO_4^{2-}	5.31	-0.07

A and B are dependent on temperature and can be calculated from the following empirical equations (Merkel and Planer-Friedrich, 2008):

$$A = \frac{1.82483 \cdot 10^6 \sqrt{d}}{(\varepsilon \cdot T_k)^{3/2}} \tag{11}$$

$$B = \frac{50.2916 \cdot \sqrt{d}}{(\varepsilon \cdot T_k)^{1/2}} \tag{12}$$

$$d = 1 - \frac{(T_c - 3.9863)^2 \cdot (T_c + 288.9414)}{508929.2 \cdot (T_c + 68.12963)} + 0.011445 \cdot e^{-\frac{374.3}{T_c}} \tag{13}$$

$$\varepsilon = 2727.586 + 0.6224107 \cdot T_K - 466.9151 \cdot \ln(T_K) - \frac{52000.87}{T_K} \tag{14}$$

Where d = density (after Gildseth et al., 1972), ε = dielectric constant (after Nordstrom et al., 1990), T_C = temperature in °Celsius (0-100 ^oC), T_K = temperature in Kelvin.

From the equations based on ion-association theory, the ionic strength-dependent activity coefficient is valid to molality of about 1. However, these ranges of ionic strength fitted for the equations are still controversial. Some authors believe that even the WATEQ DEBYE-HÜCKEL equation cannot exceed the upper limit of 0.7 molality (or sea water) whereas others consider

that this equation can fit experimental data to the ionic strength as high as 2 molality if the solution is dominated by chloride because the data were collected from the experimental results based on the chloride solutions.

2.1.2.2 Ion-interaction model

Ion-association theory is not appropriate to estimate activity coefficient at high ionic strengths. Another semi-empirical model was developed for high ionic strength conditions (Pitzer, 1973). Compared to ion-association theory or ion-pair theory, the ion-interaction model offers a different point of view. It considers all charged ions are fully separated as free ions instead of ion-pair formation. However, this type of view was later edited (Pitzer, 1991) to incorporate ion-association models to solve some inaccuracies for week electrolytes. Equations (15) to (17) show the general equations used for calculating the activity coefficient by Pitzer equations for cations, anions and neutral ions, respectively.

$$\begin{aligned}\ln\gamma_M = {} & z_m{}^2\mathrm{F} + \textstyle\sum_a m_a(2B_{Ma} + ZC_{Ma}) \ (1\ salt) \\ & + |z_M| \textstyle\sum_c \sum_a m_c m_a m_{ca} \\ & + \textstyle\sum_c m_c(2\emptyset_{Mc} + \sum_a m_a \Psi_{Mca}) \ (\geq 2 \text{ cation}) \\ & + \textstyle\sum_a \sum_{<a'} m_a m_{a'} \Psi_{Maa'} \ \ (\geq 2 \text{ anion}) \\ & + 2\textstyle\sum_n m_n \lambda_{Mn} + 3\sum_n m^2{}_n \mu_{Mnn} \ (\geq 1\ neutral) \\ & + 6\textstyle\sum_n \sum_{<n'} m_n m_{n'} \mu_{Mnn'} \ (\geq 2\ neutral) \\ & + 6\textstyle\sum_n \sum_a m_n m_a \xi_{Mna} \ \ (\geq 1\ anion, \ \geq 1\ neutral) \\ & + 6\textstyle\sum_n \sum_c m_n m_c \xi_{Mnc} \ (\geq 2\ cation, \ \geq 1\ neutral)\end{aligned} \tag{15}$$

$$\begin{aligned}\ln\gamma_X = {} & z_X{}^2\mathrm{F} + \textstyle\sum_c m_c(2B_{cX} + ZC_{cX}) \ (1\ salt) \\ & + |z_X| \textstyle\sum_c \sum_a m_c m_a m_{ca} \\ & + \textstyle\sum_a m_a(2\emptyset_{Xa} + \sum_c m_c \Psi_{cXa}) \ (\geq 2 \text{ ation}) \\ & + \textstyle\sum_c \sum_{<c'} m_c m_{c'} \Psi_{Xcc'} \ \ (\geq 2 \text{ canion}) \\ & + 2\textstyle\sum_n m_n \lambda_{Xn} + 3\sum_n m^2{}_n \mu_{Xnn} \ (\geq 1\ neutral) \\ & + 6\textstyle\sum_n \sum_{<n'} m_n m_{n'} \mu_{Xnn'} \ (\geq 2\ neutral) \\ & + 6\textstyle\sum_n \sum_c m_n m_c \xi_{ncX} \ \ (\geq 1\ canion, \ \geq 1\ neutral) \\ & + 6\textstyle\sum_n \sum_a m_n m_a \xi_{Xna} \ (\geq 2\ ation, \ \geq 1\ neutral)\end{aligned} \tag{16}$$

$$\begin{aligned}\ln\gamma_N = {} & 2\textstyle\sum_n \lambda_{Nn} m_n + 3\sum_n m^2{}_n \mu_{Nnn} \ (\geq 1\ neutral) \\ & +6\textstyle\sum_n m_N m_n \mu_{NNn} \ (\geq 2 \text{ neutral}) \\ & +6\textstyle\sum_n \sum_{<n'} m_n m_{n'} \mu_{Nnn'} \ (\geq 3\ neutral) \\ & +2\textstyle\sum_c \lambda_{Nc} m_c + 2\sum_a \lambda_{Na} m_a \\ & +\textstyle\sum_c \sum_a m_c m_a \xi_{Nca} \ (\geq 1\ cation, \ \geq 1\ anion) \\ & +\textstyle\sum_c \sum_{<c'} m_c m_{c'} \eta_{Ncc'} \ (\geq 2\ cation) \\ & +\textstyle\sum_a \sum_{<a'} m_a m_{a'} \eta_{Naa'} \ (\geq 2\ ation) \\ & +6\textstyle\sum_n \sum_c m_n m_c \mu_{Nnc} \\ & +6\textstyle\sum_n \sum_a m_n m_a \mu_{Nna} \ (\geq 1\ neutral, \geq 1\ cation, \ \geq 1\ anion) \end{aligned} \quad (17)$$

Where subscripts M, X, N stand for cation, anion, and neutral ions of interests, respectively. The subscripts c, a, n indicate other cations, anions, and neutral species. In these equations, F is a derived DEBYE-HÜCKEL limiting-law equation dependent on DEBYE-HÜCKEL parameter A (Eq. (11)). Other terms mainly determined by six types of empirical parameters, namely $\beta^{(0)}_{MX}$, $\beta^{(1)}_{MX}$, $\beta^{(2)}_{MX}$, $C^{(0)}_{MX}$, Φ_{ij}, Ψ_{ijk}, which are temperature-dependent. The first three terms, namely $\beta^{(0)}_{MX}$, $\beta^{(1)}_{MX}$, $\beta^{(2)}_{MX}$ describe the interaction of pairs of oppositely charged ions in mixed electrolyte solutions. $C^{(0)}_{MX}$ account for short-range interaction of ions and is of importance at high concentration. Φ_{ij} are mixed electrolyte parameters for interaction between ions of the same signs. Ψ_{ijk} describe interactions for cation-cation-anion and anion-anion-cation in the mixed electrolyte solutions. More details can refer to many literatures by Pitzer (Pitzer and Mayorga, 1973; Pitzer and Kim, 1974; Pitzer, 1974; Pitzer, 1991).

Besides Pitzer equations, the Specific Interaction Theory (SIT, Ciavatta,1980) is another equation based upon ion-interaction theory. It is written as

$$\log(\gamma_i) = z_j^2 \frac{0.51\sqrt{\mu}}{1 + 1.5\sqrt{\mu}} + \sum_k \epsilon_{jk} m_k \quad (18)$$

The activity coefficient calculated by the specific interaction theory (SIT) has been shown to be adequate for ionic strength between 0.5 and 3 molal (Elizalde and Aparicio, 1995), while Pitzer equation successfully fitted the behavior of mixed-salt solutions to ionic strengths of

about 6 molal (Burkin, 2001). However, the biggest disadvantage of ion-interaction theory is that it is very complex and lacks many parameters for aqueous species. Since any one species incorporated into the equations will require many parameters, it is sometimes hard to calculate the reactions accurately for the solutions containing many species. Any attempt to add the parameter based on different sources may cause inconsistency and make the results uncertain

2.1.2.3 Comparison between ion-association and ion-interaction models

Because the ion-association has been taken into account in Pitzer models, activity coefficients based on different equations will be in good agreement in less concentrated solutions. However, for high ionic strength systems, it is believed that activity coefficients for ion-interaction models are generally smaller than those predicted by ion-association models (Pearson and Berner, 1991). WATEQ DEBYE-HÜCKEL equation maybe reliable at higher ionic strength (David, 1999) under specific conditions, such as in sodium chloride dominated systems,. In addition, Merkel and Planer-Friedrich (2008) have also confirmed that the conformity of WATEQ DEBYE-HÜCKEL equation and Pitzer equations is surprisingly good with respect to calcium, sulfate and chloride (see Figure 1, 2, and 3). These provide strong evidence that the WATEQ DEBYE-HÜCKEL equation could be utilized in some high salinity solutions. However, the Davis equation may deviate significantly from the other two values at ionic strength as low as 0.3 molality (for chloride).

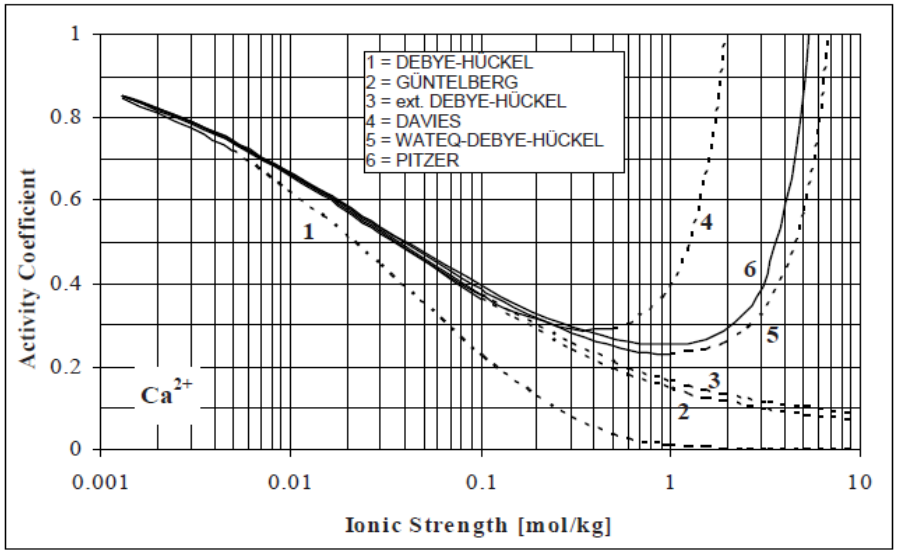

Figure 1. Comparison of activity coefficient for Ca^{2+} (Merkel and Planer-Friedrich, 2008)

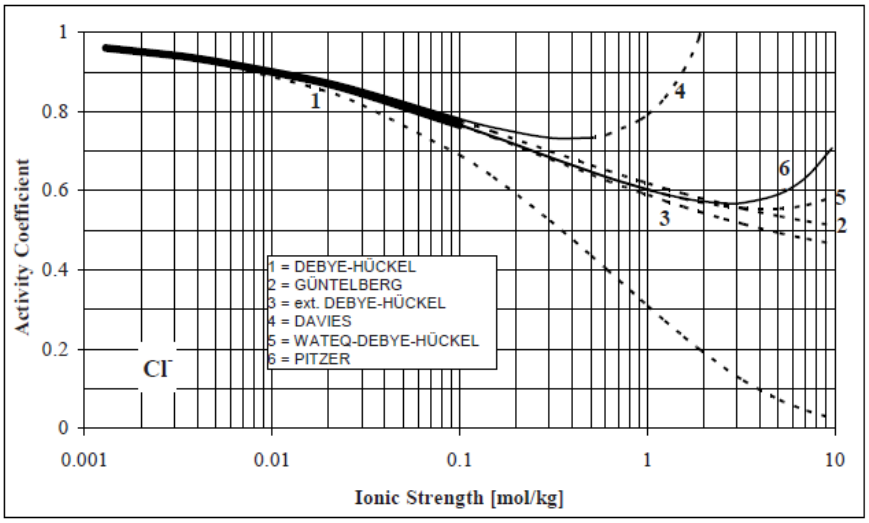

Figure 2. Comparison of activity coefficient for Cl^- (Merkel and Planer-Friedrich, 2008)

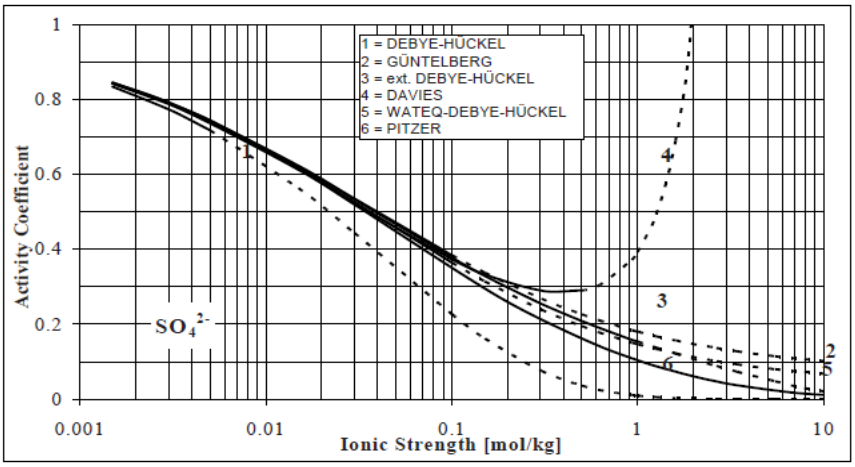

Figure 3. Comparison of activity coefficient for SO_4^{2-} (Merkel and Planer-Friedrich, 2008)

2.1.3 Saturation Index

According to the concepts mentioned in previous paragraphs, the chemical precipitation can be determined in term of Saturation Index (SI). The saturation index (SI) is the logarithm of the quotient of the ion activity product (IAP) and solubility product constant (K_{sp}).

$$SI = \log \frac{IAP}{K_{sp}} \tag{19}$$

Where IAP (Ion Activity Product) = $\alpha_M \cdot \alpha_X$. Solubility product (K_{sp}) is temperature-pressure dependent and was determined already for different minerals in the programs database. If the activities of cation and anion were known, the state of a mineral can be determined as described in Table 3.

Table 3. Relations between Saturation Index and minerals states

SI	Results
< 0	mineral dissolves
$= 0$	equilibrium
> 0	Mineral precipitates

Generally, the solubility product constant is taken from literature. Concentrations of cations and anions can be measured throughout the experiments and then have to be converted into activities based on the product of activity coefficient and concentrations. If precipitating reagents were overdosed, the minerals will precipitate until SI equals to zero. However, even supersaturation (SI > 0) doesn't mean that precipitation will happen. If the kinetics of the reactions is very slow, it can keep supersaturation for a long period.

2.2 CHEMICAL EQUILIBRIUM MODELS AND DATABASE ANALYSIS

To date, numerous reliable thermodynamic models have been developed (Phreeqc, Parkhurst and Appelo, 1999; EQ 3/6, Wolery 1992a and 1992b; MINEQL+, Westall et al., 1976; WATEQ4F, Ball & Nordstrom, 1991; etc.). The differences among them include algorithms, activity coefficient equations, and database that are included in each model.

For the species distribution calculations, there are basically two distinct categories of approaches: one is Gibbs Free Energy Minimization (GFEM); the other is Law of Mass-Action (LMA). The former one is based on the idea that all species in the system have the tendency to reach their lowest energy state. The latter one solves the thermodynamic problems based on equilibrium constants and mass balance. These two are normally equivalent at equilibrium:

$$G_0 = -\mathrm{RT}\ln K \tag{20}$$

When $\mathrm{T} = 25℃$, Eq.(20) can be converted to $G_{25℃} = -5.707\log K$. Due to the risk of unreliable free energy measurements, the algorithm based on LMA is preferred.

MINEQL+ and PhreeqcI are widely used simulation software packages for calculating chemical equilibrium based on the LMA method. However, they use different equations to

calculate the activity coefficients. MINEQL+ uses the MINTEQA2 database of thermodynamic constants as a starting point for defining the reactions in any aqueous system. This database uses Davis equation to predict the activity coefficient, which means that this model is applicable as long as the ionic strength does not exceed 0.5 molality. Below this value, the modeling results give relatively high accuracy.

PhreeqcI software package allows the selection between "WATEQ" DEBYE-HÜCKEL equation (database named Phreeqc.dat) and Pitzer equation (database named Pitzer.dat) to calculate activity corrections. Therefore, the validity of this model depends on the solution composition and the chosen database. Based on the explanation provided with this model, the "WATEQ" DEBYE-HÜCKEL equation can be used in a relatively concentrated sodium-chloride solution, because the activity coefficients of chloride is accurately represented up to the 6 molal concentration. For other strong electrolyte cations that may exist in solution, the model calculations should be accurate as long as chloride is the dominant anion. The instructions for the use of PheeqcI suggest that if the NaCl is the dominant solute in the solutions, activity coefficient calculations with "WATEQ" DEBYE-HÜCKEL equation should be accurate for the ionic strengths between 0.5 and 2 molal. Outside this range, the ion-interaction approach using the Pitzer equation should be used. However, the Pitzer database included in PhreeqcI software is not as complete as the database for "WATEQ" DEBYE-HÜCKEL equation (Phreeqc.dat) and Davis equation (MINEQL+). Several essential solubility product constant and Pitzer parameters needed for the experimental system evaluated in this study were not included in the original software and had to collected from literature. Table 4 lists the necessary solubility product constants for the system used in this study that were available in the software database.

Table 4. Solubility product constants for different minerals at 25°C

Minerals	MINEQL+4.6/log Ksp	PhreeqcI/log Ksp	Pitzer/log Ksp
Barite ($BaSO_4$)	-9.980	-9.970	Not exist
Celestite ($SrSO_4$)	-6.620	-6.630	-6.630
Gypsum ($CaSO_4$)	-4.610	-4.580	-4.581
Witherite ($BaCO_3$)	-8.570	-8.562	Not exist
Strontianite ($SrCO_3$)	-9.270	-9.271	Not exist
Calcite ($CaCO_3$)	-8.480	-8.480	-8.406

Missing solubility products for barite, witherite, and strontianite in the Pitzer database were filled with the most reliable data available in the literature as shown in Table 5.

Table 5. Recommended solubility product constants for barite, witherite, and strontianite at 25°C

Minerals	Log Ksp	Sources
Barite ($BaSO_4$)	-9.954	Robie et al. 1978
Witherite ($BaCO_3$)	-8.560	Busenbergh et al., 1984
Strontianite ($SrCO_3$)	-9.271	Millero et al. 1984

These values are also close to those shown in Table 4. To make the data comparable with each other, these missing constants based on Phreeqc.dat database were included into Pitzer database.

In the simulation code Pitzer from the PhreeqcI software, Pitzer equations are evoked. This code is based on ion-interaction theory and is suitable for very concentrated solution systems. However, since this code is parameter-dependent, any lack of necessary ion-interaction parameters will lead to inaccuracies. Some of the important parameters for Barite, Witherite, Strontianite and Calcite were not incorporated into the program and had to be added for the purpose of this study. Table 6 lists the Pitzer ion interaction parameters collected from the literature. These parameters were added to the database and used in all calculations based on the Pitzer equations.

Table 6. Pitzer ion interaction parameters adapted from the literature

Parameters	Values	Sources
B^0 Ba-SO4	-1.0	Monnin & Galinier, 1988
B^0 Sr-SO4	-0.43	Monnin & Galinier, 1988
B^0 Mg-SO4	0.221	Pabalan & Pitzer, 1987a
B^0 Ca-SO4	0.2	Greenberg & Moller (1989)
B^1 Ba-SO4	12.6	Monnin & Galinier, 1988
B^1 Sr-SO4	5.7	Monnin & Galinier, 1988
B^1 Mg-SO4	3.343	Harvie et al., 1984
B^1 Ca-SO4	3.1973	Greenberg & Moller (1989)
B^2 Ba-SO4	-153.4	Monnin & Galinier, 1988
B^2 Sr-SO4	-94.2	Monnin & Galinier, 1988
B^2 Mg-SO4	-37.23	Pabalan & Pitzer, 1987a
B^2 Ca-SO4	-54.24	Greenberg & Moller (1989)
PSI Na-Ca-Cl	-0.003	Holmes et al., 1987
PSI Na-Ca-SO4	-0.012	Greenberg & Moller (1989)
PSI Na-Ba-Cl	0.0128	Monnin, 1999
PSI Cl-SO4-Mg	-0.008	Harvie et al., 1984
THETA SO4-Cl	0.07	Greenberg & Moller (1989)

Even though many useful data have been found and successfully incorporated into the Pitzer database, there was still a lack of many parameters, especially for carbonates. It seems that there are no parameters for Ba-Sr-CO_3-HCO_3 systems published so far, which makes the calculation for these species quite uncertain. However, an earlier calculation by Milleroa et al (1984) showed that it is no necessary to add the Pitzer parameters for the interactions of CO_3^{2-} with Ca^{2+}, Ba^{2+} and Sr^{2+} at low values of P_{CO2}.

3.0 MATERIALS AND METHODS

3.1 FLOWBACK WATER CHARACTERISTICS

The chemistry in flowback water varied with location (or shale formation) and flowback period. Flowback water in this research came from three representative well sites located on southwestern counties in the vicinity of Pittsburgh: Site A, Site B, and Site C. The total dissolved solid concentration in all three well sites increase with time; however, the ionic concentration in Site C is the highest while that in Site A is the lowest. Again, these variations were ascribed to the shale formation in different locations.

To simplify and integrate the flowback chemistry, the flow-composite flowback water sample was used for this study. The mix ratio of flowback water sampled at different time was based on the flow-rate profile with time. The main chemistry characteristics of the flowback are shown in Table 7. In general, they were all concentrated brines and the solution ionic strength varied from 0.89 M to 3.41 M (calculations were based upon ionic strength equation, Eq. (5)). Sodium and chloride were the major ions that contributed the majority of solution ionic strength (86.3% in Site A, 93.5% in Site B, and 72.6% in Site C). Besides, composition of target ions (Ba, Sr, and Ca) was another obvious difference. The flowback water from Site A was characterized by low Ba and Sr concentrations and medium Ca content; Site B had high Ba and Sr concentrations but low Ca content; Ba concentration in Site C is very low but Sr and Ca contents

were very high. All in all, these three types of flowback water in this study had distinct characteristics and were a good representation of flowback water in Marcellus Shale.

Table 7. Flowback Water Characteristics, mg/L

Constituent	Site A	Site B	Site C
Na	16518	32327.8	46130.7
Ca	2224	449.1	15021
Mg	220	119.9	1720
Ba	781	2530	236
Sr	367	1400	1799
Cl	29000	52913.5	104300
Ionic Strength/M	0.89	1.55	3.41

3.2 REAGENTS AND MATERIALS

Reagents used in this study were of analytical grade (Barium Chloride, Dihydrate, Assay 99.0% min, Mallinckrodt Chemicals; Strontium Chloride, Hexahydrate, Assay 99%, Acros Organics; Sodium Chloride, Assay 99.8%, Fisher Scientific; Magnesium Chloride, Hexahydrate, Assay 100.1%, J.T.Baker; Calcium Chloride, Dihydrate, Assay 99.0~105.0%, EMD; Sodium Bicarbonate, Assay 100.2%, Fisher Chemical; Sodium Carbonate, Anhydrous, Assay 99.5%, EMD; Sodium Sulfate, Assay 100.0%, Fisher Scientific; Potassium Chloride; Nitric Acid, Assay 67~70%, Fisher Scientific) . All synthetic waters and dilutions were prepared by using carbonate free de-ionized water (with a resistance of 17.8 MΩ). Actual flowback water in this research was a mix of flowback water samples collected at different times and based on the flow rate profile

with time. All membrane filters were supplied by Whatman (0.45 µm Glass Microfibre filters, 934-AH) and Millipore (0.05 and 0.45 µm, Type VVLP).

3.3 EXPERIMENTAL PROCEDURE

The synthetic flowback waters were prepared in 1 liter volumetric flask using high purity chemicals. Each liter was then separated into 250ml volumetric flasks. The sulfate dose was added in the solid form or as a solution and carbonate dose was added in the solid form. The sulfate solution was made by adding high-purity Na_2SO_4 into deionized water to get a highly concentrated stock solution (100,000 mg/L as SO_4).

Unless specified otherwise, samples from each 250-ml volumetric flask were collected at different reaction times and filtered through 0.45 um filters. Filter paper was washed three times with de-ionized water and dried in a desiccator until SEM-EDS analysis was performed. For the cation analysis, Ba and Sr were measured using atomic adsorption spectrometry (Perkin-Elmer model 1000 AAS) with a nitrous-acetylene flame. To eliminate the interference from ionization and retard the kinetics of reaction, all of the samples were immediately diluted using 0.15% KCl & 2% HNO_3 solution after filtration. The analysis was conducted within 8 hours of sample collection. Each cation analysis was performed at least three times and the average value was used in this study

3.3.1 AAS analysis corrections by potassium chloride

Due to the complex chemistry and high salinity of flowback water, the target cations, such as Ba and Sr cannot be accurately measured using standard Atomic Absorption Spectrometry procedure with Nitrous Oxide-Acetylene flame without method alterations. Initial data indicated that chemical and ionization interferences are relatively common in AAS measurements of Ba and Sr. Several analyses for Ba and Sr were performed on the synthetic Site B flowback water; the results showed that up to 2.4-fold of Ba and 1.8-fold of Sr were measured comparing to their actual concentrations. There are two typical kinds of problems that make these results inaccurate (Agilent Technologies, Inc., 2010). One is the significant ionization when using Nitrous Oxide-Acetylene as flame. This will strongly reduce analytical sensitivity. The other is the interference from alkali and alkaline metals, such as Na and Ca. Potassium chloride was determined to be a good ionization suppressor in the solution that can minimize these effects. CaOH adsorption band at 554 nm is an interference when Ba analysis is performed at the default wavelength (553.6 nm). And Ca also represents spectral interference to Ba. However, according to some references, only very high content of calcium mixed with Ba will lead to inaccuracies.

Without addition of KCl, much lower measured values demonstrated that the ionization interferences existed in the barium analysis. On the contrary, with the addition of KCl in the solutions, only small variations were shown and rendered more accuracy. To confirm the effectiveness of KCl in the analysis of Ba and Sr in the samples, a series of solutions with different composition (see in Table 8) were measured with/out 0.15% KCl by weight. The variations of barium and strontium concentrations in different solutions were compared in Table 8, 9, 10 & Figure 4. The maximum deviation of barium concentration was within 3.2%, while that of strontium concentration was within 3.4%, which illustrate the validity of potassium

chloride use to minimize the ionization and chemical effects. These measurements showed very stable values as illustrated in Figure 4 (B and C) which means this method is not susceptible to the composition of solutions and can be utilized in relatively large range of conditions. It can be concluded that all of the barium and strontium measurements in the solutions should be done after 0.15% of potassium chloride is added to the sample.

Table 8. Composition of Test Solutions

Solution No.	Components	Concentration (mg/L)
1	Ba	2530
2	Sr	1400
3	Ba	2530
	Sr	1400
4	Ba	2530
	Sr	1400
	Ca	449
5	Ba	2530
	Sr	1400
	Ca	449
	Mg	120
6	Ba	2530
	Sr	1400
	Ca	449
	Mg	120
	Na	32327

Table 9. Ba Concentration Analysis using AA

Solution No.	Ba conc. without KCl (mg/L)	Ba conc. with KCl (mg/L)
1	980.8	2578
3	501.3	2492
4	456.1	2578
5	601.7	2612
6	1884.3	2612

Table 10. Sr Concentration Analysis using AA

Solution No.	Sr conc. With KCl (mg/L)
2	1359
3	1352
4	1352
5	1371
6	1372

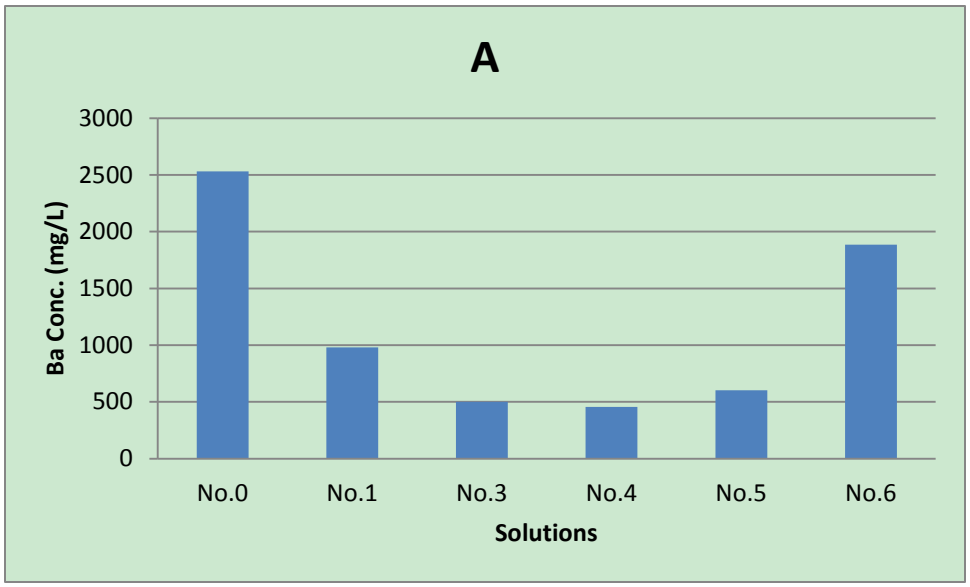

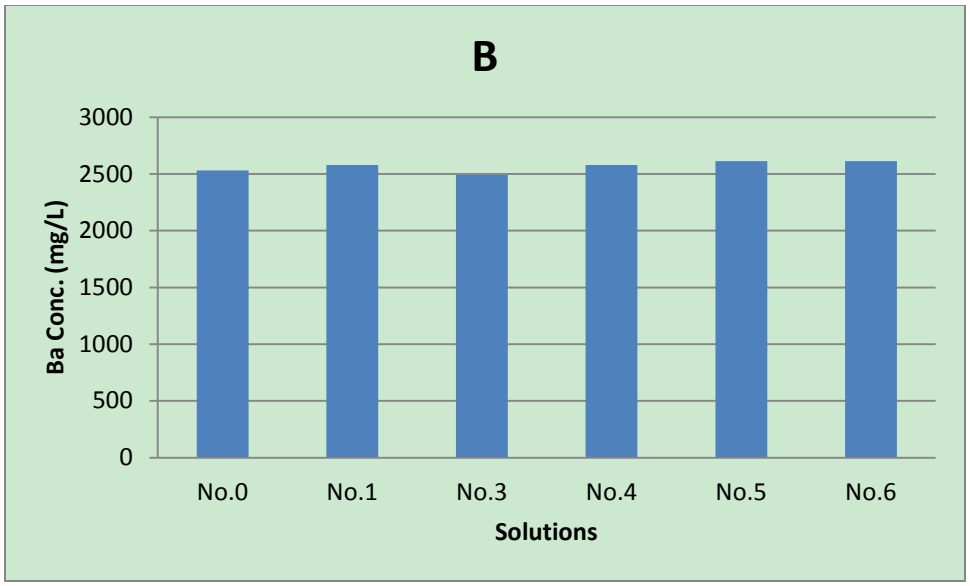

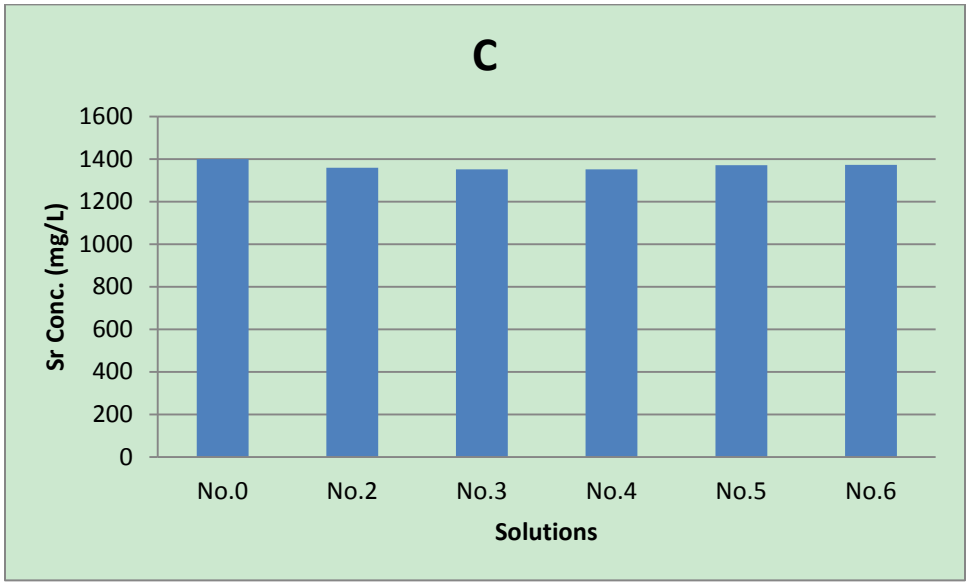

Figure 4. Comparison of Ba measurement variations (A) without KCl addition, (B) with KCl addition, (C) Sr measurement variations with KCl addition. [Ba and Sr in No.0 sample were based on calculation and showed the real concentration, Ba equals 2530 mg/L and Sr equals 1400 mg/L]

3.3.2 Experimental reliability

3.3.2.1 Membrane filter pore size selection

The choice of a proper membrane filter for sample preparation is important to ensure proper experimental results. If a significant portion of particles created through precipitation reaction is too small to be captured by a filter, they can cause erroneous results. Reports by Sheikholeslami and Ong (2003) showed that the calcium sulfate morphology is concentration-composition-dependent, which means that higher concentrations would lead to smaller particle size. Considering the similarity between gypsum and barite, it is possible that the particle size of barite may also become smaller when solution was concentrated. According to the results of SEM analysis, barite crystals are several microns in diameter. However, much smaller particle size was consistently observed in the case of Site C sample (which is the highest salinity solution in this research) mixed with 150 ppm of sulfate. Bethke (2008) suggested that 0.10 μm filter should be used to avoid the experimental error due to the passage of particulates into the filtrate.

To determine which pore size of membrane filter is appropriate, an experiment where synthetic Site C flowback water was mixed with 150 ppm of sulfate was performed and duplicate. Sample collected after 1, 3, 5, 24, and 48 hours were filtered through 0.45 μm and 0.05 μm filters. The experimental results were compared and shown in Figure 5.

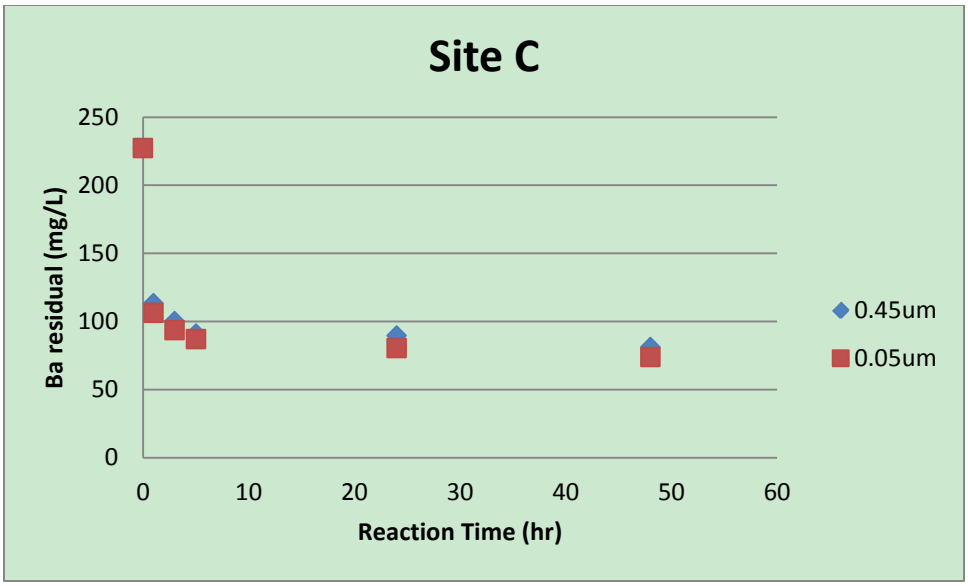

Figure 5. Barium residual comparison between 0.45 µm and 0.05 µm filters with time.

Results revealed that no more than 10.2% difference in concentration measurement was observed after 24-hours and 48-hours, which mean that only a small portion of particles smaller than 0.45 µm were formed under these conditions. Therefore, for the reminder of the study, 0.45 µm filters were used to separate solids from the solution.

3.3.2.2 Reliability of experimental measurements

To verify the accuracy of cation analysis by AAS performed at University of Pittsburgh, analytical results were further compared with samples sent to the NETL-Pittsburgh, which used ICP-OES (Optima 3000) to perform cation analysis. The synthetic flowback water sampled was mixed with different sulfate (SO_4^{2-}) dosage as indicated in Table 11. Samples were filtered through 0.45 µm filters after 24 hours of equilibration. The samples were analyzed by ICP-OES after more than 3 weeks in storage due to analytical availability (filtrations were performed again by NETL before analysis). Typically, samples were measured by AAS immediately after 24 hours of mixing. All samples were tested with 0.15% potassium chloride and 2% nitric acid

before analysis. The barium and strontium concentrations measured by different methods are compared in Table 12. Both analytical procedures returned the results that were closed to each other with deviations within 5%. The excellent fit between the values obtained by AAS at University of Pittsburgh and ICP-OES at NETL demonstrates that adding KCl to the solutions rendered AAS analysis quite accurate. Additionally, because the samples analyzed at NETL were done after more than 3 weeks, it indicates all chemical reactions reached equilibrium in 24 hours.

Table 11. Compositions for the synthetic flowback for NETL and Pitt analysis

	Flask 1	**Flask 2**	**Flask 3**
Components	0 mg/L sulfate	1000 mg/L sulfate	2000 mg/L sulfate
NaCl (mg/L)	82176.5	82176.5	82176.5
$CaCl_2 \cdot 2H_2O$ (mg/L)	1646.9	1646.9	1646.9
$MgCl_2 \cdot 6H_2O$ (mg/L)	1002.3	1002.3	1002.3
$BaCl_2 \cdot 2H_2O$ (mg/L)	4499.8	4499.8	4499.8
$SrCl_2 \cdot 2H_2O$ (mg/L)	4258.5	4258.5	4258.5
Na_2SO_4 (mg/L)	-	1478.7	2957.3

Table 12. Intercomparison of analytical accuracy

$[SO_4^{2+}]$ (mg/L)	**$[Ba^{2+}]$ (mg/L)**			**$[Sr^{2+}]$ (mg/L)**		
	Pitt	**NETL**	**Recipe**	**Pitt**	**NETL**	**Recipe**
0	2506	2440	2530	1387	1414	1400
1000	1038	1103	-	1355	1414	-
2000	10.8	9.37	-	1213	1227	-

In conclusion, the results of these experiments illustrate that the chemical and ionization interference commonly observed for barium and strontium measurements by AAS can be eliminated by using potassium chloride. Further studies provide the strong evidence that the barium and strontium measurements by using AAS with addition of 0.15% potassium chloride in the standards and samples could provide a good agreement with those measured by ICP-OES.

3.3.3 Equilibrium calculations

MINEQL+ 4.6 and Phreeqc Interactive 2.17 (named PhreeqcI later in this document) were the two computer programs used for equilibrium predictions in this study. MINEQL is software specialized for chemical equilibrium calculations and was developed by Westall et al. (1976). PhreeqcI is software for geochemical speciation calculation that was developed by US Geological Survey. The computer codes used in MINEQL+ and PhreeqcI are both based on the law of mass action. The differences between them are in databases used and in the equations used to calculate activity coefficients. The calculations based on Pitzer database are partially modified to make it available for some minerals prediction by adding thermodynamic data and relevant parameters.

4.0 RESULTS AND DISCUSSION

Sulfate (SO_4^{2-}) is a key component in Abandoned Mine Drainage (AMD) that has the ability to precipitate significant amount of divalent cations such as barium (Ba) and strontium (Sr) in the forms of Barite ($BaSO_4$) and Celestite ($SrSO_4$). Calcium (Ca) is not readily removed even with high SO_4^{2-} content since the sulfate will precipitate with Ba and Sr over Ca (K_{sp} of $BaSO_4$ is 1.1×10^{-10}, K_{sp} of $SrSO_4$ is 2.3×10^{-7}, K_{sp} of $CaSO_4$ is 4.3×10^{-5}). Studies showed that Barite crystal has the ability to accommodate Strontium and Calcium on its surface or in the lattice. In that case, Sr and Ca concentrations in the solution may be lower than those calculated by saturation of pure solid precipitation. This depends on many aspects, especially the ionic content and supersaturation degree. Although the degree of supersaturation is the significant factor that affects the removal of target cations, high salinity and complex chemistry of flowback water introduce complex aspects that will have great impact on the removal of these cations. Therefore, it is important to understand all factors that affect the chemistry of flowback water blended with AMD. The purpose of this task was to evaluate the efficiency of sulfate to remove barium and strontium under different sulfate concentrations. In addition, prediction models were used to compare with the experimental results to figure out their calculation capability. To simplify the conditions, synthetic and actual flowback water from different well sites were mixed with different dosages of sulfate in order to gain fundamental insight into the behavior of target cations in the flowback water mixed with AMD water.

4.1 KINETICS OF BARITE AND CELESTITE PRECIPITATION IN SYNTHETIC FLOWBACK WATER

In this study, an understanding of kinetics of barite ($BaSO_4$) and celestite ($SrSO_4$) precipitation is of importance for determining the state of chemical equilibrium in complex brines. A number of parameters showed significant effects on the kinetics of sulfate precipitation, including temperature, pressure, saturation index, ionic strength, scale inhibitors etc. (He et al., 1995; Risthaus et al., 2000; Jones et al., 2007; Shen et al., 2009; Fan et al., 2010). In this study, the temperature and pressure were at standard conditions (atmospheric pressure and room temperature) and the focus was on other factors. Mineral precipitation involves two stages: nucleation and crystal growth. The initial chemical reaction stage is known as induction period and it is usually completed within a couple of minutes (He et al., 1995; Fan et al., 2010). However, the equilibrium of precipitation will take much longer and the precipitation rate normally follows a second order reaction rate (Yeboah et al, 1994; Shen et al, 2008). Further study by Shen et al, (2008) found that the barite precipitation rate is also reaction-direction-dependent: equilibrium is normally reached rapidly when the reaction direction goes from under-saturation to saturation while it usually becomes relatively slow if the direction is from supersaturation to saturation. In this thesis, the situation was more like the latter one simply because reacting ions initially exceeded the saturation needs.

Synthetic flowback water samples were prepared based on a flow-composite flowback water (mix of flowback water samples collected at different times and based on the flow rate profile with time). The compositions of the waters were shown in Table 7 to simulate actual flowback water from gas production in different Marcellus Shale well sites. In the case of flowback water treatment with sulfate only, barium and strontium precipitate and their

concentrations in the liquid phase decreases with reaction time. On the other hand, the removal of Ba and Sr also depends on the amount of sulfate added. The kinetics of precipitation was measured by determining the aqueous Ba and Sr concentrations at different reaction time during the experiment.

The induction period was not an important concern in this study; the profile was not shown here. However, based on the visual observations for most of the runs when the flowback water was mixed with sulfate, the mixture turned turbid within only a few seconds, which indicated extremely rapid barium sulfate nucleation. This is much faster than the nucleation rates found by other researchers (He et al, 1995; Fan et al, 2010). A summary of experimental conditions, including the concentration measurements of ions of concern, calculations of activities, ionic strengths, and saturation indices, is given in Table 13.

Figure 6 and Figure 7 depict the changes in Ba and Sr concentrations in the solutions with time, respectively. Table 14 clearly shows that the removal efficiency for Ba was much higher than that for Sr in all cases. To achieve high Sr removal, much more sulfate is needed than in the case of Ba. These results indicate that sulfate is an excellent removal reagent for Ba but not as good for Sr. The reason is simply because barite solubility is nearly three orders of magnitude lower than that of celestite ($K_{sp,BaSO4} = 1.072\times10^{-10}$ vs. $K_{sp,SrSO4} = 2.291\times10^{-7}$).

Data in Figures 6 and 7 also demonstrated that, barite precipitation was much faster than celestite. In the cases of Site A and Site B flowback water, the differences in time to reach equilibrium between Ba and Sr were very significant. The Ba precipitation was completed within half an hour, sometimes even minutes, but Sr concentration did not stabilize even after 24 hours. Figure 8 clearly indicate that strontium precipitation is such a slow process that the equilibrium needed even weeks to be achieved. In the Site C flowback water, even though strontium

precipitation rate is still slower than that of barium, the differences were not that large. Barium required 3 to 24 hours to reach equilibrium, which depends on the amount of sulfate added, and strontium also became stable around 24 hours (Figure 6(c) & Figure 7(c)). The leading reason for this behavior is the effect of supersaturation. The thermodynamic data shown in Table 13 as Saturation Index (SI) show that barite in Site A and Site B flowback water has higher saturation indices for barite (3.91~4.78) than for celestite (2.2~3.03). Hence, faster precipitation rate than the one observed in Site C flowback water is a strong proof that higher saturation index leads to a faster precipitation rate. Furthermore, the ionic strength of solution and the concentrations of other divalent ions, especially Sr and Ca may also have impacts on the barite precipitation kinetics. Table 13 shows that the initial ionic strength of the Site A and B mixtures were relatively low and that Ba activities were close to Sr activities. However, in the case of Site C flowback water, not only was the ionic strength dramatically increased but the strontium activity was more than 20 times higher than the barium activity (α_{Sr} = 0.01165 and α_{Ba} = 0.0005679). As a result, the equilibrium for Ba precipitation needs much more time to be achieved. This is reasonable because higher salinity and other divalent cations will generate stronger competitions for barite to be formed. It is very interesting to note that the Sr variations shown in Figure 7(c) initially decreased with low sulfate concentration and then increased with time. It is possible that Sr was precipitated at first as celestite because of its much higher activities and then was substituted by Ba through isomorphic substitution because the equilibrium was driven by supersaturation.

Table 13. Measured initial Ba and Sr Concentrations in Different Synthetic Flowback Waters and Corresponding Ionic Strengths, Activities and Saturation Indices with Respect to Barite and Celestite.

Flowback Name	$[SO_4^{2-}]$	$[Ba^{2+}]$	$[Sr^{2+}]$	IS	α_{SO4}	α_{Ba}	α_{Sr}	SI_{BaSO4}	SI_{SrSO4}
Site A	1000	730	376	0.9495	7.806 e-4	1.115 e-3	1.051 e-3	3.91	0.55
	2000	730	376	0.9822	1.542 e-3	1.126 e-3	1.106 e-3	4.21	0.83
	3000	730	376	1.017	2.284 e-3	1.139 e-3	9.854 e-4	4.39	0.98
Site B	1000	2506	1387	1.642	5.588 e-4	3.763 e-3	4.396 e-3	4.29	1.03
	2000	2506	1387	1.677	1.104 e-3	3.830 e-3	4.309 e-3	4.60	1.31
	3000	2506	1387	1.712	1.637 e-3	3.898 e-3	4.227 e-3	4.78	1.48
Site C	150	232	1817	3.620	2.962 e-5	5.679 e-4	1.165 e-2	2.20	0.18
	500	232	1817	3.633	9.858 e-5	5.717 e-4	1.163 e-2	2.72	0.70
	1000	232	1817	3.652	1.967 e-4	5.772 e-4	1.159 e-2	3.03	1.00

- IS: Ionic Strength.
- SI: Saturation Index is the logarithm of Ω (Ω is the ratio of IAP/K_{sp}, where IAP = Ion Activity Product, $\alpha_{A+}\alpha_{C-}$).
- $K_{sp,BaSO4} = 1.072\times10^{-10}$, $K_{sp,BaSO4} = 2.291\times10^{-7}$.
- All values are at initial state.
- Unit for IS and α_X is Molality instead of Molarity based on PhreeqcI program, [XX] in ppm, Ω is dimensionless.
- Calculations were based on Pitzer equations.

Table 14. Ba and Sr removal efficiency in terms of sulfate at different mixing conditions. The data was based on the experimental results. Note that sulfate consumption was estimated by Pitzer model calculations.

Mixtures	Ba removal efficiency	Sr removal efficiency	SO4 consumption
Site A+1000ppm SO4	100.00%	15.80%	62.34%
Site A+2000ppm SO4	100.00%	68.12%	41.18%
Site A+3000ppm SO4	100.00%	-	-
Site B+1000ppm SO4	58.58%	2.31%	99.99%
Site B+2000ppm SO4	99.57%	12.55%	94.80%
Site B+3000ppm SO4	99.89%	56.52%	91.22%
Site C+150ppm SO4	72.41%	1.10%	95.42%
Site C+500ppm SO4	98.36%	9.25%	77.41%
Site C+1000ppm SO4	100.00%	13.98%	84.81%

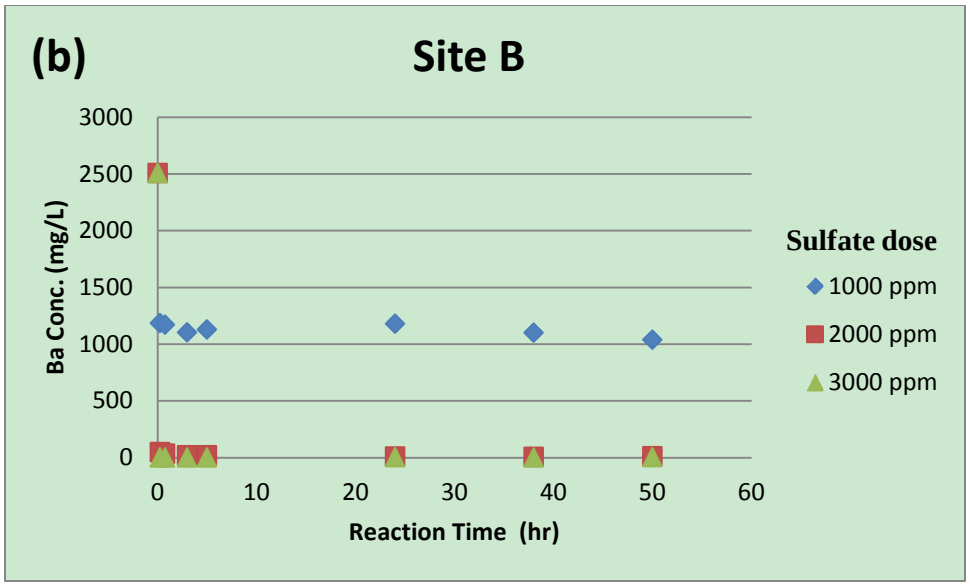

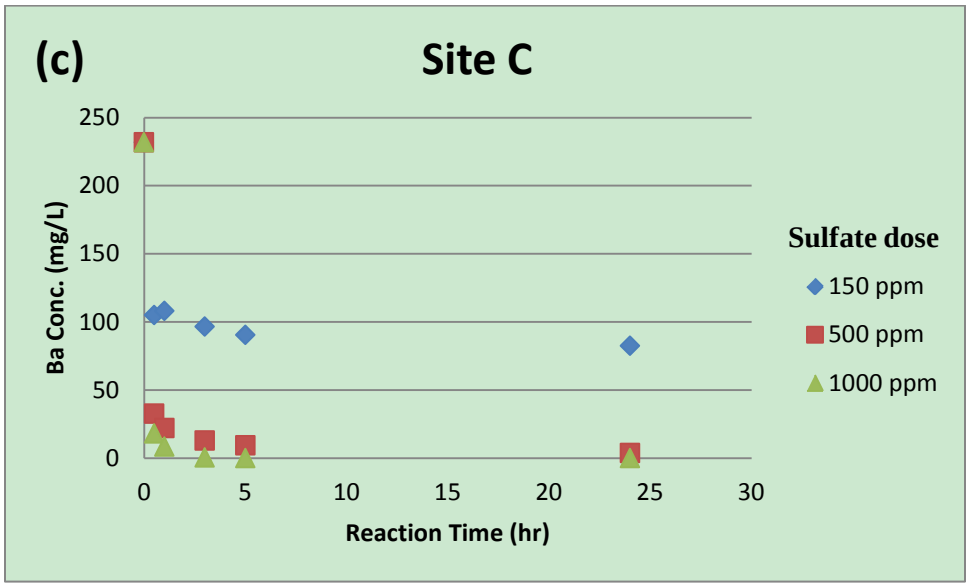

Figure 6. Variations of barium concentration with time for (a) synthetic Site A flowback water, (b) synthetic Site B flowback water, and (c) synthetic Site C flowback water mixed with different dosages of sulfate added in a solid form. Experiments were conducted at standard conditions and all the samples were filtered through 0.45µm filters before analysis.

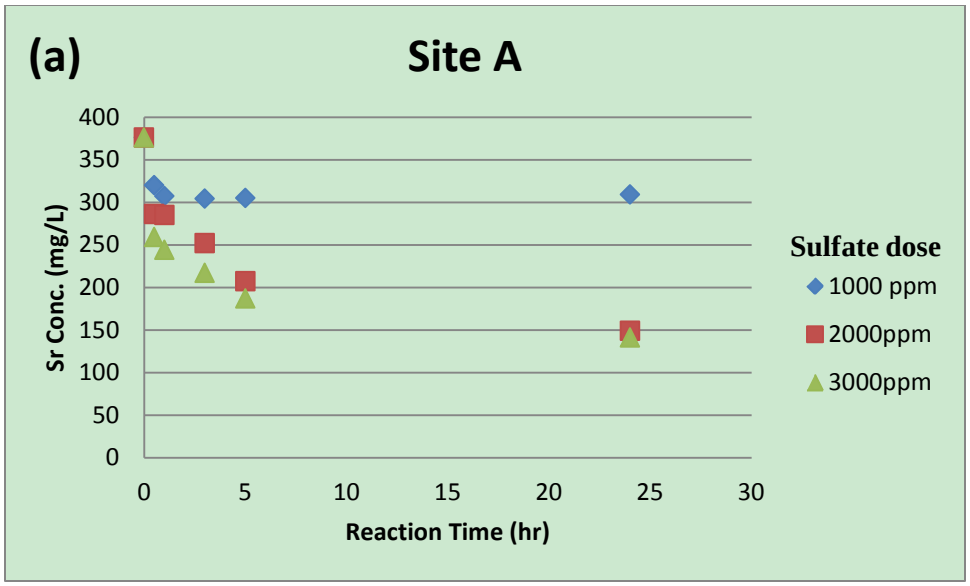
(a)
Site A
Sr Conc. (mg/L)
400
350
300
250
200
150
100
50
0
0
5
10
15
20
25
30
Reaction Time (hr)
Sulfate dose
1000 ppm
2000ppm
3000ppm

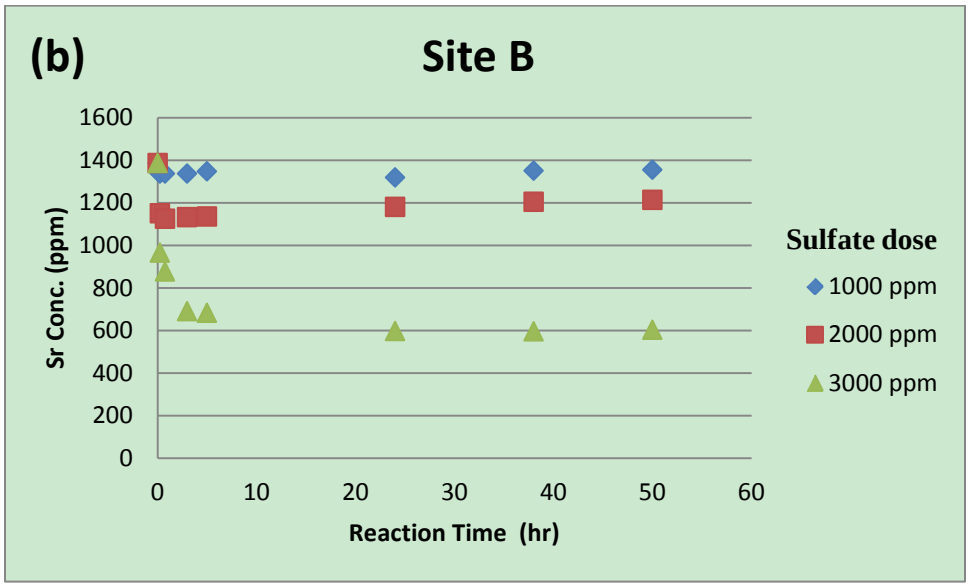
(b)
Site B
Sr Conc. (ppm)
1600
1400
1200
1000
800
600
400
200
0
0
10
20
30
40
50
60
Reaction Time (hr)
Sulfate dose
1000 ppm
2000 ppm
3000 ppm

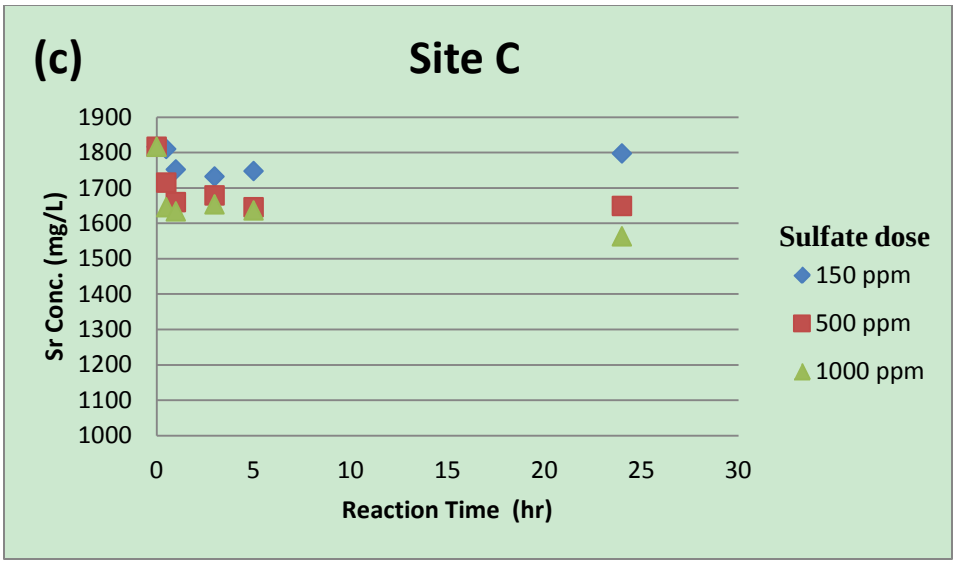

Figure 7. Variations of strontium concentration with time for (a) synthetic Site A flowback water, (b) synthetic Site B flowback water, and (c) synthetic Site C flowback water mixed with different dosages of sulfate added in a solid form. Experiments were conducted at standard conditions and all the samples were filtered through 0.45µm filters before analysis.

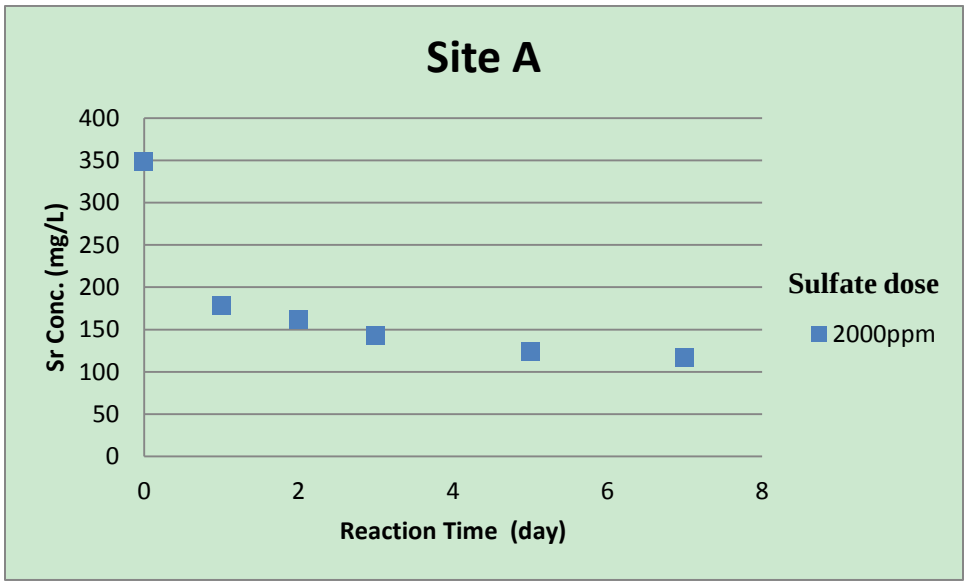

Figure 8. Dissolved strontium concentrations versus time for strontium sulfate precipitation kinetics over the extended period of time.

4.2 INFLUENCE OF CALCIUM ON BARITE AND CELESTITE REMOVAL IN SYNTHETIC FLOWBACK WATER

The solubility of barite and celestite in electrolyte solutions will increase when the solution ionic strength increases (Blount, 1977; Reardon & Armstrong, 1987). However, due to the different tendencies of cations to interact with sulfate, their impact on the behavior of Ba and Sr is different. Most studies have shown good agreement of solubility of barite and celestite under different electrolyte solutions up to ionic strength of several molarities. The only discrepancy was found when barite and celestite formed in calcic solutions (Monnin and Galinier, 1988). The interest concerning the effect of calcium on barite precipitation increased recently (Hennessy and Graham, 2002; Jones et al., 2004). The researchers found an inhibitory effect of Ca even much greater than that of Na with equivalent ionic strength. Additionally, the inhibitory effect of calcium would become obvious only for concentrations of calcium above 0.25 mM (10ppm). The studies suggest that there will be higher barium concentration at equilibrium and slower precipitation rate even with low content of calcium in solution.

One of the major differences in different Marcellus Shale flowback waters comes from significant variations of calcium concentration, which is the highest in Site C and lowest in Site B. Considering the experimental conditions in the literature, synthetic flowback water based on Site A was selected to examine calcium effect. Two sets of experiments were conducted to determine the impact of the presence of calcium on the precipitation of barium and strontium sulfate. Synthetic Site A flowback water was prepared with different calcium concentrations (0 ppm, 500 ppm, and 1000 ppm) and sodium chloride was used to make the ionic strength equal in each solution. To be able to study the calcium influence on barium sulfate precipitation, a lower initial sulfate concentration of 400 ppm was selected to allow a measurable residual Ba

concentration at equilibrium (Table 15). Much higher sulfate concentration of 2000 ppm was chosen to study the impact of Ca on strontium sulfate precipitation. The reason for such different sulfate dosage in the two sets of experiment is because of considerable solubility differences between barite and celestite in the electrolyte solution.

Table 15. Residual dissolved barium concentration (ppm) in the presence of different calcium concentrations in synthetic Site A flowback water with 400 ppm sulfate.

Time (hour)	0ppm calcium	500ppm calcium	1000ppm calcium
0	747	747	747
0.5	276	273	254
1	248	241	229
3	245	220	230
5	223	210	210
24	204	199	171

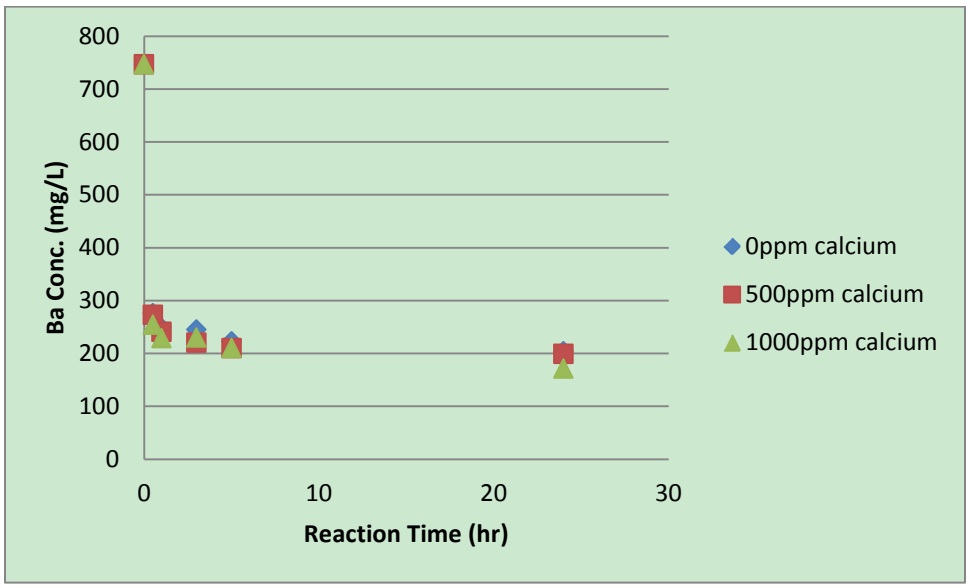

Figure 9. Dissolved barium concentration profile for different concentrations of calcium with time in synthetic Site A flowback water with 400 ppm sulfate. Ionic strength in these 3 solutions was identical.

The dissolved barium concentration profile with time (Figure 9) did not reveal any influence of calcium on barite precipitation kinetics for calcium concentrations up to 1000 ppm. However, continuous gradual decrease in barium concentrations suggests that the equilibrium state is not achieved in at 24 hours. Therefore, an extended experiment using synthetic Site A flowback water (2224 ppm calcium added) mixed with 400 ppm sulfate was performed. The reaction last for 7 days (Figure 10). These extended profiles showed that the barite precipitation did reach equilibrium within the very first day.

Results observed in this study were contrary to those reported by Jones et al. (2004) that showed that calcium would increase the solubility of barite much greater than sodium under equivalent ionic strength condition. It is important to note that the solution in this research had much higher sodium chloride concentration. Therefore, it is possible that high ionic strength used in this study completely washed the influence of calcium.

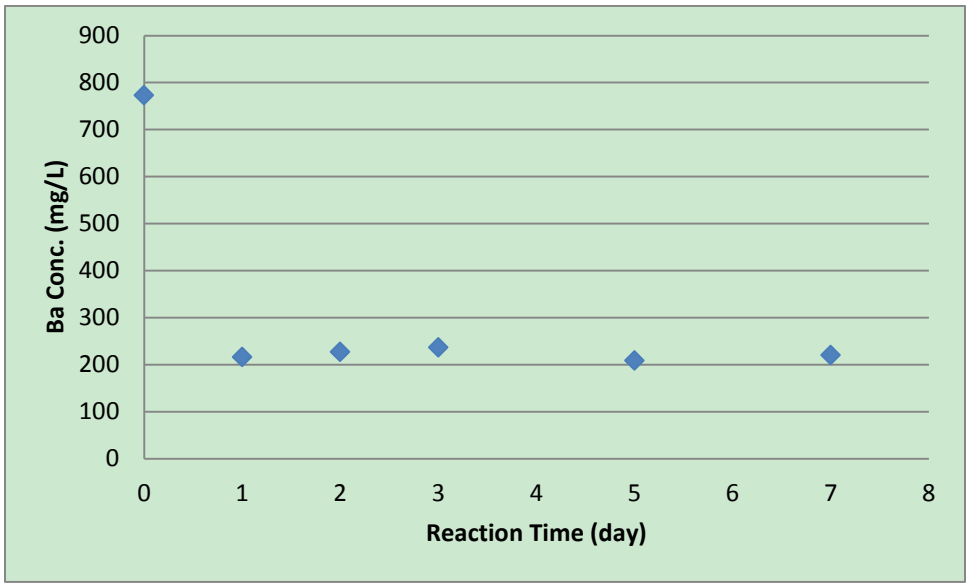

Figure 10. Dissolved barium concentration profile for synthetic Site A flowback water mixed with 400 ppm sulfate.

Experimental results were compared with equilibrium calculations (Figure 11) using Davis equation (MINEQL+ 4.6), "WATEQ" DEBYE-HÜCKEL equation and Pitzer equations (Phreeqc Interactive 2.17). All the three models predicted the same Ba values at equilibrium for all cases, suggesting that Ca has no impact on thermodynamic calculations. Differences between measured and predicted Ba concentration (up to 15.9% off) were more pronounced for lower Ca concentrations (0 and 500 ppm). One reason may be the measurement error of initial barium concentration. Calculations revealed that when sulfate is insufficient to completely precipitate barium, even 3% error in initial Ba concentration can lead up to 15% difference in equilibrium predictions for Site A flowback water mixed with 400 ppm sulfate.

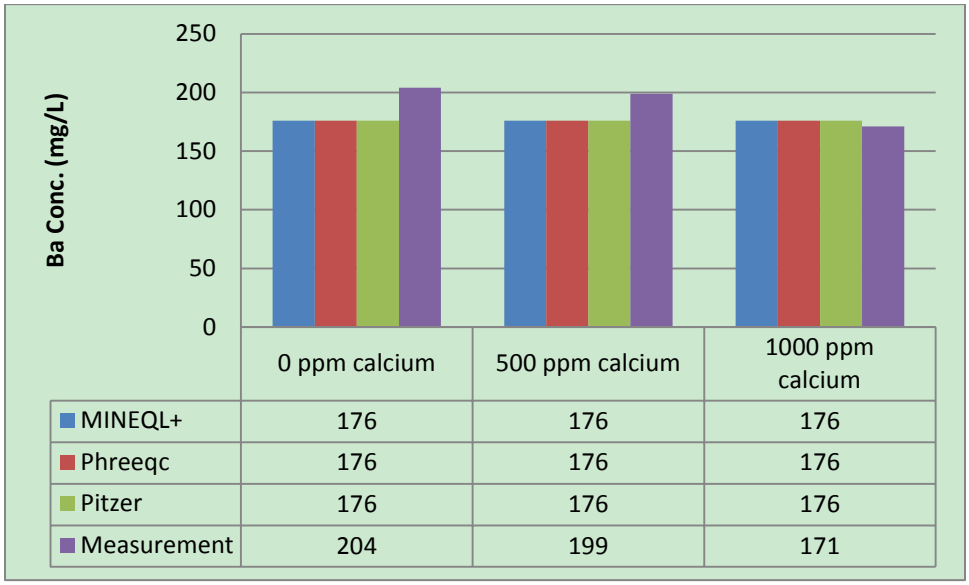

Figure 11. Dissolved barium concentration at equilibrium for different concentrations of calcium in synthetic Site A flowback water mixed with 400 ppm sulfate. Experimental results are compared with equilibrium prediction by MINEQL+4.6 and Phreeqc Interactive 2.17. Note that the initial barium concentrations were different.

As indicated earlier, celestite solubility is much greater than that of barite and a much higher sulfate dosage is required to test the impact of Ca on the celestite precipitation. It was decided to use 2000 ppm of sulfate for the Site A flowback water. However, under such high sulfate content, no Ba could be detected after 30 minutes. As can be seen from Figure 12, calcium concentration up to 1000 ppm does not show any significant impact on the kinetics of strontium sulfate precipitation. However, according to the experiment with Site A synthetic water that contained 2224 ppm of calcium, strontium precipitation lasted for days when 2000 ppm sulfate was added to the solution (Figure 13).

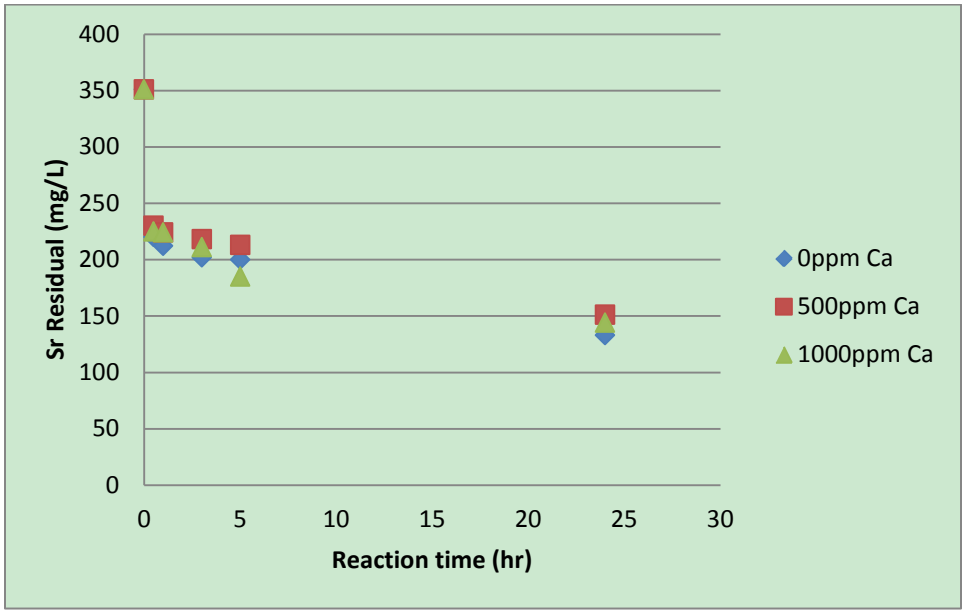

Figure 12. Dissolved strontium concentration profile for different concentrations of calcium in synthetic Site A flowback water with 2000 ppm sulfate. Ionic strength in these 3 solutions was identical.

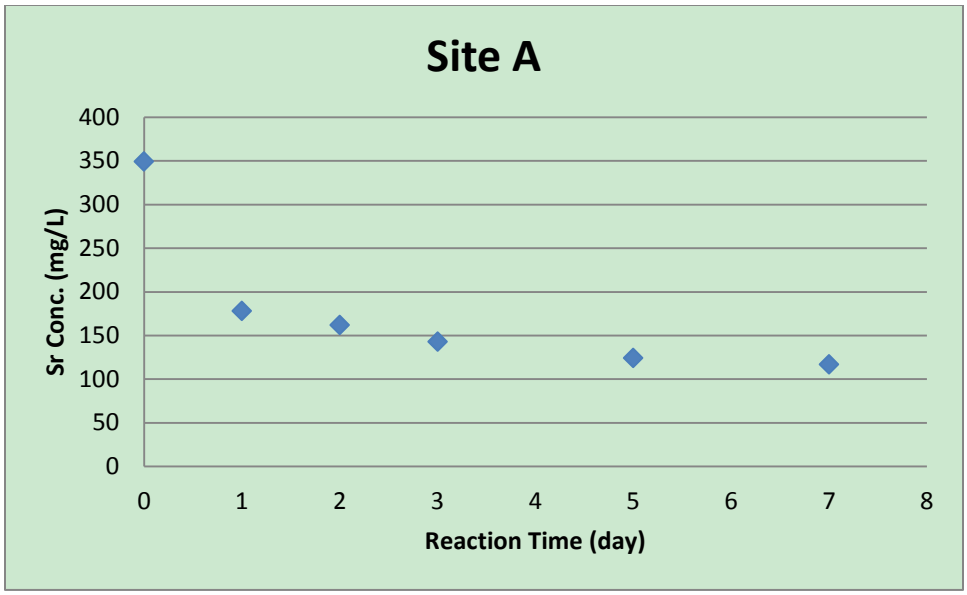

Figure 13. Dissolved strontium concentration profile for synthetic Site A flowback water mixed with 2000 ppm sulfate.

Modeling results displayed in Figure 14, on the other hand, indicate that the celestite solubility increases with an increase in Ca concentration. These results are similar to those found in studies of Ca impact on $BaSO_4$ precipitation, where $BaSO_4$ solubility increases either due to surface poisoning to hinder barium sulfate reaction or due to incorporation into barite lattice to increase its internal free energy. Study by Monnin and Galinier (1988) showed that celestite solubility becomes even higher than that of gypsum ($CaSO_4 \cdot 2H_2O$) when the $CaCl_2$ concentration increases up to a point. Considering a much higher sulfate dose (2000 mg/L SO4 in celestite experiments vs. 400 mg/L SO4 in barite experiments) and higher solubility (celestite solubility is three orders of magnitude higher than that of barite) in this case, it is possible that Ca and Sr have a strong competition for sulfate and the formation of $CaSO_4 \cdot 2H_2O$ is thus formed. This can increase celestite solubility because less free sulfate ion is available to precipitate strontium in the solution.

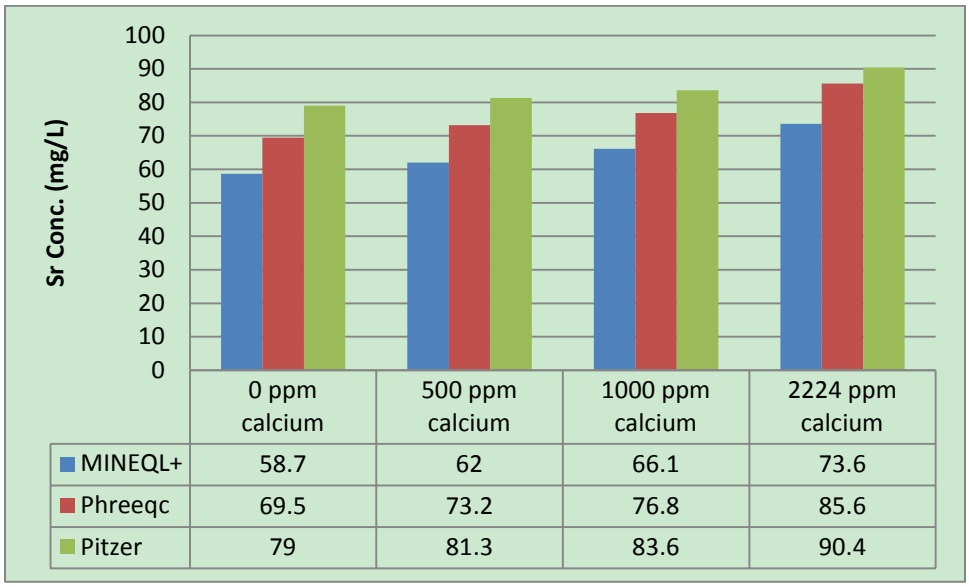

Figure 14. Dissolved strontium concentration at equilibrium for different concentrations of calcium in synthetic Site A flowback water mixed with 2000 ppm sulfate.

The key conclusion from this part of work is that barium precipitation can be predicted by any of the three equations evaluated in this study, while strontium precipitation is a slow process and equilibrium may take even more than 7 days to achieve. Calculations based on three different models showed that calcium has no effect on the solubility of barite but the celestite solubility becomes higher when calcium concentration increases.

4.3 EQUILIBRIA PREDICTIONS IN SYNTHETIC FLOWBACK WATER

The aim of this part of work is to evaluate the ability of different chemical equilibrium models to predict sulfate equilibrium in synthetic flowback water. It is well known that the models based on different activity coefficient equations have their own ionic strength range of application and

any attempt to exceed the limit may lead significant deviation from the observations. However, considering the very special cases in this research, which is the high salinity brine water with complex composition that is dominated by sodium chloride, it may be possible to extend model applicability for higher range of ionic strengths. Calculations in Pitzer model use semi-empirical equations and depend on a large number of parameters. However, the database for the Pitzer model in PhreeqcI program is missing some parameters that are essential for the Marcellus Shale flowback water and new data have been collected from the literature. The experimental equilibrium data are compared with model prediction to find the calculation accuracy in multi-electrolyte mixtures with a wide range of ionic strengths (0.95~3.65 molality) shown in Table 16. Synthetic Site A, Site B and Site C flowback waters were chosen to represent flowback waters in Marcellus Shale

Table 16. Initial Barium and Strontium Concentrations in Different Synthetic Flowback Waters and Corresponding Initial Activities, Ionic Strengths, and Saturation Indices with Respect to Barite and Celestite.

Flowback Name	$[SO_4^{2-}]$	$[Ba^{2+}]$	$[Sr^{2+}]$	IS	α_{SO4}	α_{Ba}	α_{Sr}	SI_{BaSO4}	SI_{SrSO4}
Site A	1000	730	376	0.9495	7.806 e-4	1.115 e-3	1.051 e-3	3.91	0.55
	2000	730	376	0.9822	1.542 e-3	1.126 e-3	1.106 e-3	4.21	0.83
	3000	730	376	1.017	2.284 e-3	1.139 e-3	9.854 e-4	4.39	0.98
Site B	500	2440	1414	1.624	2.806 e-4	3.631 e-3	4.527 e-3	3.98	0.74
	1000	2506	1387	1.642	5.588 e-4	3.763 e-3	4.396 e-3	4.29	1.03
	1400	2451	1376	1.655	7.781 e-4	3.706 e-3	4.326 e-3	4.43	1.16
	1800	2451	1376	1.669	9.956 e-4	3.732 e-3	4.292 e-3	4.54	1.27
	2000	2506	1387	1.677	1.104 e-3	3.830 e-3	4.309 e-3	4.60	1.31
	2400	2451	1376	1.690	1.318 e-3	3.772 e-3	4.434 e-3	4.67	1.38
	2800	2451	1376	1.704	1.530 e-3	3.799 e-3	4.209 e-3	4.73	1.45
	3000	2506	1387	1.712	1.637 e-3	3.898 e-3	4.227 e-3	4.78	1.48
Site C	150	232	1817	3.620	2.962 e-5	5.679 e-4	1.165 e-2	2.20	0.18
	500	232	1817	3.633	9.858 e-5	5.717 e-4	1.163 e-2	2.72	0.70
	1000	232	1817	3.652	1.967 e-4	5.772 e-4	1.159 e-2	3.03	1.00

- IS: Ionic Strength.
- SI: Saturation Index is the logarithm of Ω (Ω is the ratio of IAP/K_{sp}, where IAP = Ion Activity Product, $\alpha_{A+}\alpha_{C-}$).
- $K_{sp,BaSO4} = 1.072\times10^{-10}$, $K_{sp,BaSO4} = 2.291\times10^{-7}$.
- Unit for IS and α_X is Molality instead of Molarity based on PhreeqcI program, [XX] in ppm, Ω is dimensionless.
- Calculations were based on Pitzer equations.

The first set of experiments was conducted on synthetic Site A flowback water which has lowest ionic strength (around 0.89 M) among the three flowback waters. Site A flowback water also has low concentration of strontium (367 ppm) and medium concentrations of barium and calcium (781 ppm of Ba and 2224 ppm of Ca). This water was mixed with 400 ppm, 1000 ppm, 2000 ppm, and 3000 ppm of sodium sulfate powder and the equilibrium data were collected after 24 hours of mixing. The experimental results were compared with calculations based on different models in Figure 15 and 16.

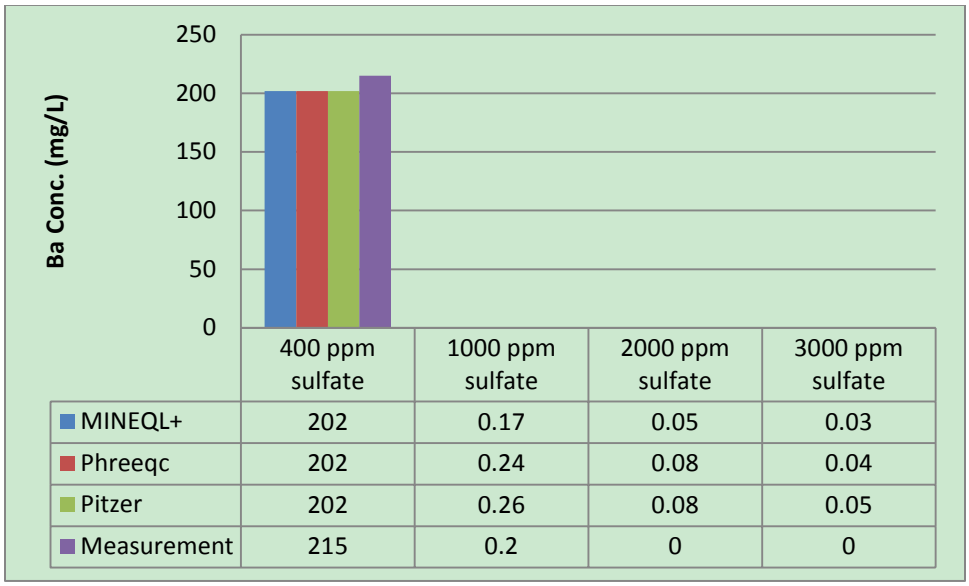

	400 ppm sulfate	1000 ppm sulfate	2000 ppm sulfate	3000 ppm sulfate
MINEQL+	202	0.17	0.05	0.03
Phreeqc	202	0.24	0.08	0.04
Pitzer	202	0.26	0.08	0.05
Measurement	215	0.2	0	0

Figure 15. Barium concentration comparison between experimental results and calculations. Measurements were the data collected based on 24 hours reaction.

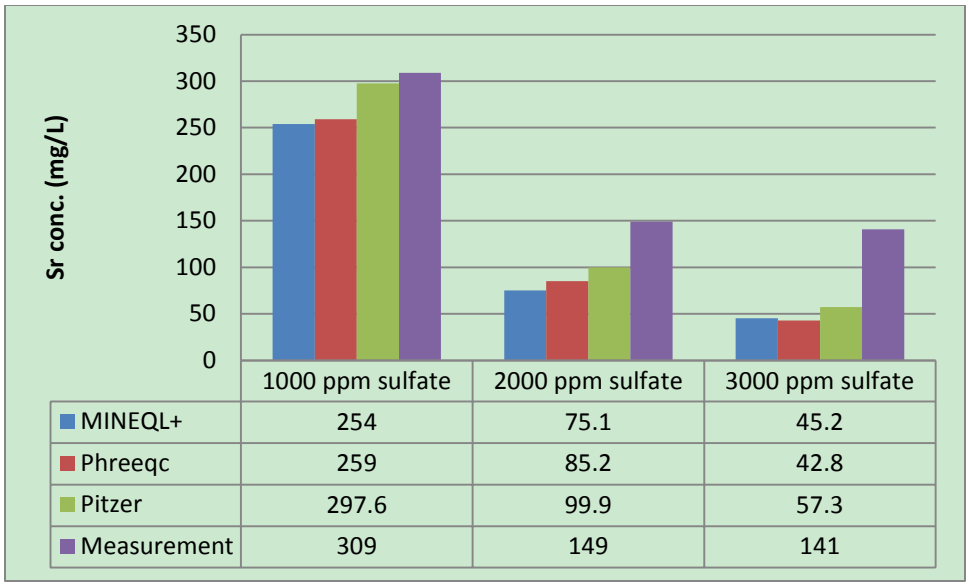

	1000 ppm sulfate	2000 ppm sulfate	3000 ppm sulfate
MINEQL+	254	75.1	45.2
Phreeqc	259	85.2	42.8
Pitzer	297.6	99.9	57.3
Measurement	309	149	141

Figure 16. Strontium concentration comparison between experimental results and calculations. Measurements were the data collected based on 24 hours reaction. The 400 ppm sulfate data was not included because of no precipitation of celestite was formed

Barium concentrations predictions based on the three models showed almost identical values at equilibrium and they were all in excellent agreement with the experimental results. The decreased barium concentration was due to the formation of barite precipitation which was predicted by all the three models and it is confirmed by the SEM-EDS analysis. However, Figure 16 depicted significant deviation between the calculations and experimental results when adding 2000 ppm and 3000 ppm of sulfate (up to 144% off). Only Pitzer model showed good agreement in the case of 400 ppm sulfate mixture (3.8% off for Pitzer, 19.3% for WATEQ, and 21.7% for Davis). All calculations made by Davis equation and WATEQ DEBYE-HÜCKEL equation showed an obvious deviation from the measurements. The deviation increased with the initial sulfate concentration.

One hypothesis to explain this discrepancy is that the barium sulfate formation rate is as fast as sodium sulfate dissolution. In that case, barium sulfate could form on the surface of

sodium sulfate crystals, thereby decreasing the amount of sulfate available for strontium precipitation. To verify this hypothesis, an experiment was performed by mixing the synthetic Site A flowback water with 2000 ppm of pre-dissolved sodium sulfate (a stock solution of sodium sulfate with the concentration as high as 100,000 mg/L as SO_4 was prepared). The experimental results was then compared with previous ones and shown in Figure 17.

Figure 17. Experimental results for kinetics of Sr removal from Site A synthetic flowback water with the same sulfate dosage. Dose I was 2000 ppm of sulfate added in crystal form while Dose II was 2000 ppm of sulfate added as solution.

The resulting precipitation kinetics was faster when sodium sulfate solution was used than when sodium sulfate crystals were added to the Site A flowback water, which can be explained by faster dispersion of sulfate in the solution. Figure 17 suggest there are differences in celestite precipitation when sulfate crystal or sulfate solution are used. However, it does not support the hypothesis that barite is forming on the surface of sodium sulfate crystals to reduce the availability of sulfate to react with strontium.

In sulfate precipitation, celestite has much slower precipitation kinetics compared with that of barite. It is possible that the Sr precipitation did not reach equilibrium after 24 hours. To confirm this hypothesis, experiments were conducted for extended period of time. The 2000 ppm of sulfate was added to synthetic site A flowback water as an example. Figure 18 revealed that the precipitation of celestite will continue for days and the agreement between predictions and measurement after 7 days of reaction was greatly improved. The calculation based on Pitzer equations was still the best of all indicating its outstanding performance in high ionic strength solutions.

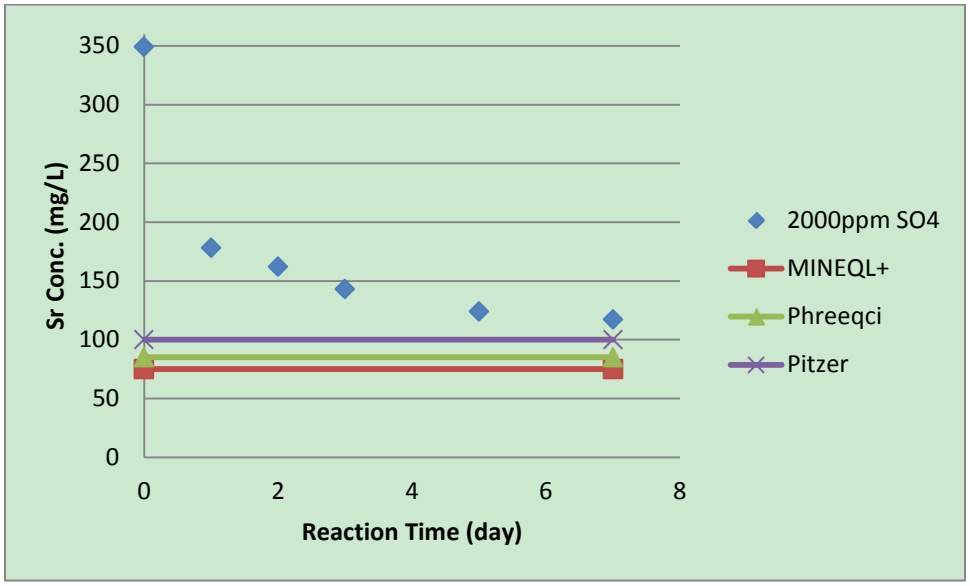

Figure 18. Strontium concentration in synthetic Site A flowback water supplemented with 2000 ppm sulfate during 7 days of contact.

The second set of experiments was conducted on synthetic Site B flowback water with the same ions. This type of water has higher ionic strength solution (1.55 M), higher concentration of Ba and Sr (2530 ppm of Ba and 1400 ppm of Sr) but lower Ca concentration

(499 ppm). Extensive sulfate dosages up to 3000 mg/L were mixed with the synthetic water (Table 17) and data were collected after 48 hours of reaction.

Table 17. Comparison between experimental results and calculations for Site B flowback water. Davis equation was used in MINEQL+ 4.6 program, while WATEQ equation and Pitzer equations were used in PhreeqcI program. Measured data were collected after 48 hours of mixing.

$[SO_4^{2-}]$ (mg/L)	$[Ba^{2+}]$ (mg/L)				$[Sr^{2+}]$ (mg/L)			
	Measured	Davis eq.	WATEQ eq.	Pitzer eq.	Measured	Davis eq.	WATEQ eq.	Pitzer eq.
500	1762	1785	1791	1791	1387	1387	1387	1387
1000	1038	1016	1076	1076	1355	1376	1376	1376
1400		439	450	450	1348	1376	1376	1376
1800		0.9	1.64	1.54	1350	1341	1372	1376
2000	10.8	0.8	1.49	1.28	1213	1200	1244	1255
2400		0.6	1.04	0.9	917	812	870	884
2800		0.34	0.68	0.6	626	495	568	587
3000	2.1	0.26	0.56	0.5	559	386	469	490

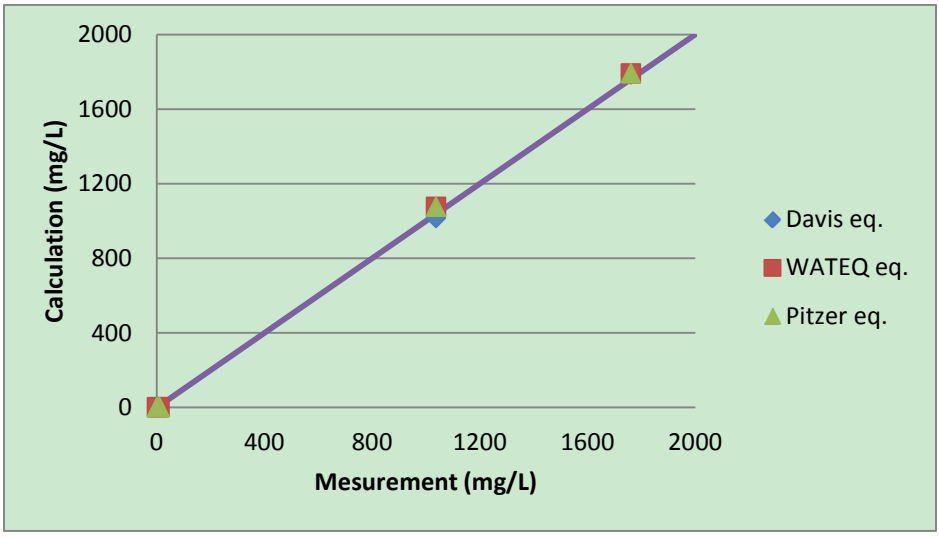

Figure 19. Comparison of measured Ba results with equilibrium data predicted by MINEQL+ and PhreeqcI for Site B flowback water.

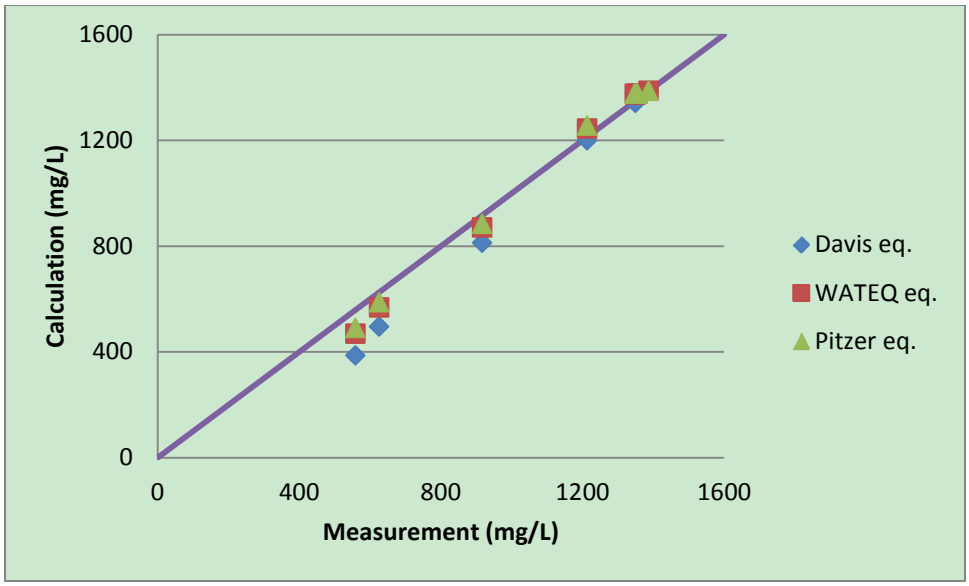

Figure 20. Comparison of measured Sr results with equilibrium data predicted by MINEQL+ and PhreeqcI for site B flowback water.

Comparing the experimental results of dissolved species of interest (i.e. barium and strontium) under different sulfate doses with the results predicted by Davis equation, WATEQ DEBYE-HÜCKEL equation and Pitzer equations revealed that all experimental results were close to equilibrium prediction for barium (Figure 19). The relatively large deviations at low Ba concentrations may be due to experimental error since the dissolved concentrations of Ba in the case of large addition of sulfate were very low (below the barium standard which is 5 ppm) and thus could not be determined precisely. On the other hand, calculations based on Davis equation could not accurately predict Sr concentrations for high sulfate dosage (Figure 20), but worked quite well (1.0% off) for an initial sulfate concentration below 2000 ppm. PhreeqcI predictions based on either WATEQ DEBYE-HÜCKEL equation or Pitzer equations were in fairly good agreement with experimental data for all sulfate concentrations tested in this study, with calculations based on Pitzer model being slightly better.

The last set of experiments was conducted by using synthetic Site C flowback water mixed with different doses of sulfate (Table 18). This water had very of high salinity (3.41 M) with elevated content of calcium (15021 mg/L) and strontium (1799 mg/L) but very low concentration of barium (236 mg/L). The comparison between measured and predicted values was performed using the experimental data collected after 24 hours of mixing.

Table 18. Comparison between experimental results and calculations with Site C flowback water. Davis equation was performed in MINEQL+ 4.6 program, while WATEQ equation and Pitzer equations were utilized in PhreeqcI program.

$[SO_4^{2-}]$ (mg/L)	$[Ba^{2+}]$ (mg/L)				$[Sr^{2+}]$ (mg/L)			
	Measured	Davis eq.	WATEQ eq.	Pitzer eq.	Measured	Davis eq.	WATEQ eq.	Pitzer eq.
150	82.4	26.1	38.8	32.6	1747	1812	1812	1812
500	3.8	1.1	3.5	2.2	1649	1629	1617	1645
1000	0	0.8	2.6	1.6	1409	1209	1202	1236

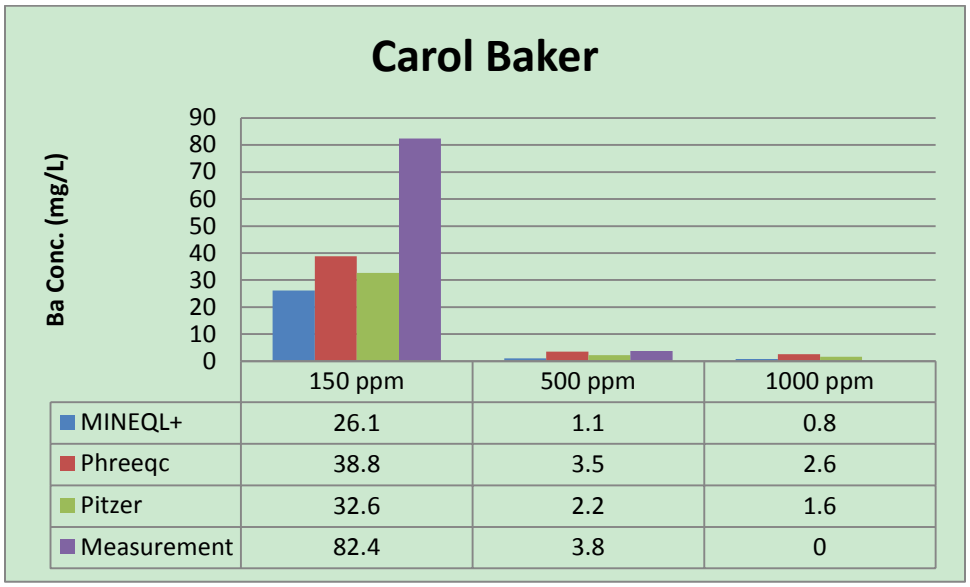

Figure 21. Barium concentration comparison between experimental results and calculations. Measurements were the data collected based on 24 hours reaction.

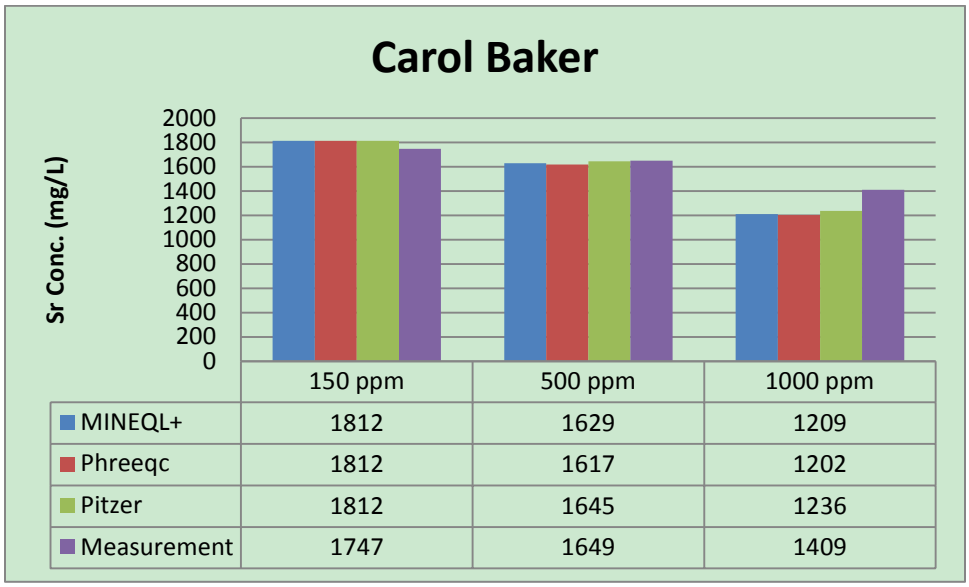

Figure 22. Strontium concentration comparison between experimental results and calculations. Measurements were the data collected based on 24 hours reaction.

As can be seen in Figure 21 and 22, all three models provided fairly good predictions for both barium and strontium concentrations. The only exception is Ba prediction after the addition of 150 ppm of sulfate.

To figure out the discrepancy in this study, further experimental results on sulfate residuals in Site C synthetic flowback water mixed with 150 mg/L and 1000 mg/L are shown in Figure 23. The measurements were based on the data collected after 4 weeks. It is clear that the agreements are improved when the predictions are compared with data collected after 4 weeks.

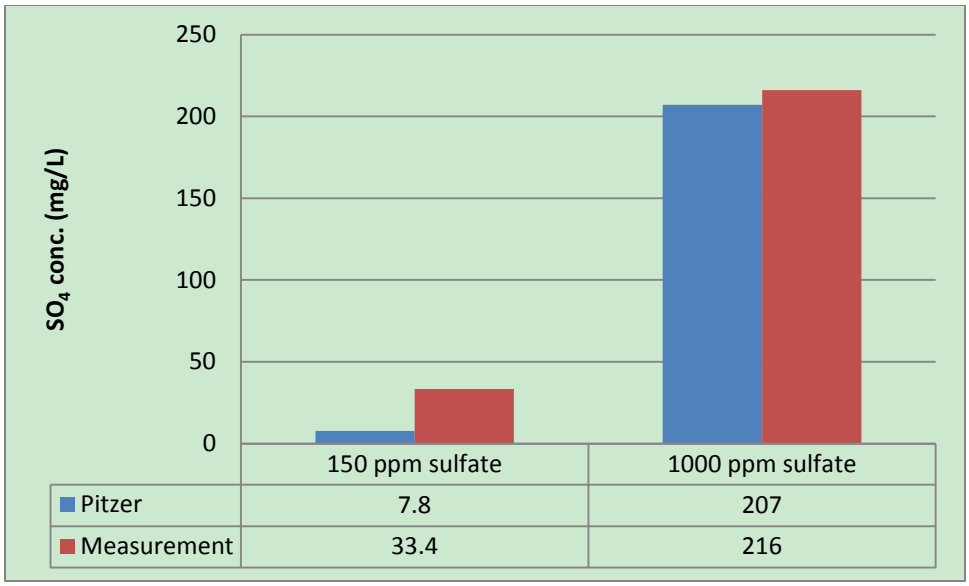

Figure 23. Sulfate concentration comparison between experimental results and calculations. Measurements were the data collected based on 4 weeks.

Visual observations showed that in the presence of such low barium and sulfate doses, the development of turbidity in solution required several minutes instead of few seconds which was the case in other experiments. This observation can be explained with high salinity and low supersaturation. This experiment with low Ba and SO_4 concentration was extended for extended 49 days and the results are shown in Figure 24.

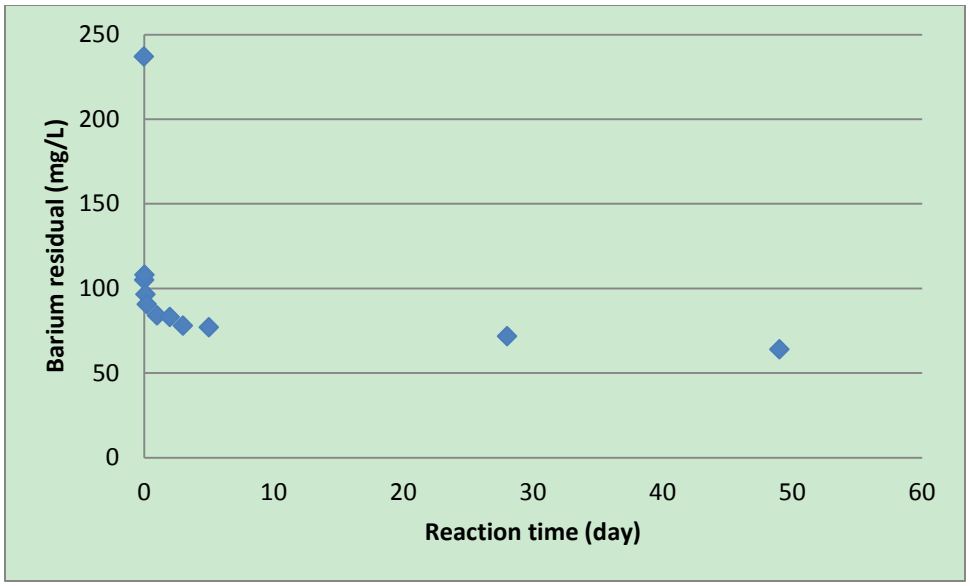

Figure 24. Barium precipitation kinetics in the mixture of Site C flowback water and 150 ppm sulfate.

Figure 24 clearly indicates that the barium in solution gradually decreases and does not reach equilibrium even after 49 days of reaction time. Previous studies have shown that solution composition besides ionic strength will impact the morphology of barite. It is possible that other high concentrated ions in the solution can be incorporated into barite crystal lattice, which will increase the internal energy and make the crystal unstable. This behavior can greatly reduce the precipitation rate and make the equilibrium hard to reach. Therefore, an experiment with solution of identical ionic strength as synthetic Site C flowback water but with varying composition (Table 19) was initiated by mixing the solution with 150 ppm of sulfate.

Table 19. Composition of simplified experimental solutions

	Composition	Ionic Strength	Initial Ba conc.	Ba conc. After 24 hours
Solution 1	$BaCl_2 + NaCl + NaSO_4$	3.41	236	37
Solution 2	$BaCl_2 + NaCl + SrCl_2 + NaSO_4$	3.41	236	79

The experimental results collected after 24 hours of reaction are shown in Figure 25. It revealed that the high ionic strength was not the reason for slow kinetics of barite precipitation because equilibrium calculations are in agreement with experimental data for solution 1. However, high initial concentration of Sr greatly influenced Ba behavior. Barium concentration measured in Solution 2 was in good agreement with the test shown in Figure 21 which was performed using the complete synthetic Site C flowback water mixed with 150 ppm of sulfate. Strontium ion has similar radius and properties to barium (sulfate structure etc.) and can easily be incorporated into barite lattice. As shown Figure 7 (c), strontium in synthetic Site C flowback solution supplemented with 150 ppm sulfate dramatically decreased within first 5 hours and then increased with time during the first 24 hours. This observation is in agreement with studies that showed that co-precipitation of (Ba, Sr)SO_4 could occur in solution but is of limited impact on the solubility of $BaSO_4$ (Prieto, 2009). The dominant impact of Sr demonstrated in these experiments is that it could extend the Barite precipitation time rather than solubility when the supersaturation of barite is low in Sr-rich solution.

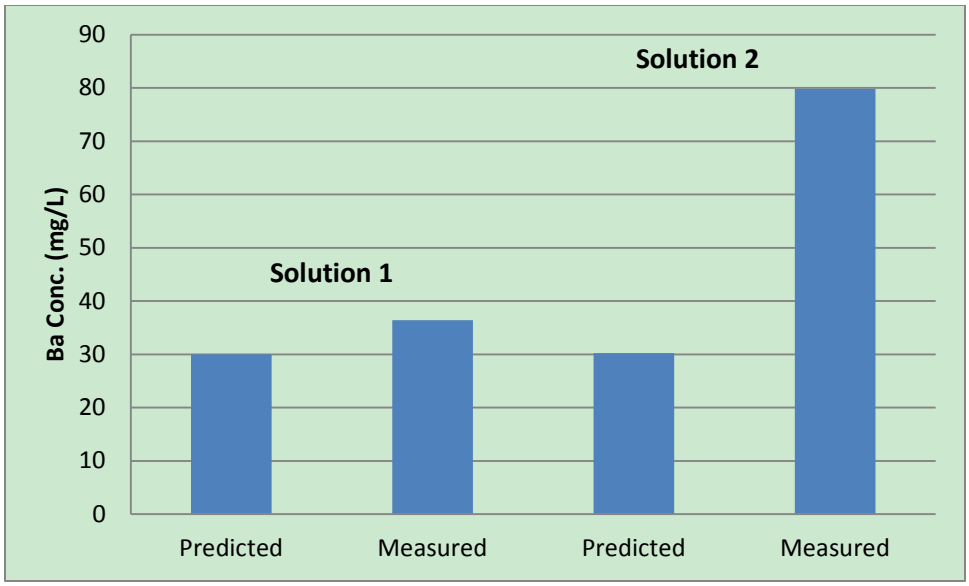

Figure 25. Comparison of measured Ba concentrations with those calculations based on Pitzer model.

Based on the data presented in this section, it can be concluded that both MINEQL+ and PhreeqcI (based on the different equations) can predict Ba precipitation quite well. The only exception was the case with high ionic strength solution mixed with low sulfate dose. Evidence has shown that this deviation was mainly due to the slow kinetics (which means the equilibrium needs much more time to be reached) that was caused by high Sr/Ba ratio in solution. On the other hand, PhreeqcI predictions based on Pitzer model were in fairly good agreement with experimental data for Sr at a wide range of ionic strengths, and solution compositions. MINEQL+ predictions for Sr were valid only when low sulfate dose was used. MINEQL+ predictions start to show significant deviation from experimental results when strontium removal ratio exceeds 14%. It is clear that the solubilities calculated by the Pitzer equations are higher than those predicted by the other two equations. This is in agreement with other studies which suggested that activity coefficient values for ion-interaction models (Pitzer equations) are generally smaller than those appropriate for ion-association models (Pearson and Berner, 1991).

4.4 COMPARISONS OF CHEMICAL EQUILIBRIA IN SYNTHETIC AND ACTUAL FLOWBACK WATER

The actual flowback water is a much more complex matrix than the synthetic water which contains only salts. Presence of organic material from either the rock formation or from the chemicals injected in the fracturing fluid may have an impact on the precipitation kinetics, concentrations at equilibrium and crystal size and morphology. Whether the organic substances can inhibit or accelerate the precipitation is still being disputed in the literatures (Hennessy and Graham, 2002; Jones et al. 2004; Smith et al. 2004; Jones et al. 2008; Hamdona and Hamza, 2009). Most studies suggest that organics, such as commercial antiscalants and polyphosphonates, could retard the precipitation even at very low concentrations. However, some other organics like methanol could promote the precipitation, which is quite opposite of what would be expected based on the classical nucleation theory. The actual flowback collected from the well sites does include organics, but the nature and their concentrations are not readily available.

An experiment was carried out by mixing the actual Site A flowback water with crystal sodium sulfate, and comparing with the results obtained for the synthetic flowback water from Site A. The sulfate doses selected for this experiment were 1000, 2000, and 3000 ppm. Barium residuals were all nearly zero because the sulfate added was in excess with respect to barium. Strontium concentration profiles are similar to those obtained using the synthetic flowback water, although a slight decrease of the precipitation rate can be noted when testing the real flowback water (Figure 26). For the experiment with 1000 ppm sulfate, the curve obtained with the real flowback water lies under the one obtained with the synthetic water, but the initial strontium concentration in actual flowback water is also lower. Considering the other two doses, more Sr

was removed in the case of synthetic water indicating that the solubility in actual flowback water was higher than that in the synthetic water.

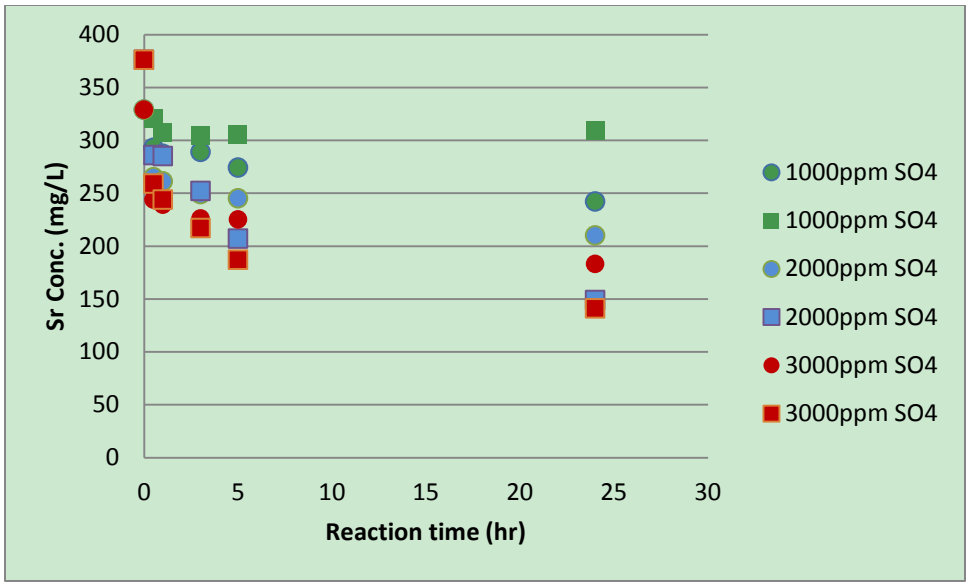

Figure 26. Dissolved strontium concentration profiles for different sulfate additions to synthetic and actual flowback water.

The experiment using 2000 ppm of sulfate added as a solution (compard to the previous experiment where crystal sodium sulfate was used) was also repeated with the real Site A flowback water and the results are shown on Figure 27. According to the SEM-EDS analysis for the case of 2000 ppm sulfate in synthetic and actual water (Figure 28 and 29), slightly more cluster crystals were formed in the synthetic water. However, the composition of crystal was almost the same (an average 16% of Sr in the crystal in synthetic water and 16.6% in the actual water.

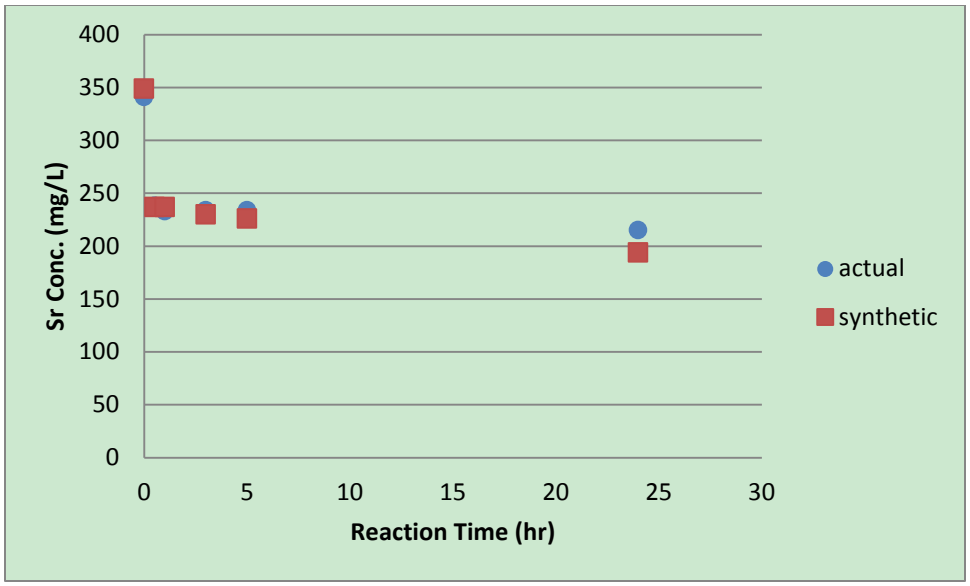

Figure 27. Dissolved strontium concentration profiles with 2000 ppm sulfate addition to synthetic and actual flowback water.

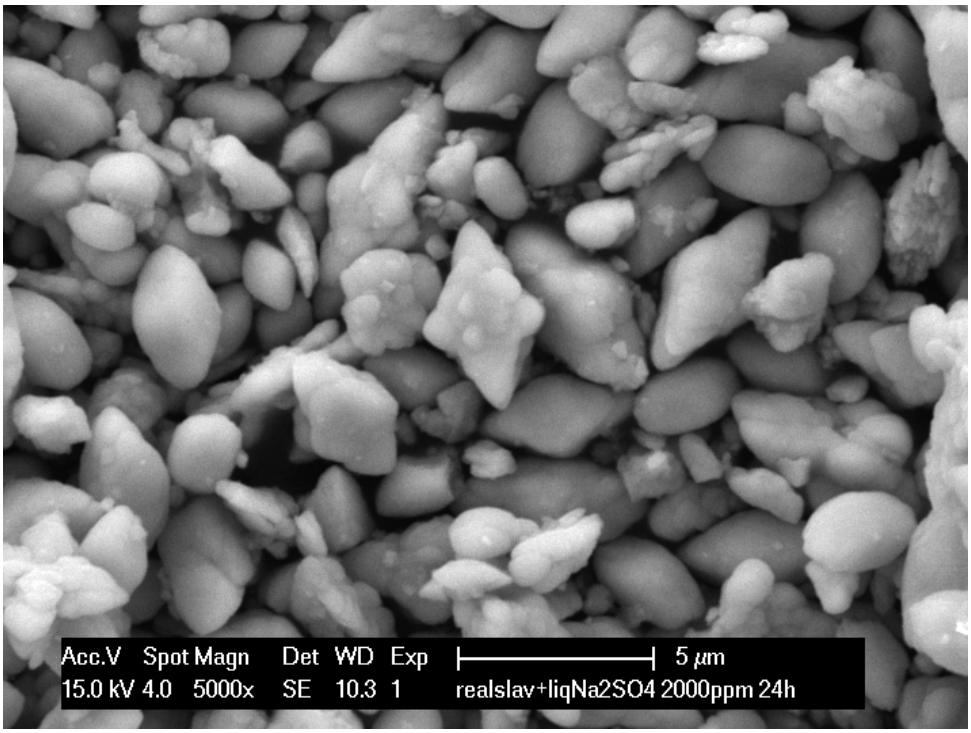

Figure 28. SEM picture of the deposit in actual Site A flowback water mixed with 2000 ppm of sulfate after 24 hours reaction.

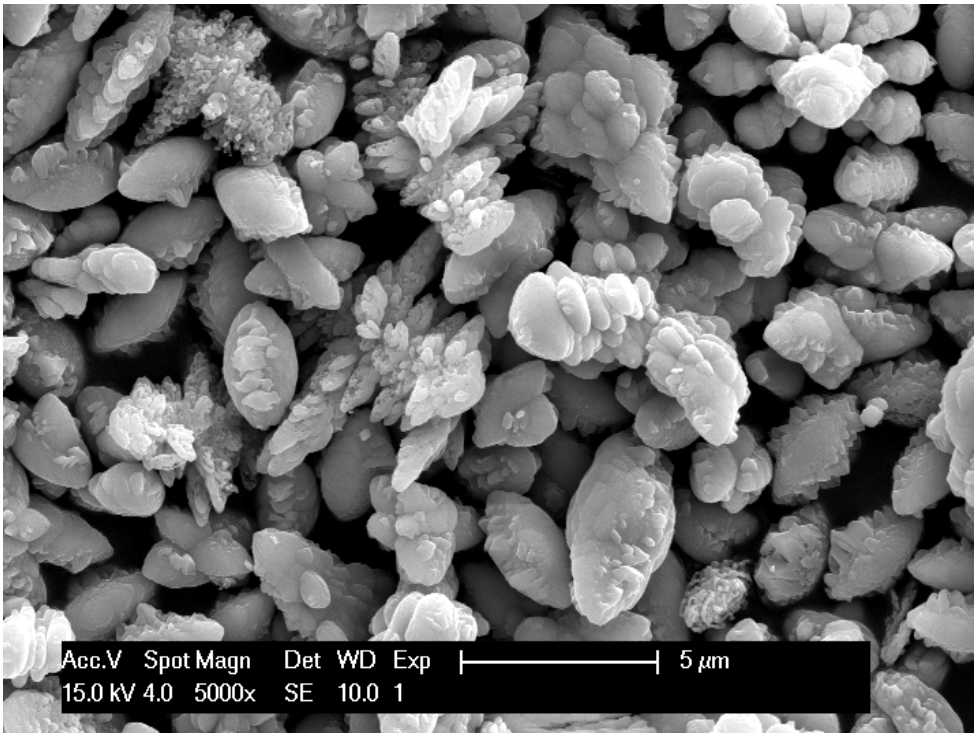

Figure 29. SEM picture of the deposit in synthetic Site A flowback water mixed with 2000 ppm of sulfate after 24 hours reaction.

When a solution of liquid sulfate is mixed with the flowback water, there is no significant difference in the strontium precipitation rate and extent between the actual and synthetic flowback waters. The reason for this is not clear so far.

The calculations based on the chemical equilibrium programs were then compared with the measurements (Figure 30). Although the results are similar to those in synthetic Site A flowback water case (Figure 16) where significant discrepancy was due to the fact that the equilibrium was not reached in 24 hours, it is clear that the discrepancy is even larger in actual flowback water. This further supports the hypothesis that unknown organics present in the actual flowback water further reduce the precipitation of Sr.

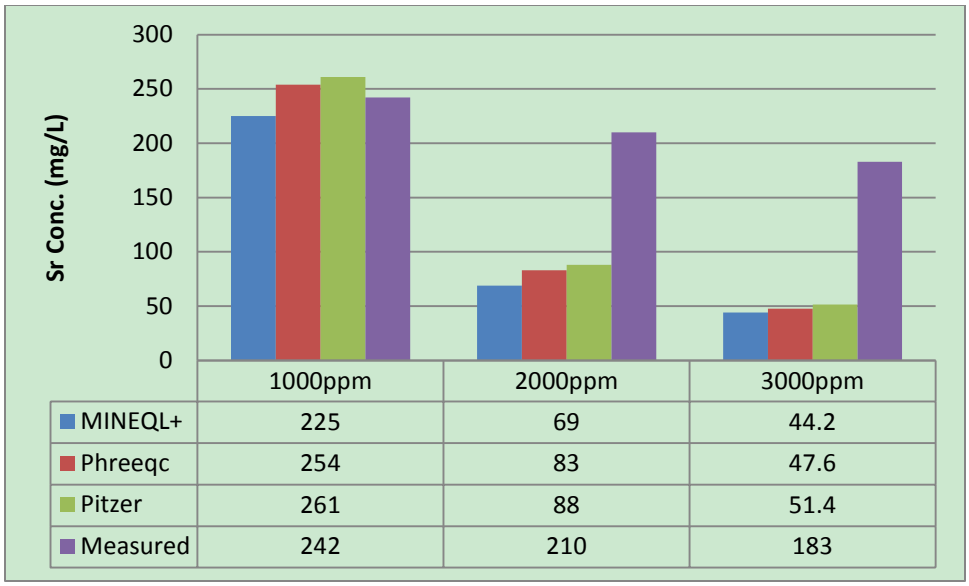

Figure 30. Comparison between equilibrium predictions and experimental results for strontium after 24 hours in actual Site A flowback water.

To verify the impact of organics on barite precipitation, experiments with actual Site A flowback water were conducted with lower sulfate dosage. The sulfate doses were 400 ppm and 600 ppm. Compared with Figure 9 and 10, barium was stabilized even faster in actual flowback water (about 1 hour in Figure 31 compared to 5 hours in Figure 9). Figure 32 showed that barite precipitation was less than predicted, which means the barite is more soluble when organics are present in the actual flowback water.

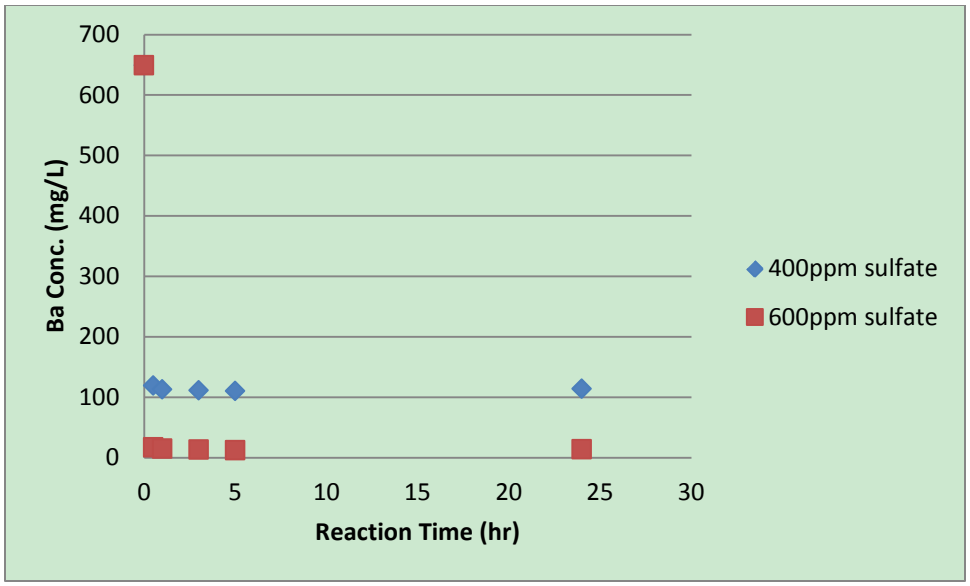

Figure 31. Dissolved barium concentration profiles for actual Site A flowback water with different sulfate concentrations.

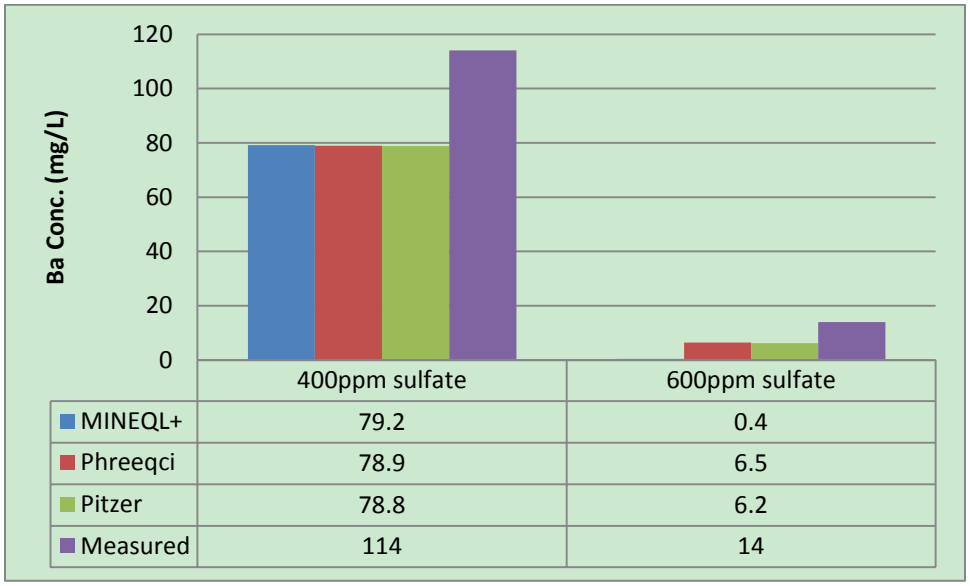

Figure 32. Comparison between equilibrium predictions and experimental results for barium after 24 hours in actual Site A flowback water.

In conclusion, organics present in the actual Site A flowback water have limited impact on the kinetics of barite and celestite precipitation. Compare with experimental results in actual

flowback water, it is clear that these organics have negative effect on barite solubility. This finding is in agreement with previous studies (Hennessy and Graham, 2002; Jones et al. 2008) with calcium and magnesium. They revealed that the organic inhibitor could promote addition of calcium into the barite lattice or on the surface of the crystal, which would elevate the internal energy of barite or celestite and make the structures unstable. The ultimate result is an increase in the solubility of target minerals. The predictions by all three equilibrium models showed a significant discrepancy with experimental results for both barite and celestite.

4.5 COMBINED USE OF SULFATE AND CARBONATE FOR THE REMOVAL OF TARGET CATIONS

Experimental results and equilibrium predictions in previous sections have shown that Ba^{2+} in solution is strongly affected by sulfate dose. However, Sr^{2+} can be only partially removed as celestite ($SrSO_4$) even with very high sulfate dose. In addition, removal of Ca^{2+} was below 0.1% (based on SEM-EDS analysis) under experimental conditions investigated earlier. To increase the removal of Sr and Ca or to decrease the use of sulfate for precipitating Ba and Sr (industry is concerned about high sulfate residual in the injection water), carbonate could be a fairly good precipitant for these target ions (K_{sp} of $BaCO_3$ is 2.74×10^{-9}, K_{sp} of $SrCO_3$ is 5.36×10^{-10}, K_{sp} of $CaCO_3$ is 3.93×10^{-9}, 25°C). Solubility of strontium carbonate is 2 orders of magnitude lower than strontium sulfate, while the calcium carbonate is 4 orders of magnitude less soluble than calcium sulfate. However, introducing a new reacting ion into the matrix could create numerous species and reactions, which can make the situation even more complex than previous task. The purpose of this task was to explore and evaluate the influence of combined sulfate and carbonate on the

removal of target ions in synthetic and actual flowback water. Equilibrium calculations based on different models were also performed to help interpret the experimental results. It should be clear that calculations based on the Pitzer equations still lacks many thermodynamic data and relevant parameters which could lead to significant discrepancies. Even though some essential data have been correctly incorporated into the model, the inconstancies of data based on different sources may make the results uncertain. However, this model is still under use for its great advantage in complex brines with high ionic strength. In this task, only one type of flowback water, namely Site A flowback water was evaluated.

4.5.1 Removal of target cations in synthetic flowback water at pH 6

The purpose of this task was to evaluate the efficiency of bicarbonate combined with sulfate to remove Ba, Sr and Ca under different HCO_3 dosages (2500 mg/L, 3500 mg/L, and 4500 mg/L). To be able to study the impact of bicarbonate on barium precipitation, low sulfate dosage (400 ppm sulfate as liquid form) was selected to allow part of Ba^{2+} to stay in solution. A series of samples was collected after 1 hour, 3 hour, 5 hour and 24 hour and analyzed for key constituents.

The pH was measured each time after filtration and the results revealed that the pH decreases with time and stabilizes around 6.1, which is close to the value predicted by the equilibrium model (Figure 33). Ba, Sr and Ca removal results with time can be seen in Figure 34, 35 and 36.

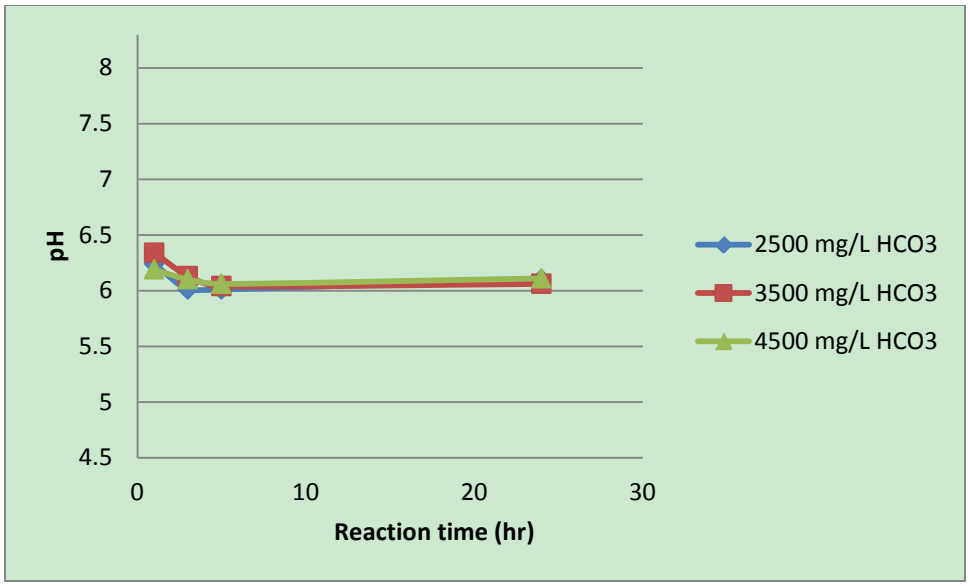

Figure 33. pH of synthetic Site A flowback water with 400 mg/L SO_4 and varying doses of bicarbonate.

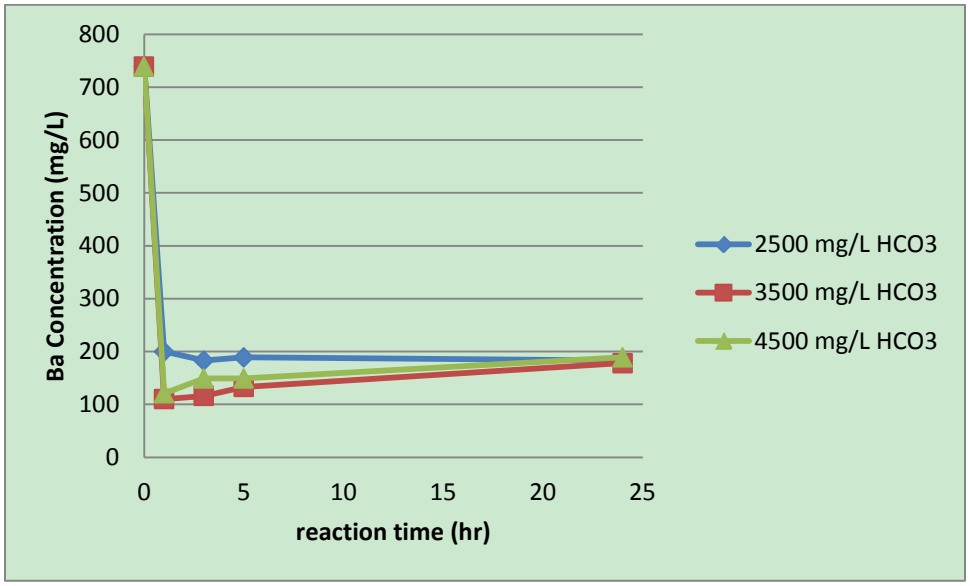

Figure 34. Ba concentration profiles for different bicarbonate doses [synthetic Site A flowback water, 400 mg/L SO_4].

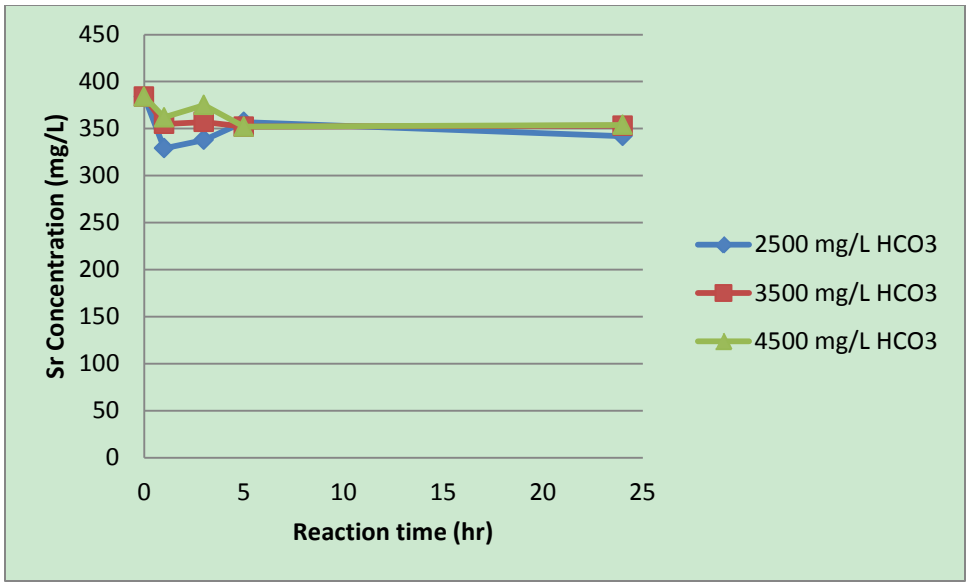

Figure 35. Sr concentration profiles for different bicarbonate doses [synthetic Site A flowback water, 400 mg/L SO_4].

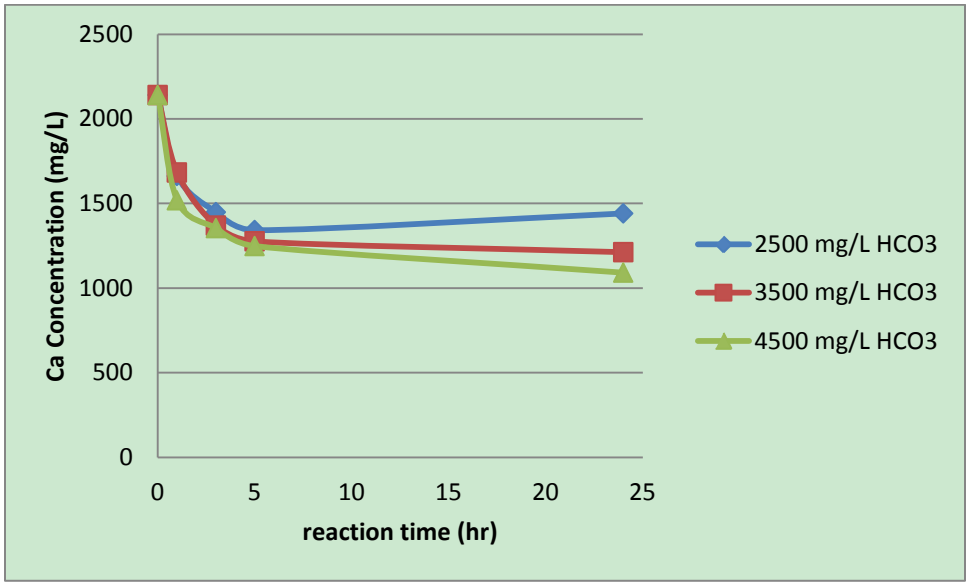

Figure 36. Ca concentration profiles for different bicarbonate doses [synthetic Site A flowback water, 400 mg/L SO_4].

The barium residual concentration profiles are slightly affected by the presence of high concentrations of bicarbonate (Figure 34). The Ba concentration decreases after 1 hour for

bicarbonate concentration greater than 3000 mg/L and then increases with time. The solubility product of witherite ($BaCO_3$) is higher than the one for calcite ($CaCO_3$). If the solubility product only is considered, $BaCO_3$ should precipitate faster than $CaCO_3$. However, the supersaturation values with respect to $BaCO_3$ and $CaCO_3$ also have an impact on the precipitation kinetic. Supersaturation with respect to $CaCO_3$ is 10 times higher than supersaturation with respect to $BaCO_3$ (α_{Ca2+} = 0.01402 and α_{Ba2+} = 0.001148). It is possible that barium was precipitated as carbonate at first and then was substituted by calcium ions through some exchange process.

Experimental results after the 24-hour run were compared with predictions (Figure 37) using Davies equation (MINEQL+) and Pitzer equation (Phreeqci). Both models give identical results and do not predict any $BaCO_3$ precipitation for the bicarbonate concentrations tested. The discrepancies between the calculated and measured value can be as high as 12.5%. This may result from the co-precipitation of Ba with $CaCO_3$, which cannot be predicted by the equilibrium models. A partitioning coefficient k can be used to relate the ratio of a trace element (here Ba^{2+}) in a solid phase (here $CaCO_3$) to the ratio of Ba^{2+} and Ca^{2+} in the liquid phase:

$$\frac{X_{BaCO3}}{X_{CaCO3}} = k\frac{[Ba^{2+}]_f}{[Ca^{2+}]_f}$$

Where, X_{BaCO3} and X_{CaCO3} are molar ratios of Ba and Ca, respectively, in the solid phase, and $[Ba^{2+}]_f$ and $[Ca^{2+}]_f$ are the concentrations of ions in solution at equilibrium.

Figure 37. Barium residual concentration at equilibrium for different bicarbonate doses [synthetic Site A flowback water, 400 mg/L SO_4].

Pingitore and Eastman (1984) measured experimental partitioning coefficient k of Ba into calcite and found an average value of 0.06 ± 0.01. Depending on the relative initial Ba and Ca concentrations in solution, the authors measured values ranging from 0.038 to 0.118. The partitioning coefficient for Ba calculated for the experiment with 2500 mg/L HCO_3^- is equal to 0.3, which is much higher than that determined by Pingitore and Eastman. However, values up to 3 were measured by Kitano et al. (1971), who demonstrated that k is highly affected by agitation speed, presence of magnesium in the solution and crystalline form of the calcium carbonate (calcite or aragonite).

The Strontium residual concentration profiles with time do not show significant effect of the presence of bicarbonate (Figure 35). However, equilibrium calculations predict that in the case of 4500 ppm bicarbonate, there should some strontianite ($SrCO_3$) precipitation, which did not occur in this experiment (Figure 38) because strontianite precipitation in generally inhibited at low pH because of low carbonate concentration in solution.

	2500-400	3500-400	4500-400
MINEQL+	384	384	358
Phreeqc	384	383	304
Pitzer	384	363	285
Measurement	357	353	354

Figure 38. Strontium residual concentration at equilibrium for different bicarbonate doses [synthetic Site A flowback water, 400 mg/L SO4].

The results for calcium are profiled on Figure 36 show that Ca removal depends on the concentration of bicarbonate ion in solution. Similar predictions are obtained from MINEQL+ and Phreeqci (Figure 39).

	2500-400	3500-400	4500-400
MINEQL+	1623	1279	1018
Phreeqc	1418	1067	821
Pitzer	1451	1106	853
Measurement	1441	1212	1091

Figure 39. Calcium residual concentration at equilibrium for different bicarbonate doses [synthetic Site A flowback water, 400 mg/L SO_4].

The predicted concentrations gradually deviate from the experimental results when the bicarbonate concentration increases. Since the sodium bicarbonate needs relatively long time to dissolve, there may be a competition between the sodium bicarbonate dissolution and the calcium carbonate precipitation. If calcium carbonate precipitates on sodium bicarbonate crystals, the amount of bicarbonate available for Ca precipitation is reduced. Another possible reason is the co-precipitation of Ba or other cations with Ca, which would increase the crystal solubility.

The experimental results revealed that HCO_3 was not an effective precipitant for Sr and Ca removal with no pH adjustment. The Sr could not be removed even with very high of HCO_3 (4500 mg/L). By comparing the measurements with calculations, the discrepancies mainly existed in Ba and Ca concentrations. The deviation for barium prediction was 6.0%~12.5% while it was 1%~28% for calcium. Co-precipitation, slow dissolution of $NaHCO_3$, slow precipitation and missing ion interaction parameters for $BaCO_3$ and $SrCO_3$ are possibilities to explain the discrepancy between measured and predicted results.

4.5.2 Removal of target cations in synthetic flowback water at pH 8

Previous series of experimental results revealed that bicarbonate (HCO_3^-) alone without pH adjustment was not an effective precipitant for Sr and Ca removal. The Ca residual in the solution still remained at fairly high levels after mixing with high bicarbonate dose: only half of the Ca was removed even with a molar ratio of HCO_3/Ca as high as 1.33. In addition, strontium and barium carbonate did not precipitate at low pH (around 6.1). Since the carbonate precipitation is very sensitive to pH (it controls the composition of carbonate in solution), a straightforward method to increase the removal is to utilize carbonate (CO_3^{2-}) instead of bicarbonate (HCO_3^-) as precipitant by maintaining the pH at a higher levels.

Experiments were conducted to investigate the removal of target cations when utilizing a mixture of sulfate and carbonate as precipitants at higher pH. By this way, the pH of the solutions could be greatly increased. The sulfate dose was 400 mg/L for all runs. At this dosage, barium cannot be completely removed so that the influence of carbonate on barium precipitation can be examined. The experimental results are compared with the predictions to evaluate the predictive capabilities of three different equilibrium models (MINEQL+, PhreeqcI, and Pitzer). Well site A was chosen and mixed with combined sulfate and carbonate to investigate the chemistry including kinetics and equilibrium.

A liquid Na_2SO_4 solution and Na_2CO_3 crystals were added to the synthetic flowback water. The initial pH increase is simply due to the addition of CO_3^{2-}. Samples were collected after 1, 3, 5, 24 hours to provide insight into the kinetics of chemical precipitation in the presence of both sulfate and carbonate.

Experimental results for synthetic water revealed that the pH increases with time because the carbonate added in a closed system and reaches equilibrium after 5 hours (Figure 40). The final pH depends on the carbonate dose: the higher carbonate dose, the higher the final pH. Compared to the HCO_3^- approach in previous progress report, the pH was increased by 2 units.

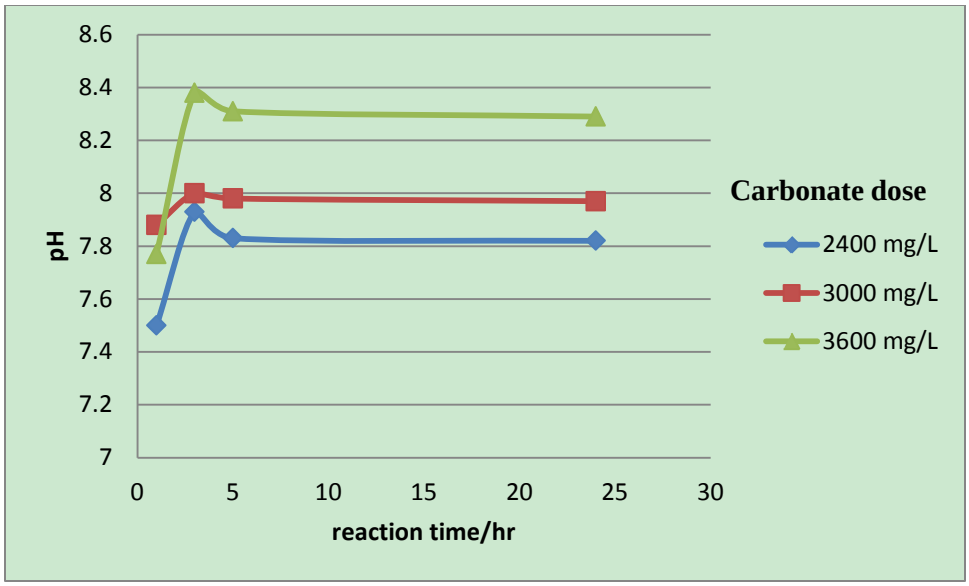

Figure 40. pH measurements with time in synthetic Site A Flowback water with 400 mg/L SO4 and different carbonate doses.

The experimental results for Ba under this condition showed a fast precipitation (profile not shown). Data after 24 hours are compared with equilibrium predictions using Davies equation (MINEQL+), "WATEQ" Debye Huckel equation (PhreeqcI database), and Pitzer equations (Pitzer database). The latter two models show no influence of CO3 on Ba (Figure 41). MINEQL+ shows that the precipitate of witherite is supposed to form with the carbonate dosage of 3600 mg/L. The Davies equation used by MINEQL+ works for an ionic strength (I) under 0.5 molal, while in this case, I = 0.82 molal. Higher ionic strength limits the metallic ions precipitation (shown by PhreeqcI and Pitzer models).

However, the experimental data demonstrate that Ba residual concentration is affected by adding CO_3 in all three dosages and significant discrepancies exist in the Ba predictions (Figure 41). These predictions by the simulation programs here were based upon pure solid calculation, which seldom happens in multi-electrolytes system. Numerous studies have demonstrated that Ba, Sr and Ca could be incorporated together during carbonate precipitation. Considering the

$CaCO_3$ lattice and the ionic radii of the metals in solution, the orthorhombic aragonite can uptake significant amounts of Ba and Sr from the solution. The co-precipitation or solid solution can be calculated through the use of partitioning coefficient but this specific parameter is not constant and depends on several factors, such as initial Ba/Ca ratio, Mg presence, temperature and mixing. Another possible reason for this discrepancy may be the result of inaccurate pH measurement. In concentrated brines, the reading from the pH meter can be lowered.

Figure 41. Barium residual concentration at equilibrium for different carbonate doses [synthetic Site A flowback water, 400 mg/L SO4, pH 8].

Sr precipitation needs more time to reach the equilibrium (profiles not shown). This is because the precipitation kinetic is driven by the supersaturation and the initial Sr concentration is relatively low. Strontium residual concentration comparison with predictions (Figure 42) revealed that carbonate concentration has an obvious positive impact on Sr precipitation. The discrepancy between measurements and predictions are probably due to co-precipitation effect, lack of Pitzer ion interaction parameters, and pH measurements.

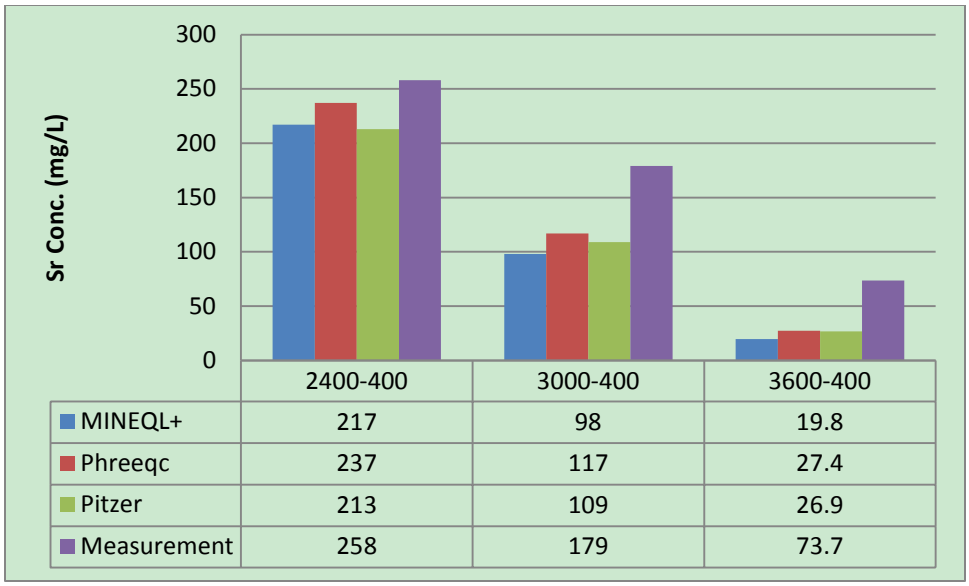

Figure 42. Strontium residual concentration at equilibrium for different carbonate doses [synthetic Site A flowback water, 400 mg/L SO4, pH 8].

Experimental results for Ca depicted on Figure 43 reflect the Ca removal depending on carbonate dosage and solution pH. Improved removal of Ca in comparison with the bicarbonate case is due to the increased solution pH (nearly 2 units). Similar predictions are obtained from these three models and there is a better agreement when using Pitzer model.

Figure 43. Cacium residual concentration at equilibrium for different carbonate doses [synthetic Site A flowback water, 400 mg/L SO4, pH 8].

Based on this part of study, it is clear that carbonate could greatly enhance the removal of all metal ions of interests. However, the discrepancies became even larger for barium and strontium predictions. Co-precipitation, initial experimental errors, and lack of Pitzer parameters for $BaCO_3$ and $SrCO_3$ are still suspect reasons for these differences.

4.5.3 Removal of target cations in synthetic flowback water at pH 10

To further investigate the removal of target ions by sulfate and carbonate, experiments similar to those described in section 4.5.2 were carried out but pH was initially increased to 10 with NaOH. Samples were collected after 1, 3, 5, 24, and 48 hours to provide insight into the kinetics of chemical precipitation in the presence of both sulfate and carbonate.

The pH was recorded each time after sample filtration. Figure 44 indicates that the solution pH remained relatively stable in the first 5 hours and then slightly decreased.

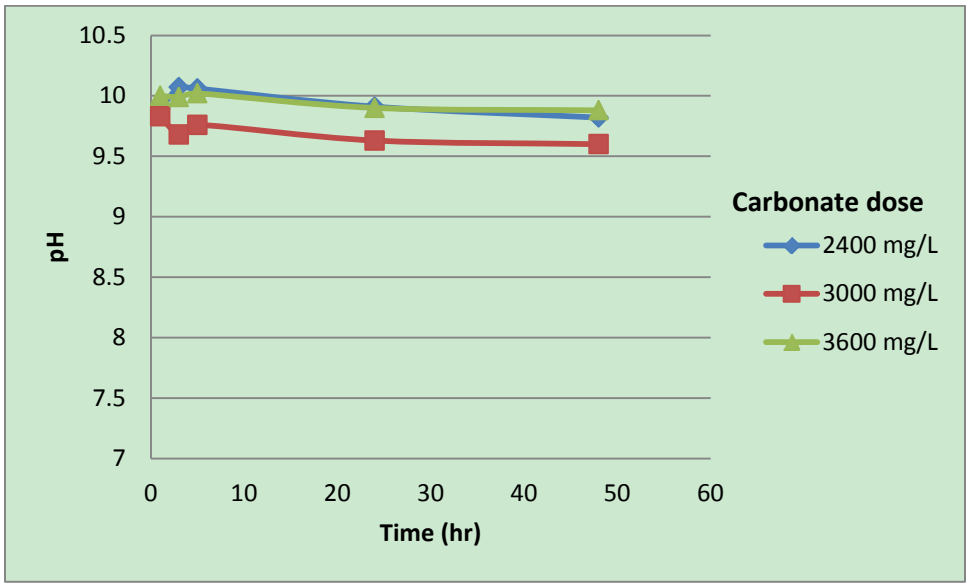

Figure 44. pH of synthetic Site A flowback water with 400 mg/L SO_4 and varying doses of carbonate.

Figure 45 reveals that Ba can be precipitated with carbonate as the increase in carbonate dose leads to a decrease in Ba concentration. The concentration of Ba decreased dramatically initially and then slowly increased with time. One possible reason for such behavior is that $BaCO_3$ (witherite, Table 20) is initially precipitated with relatively fast kinetics but that Ba is then slowly substituted with Ca because calcite had much higher supersaturation ratio than $BaCO_3$. The other possibility is the adsorption of Ba onto initial $CaCO_3$ precipitate with slow release as the crystals of $CaCO_3$ begin to solidity.

Table 20. Solubility Product of Target Chemicals

	Barite	**Witherite**	**Calcite**	**Aragonite**	**Strontianite**
Log K_{sp}	-9.97	-8.562	-8.480	-8.336	-9.271

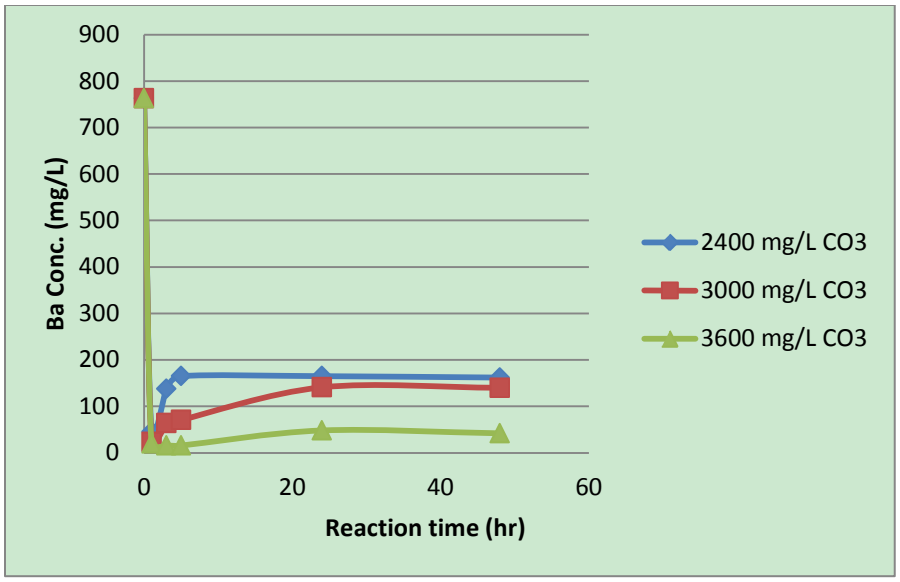

Figure 45. Ba concentration profiles for various CO_3 concentrations [synthetic Site A flowback water, 400 mg/L SO4, pH 10].

The experimental results after 48-hour were compared with predictions (Figure 46) using Davies equation (MINEQL+), and extended Debye Huckel equation and Pitzer equations (PhreeqcI). The equilibrium predictions indicate that Ba should not precipitate even when 3000 ppm of carbonate is added to this solution. However, the measurements show that, Ba concentration in solution decreases with an increase in carbonate dose. One hypothesis is the Ba is adsorbed on or incorporated into the calcite because evidence on some literatures (Dietzel et al., 2004; Terakado and Taniguchi, 2006) showed that with the help of Mg present, the calcite will convert into aragonite which has higher tendency to accommodate Ba in its lattice. However, further analysis on the crystals collected from the membrane filters (Figure 47) shows that there is no aragonite formed in the solution (all formed $CaCO_3$ are calcite).

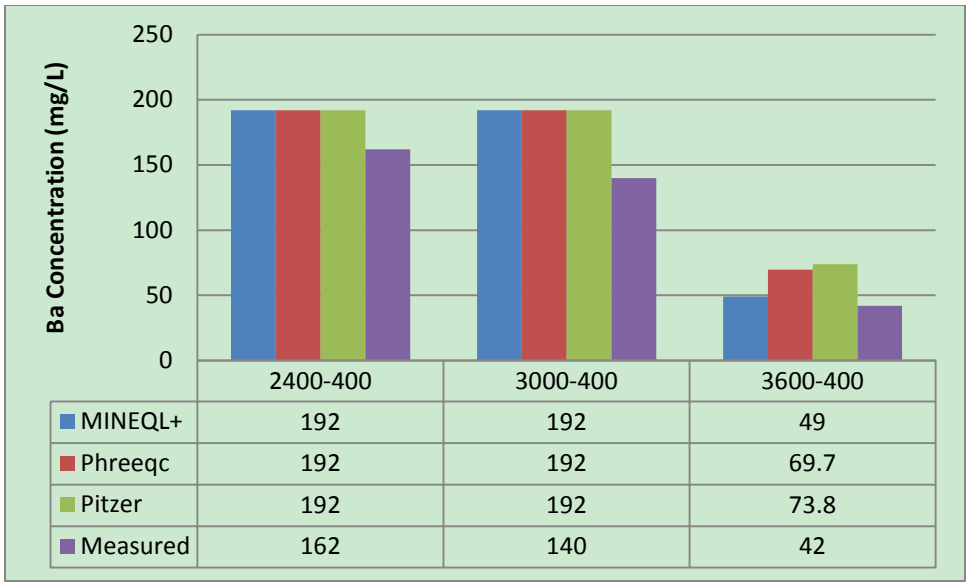

Figure 46. Measured and predicted Ba residual concentration at equilibrium for different carbonate doses [synthetic Site A flowback water, 400 mg/L SO_4, pH 10].

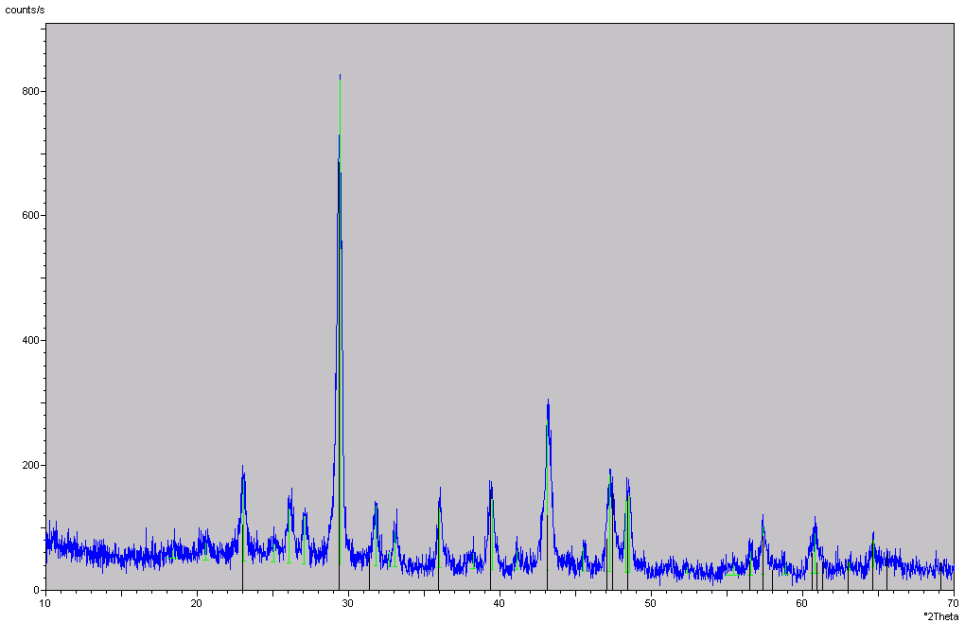

Figure 47. XRD analysis on the crystals collected from synthetic Site A flowback water mixed with 2400 mg/L of carbonate and 400 mg/L of sulfate at pH 10 after 1 hour reaction.

Another hypothesis is that after firstly adding caustic (NaOH) into the solution, the brucite ($Mg(OH)_2$) is formed. Its milk-like appearance as flocs makes it easily accommodate Ba into its structure. The EDS detects a mix of Ca, Sr, Mg, Ba, S, and O in all the analyzed crystals and Mg takes a significant percentage (about 13% in average after 1 hour). This formation can further explain the phenomenon that the Ba concentration decreased dramatically and then increase with time because Ba may be released from brucite by vigorously agitating.

The discrepancies between calculations and experimental measurements are even greater for strontium. Similar to behavior of Ba, Sr also experiences significant initial removal in solution with a slow increase in dissolved concentration (Figure 48). The difference between equilibrium prediction and experimental measurement ranges from 48 to 1400% (Figure 49). Once again, co-precipitation of Sr with $CaCO_3$ instead of pure $SrCO_3$ and the formation of brucite might be the reasons for this discrepancy.

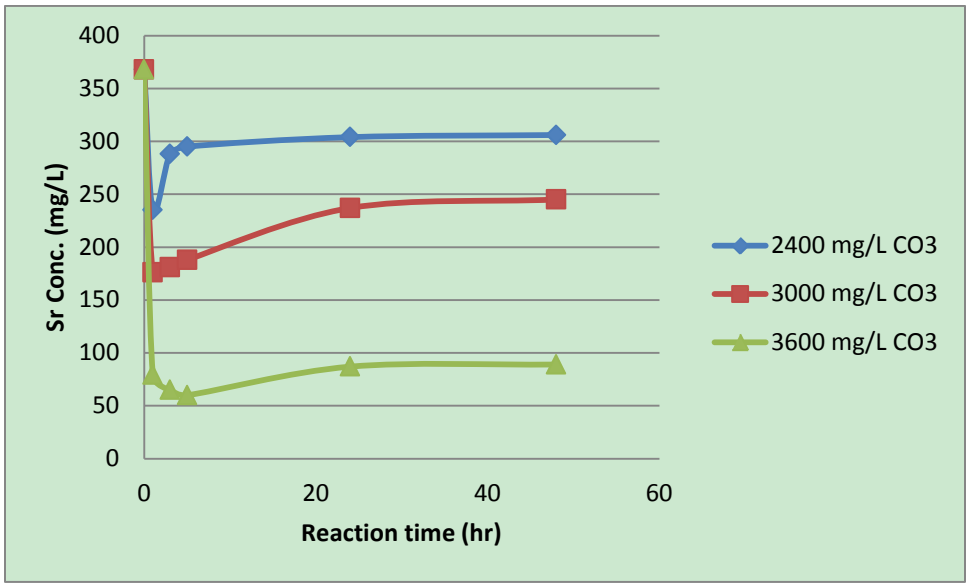

Figure 48. Sr concentration profiles for various CO_3 concentrations [synthetic Site A flowback water, 400 mg/L SO_4, pH 10].

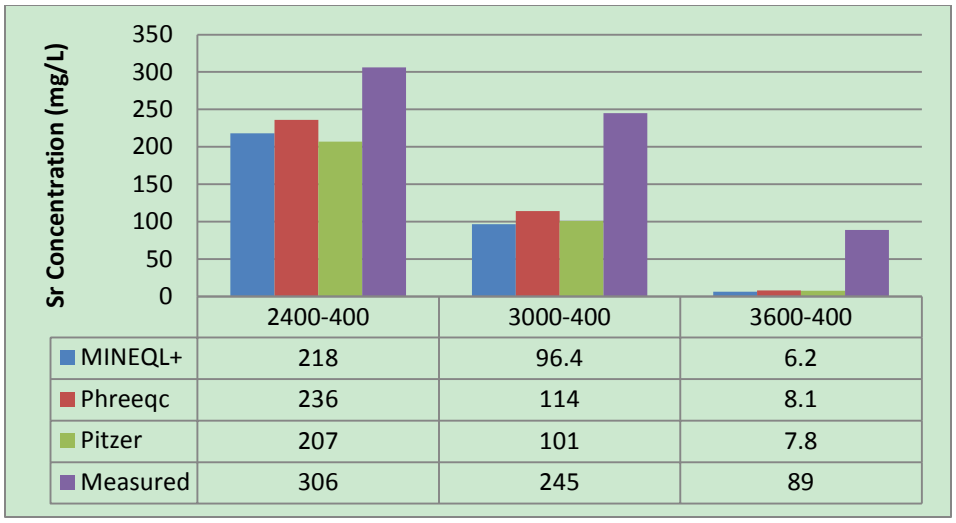

Figure 49. Measured and predicted Sr residual concentration at equilibrium for different carbonate doses [synthetic Site A flowback water, 400 mg/L SO_4, pH 10].

Calcium profiles on Figure 50 show that it can be easily removed by carbonate precipitation at pH around 10. Ca concentration reaches equilibrium after 3 hours and remains stable for the duration of the experiment. Comparison of measured and predicted Ca concentration shown on Figure 51 reveals reasonable agreement between theory and experiments.

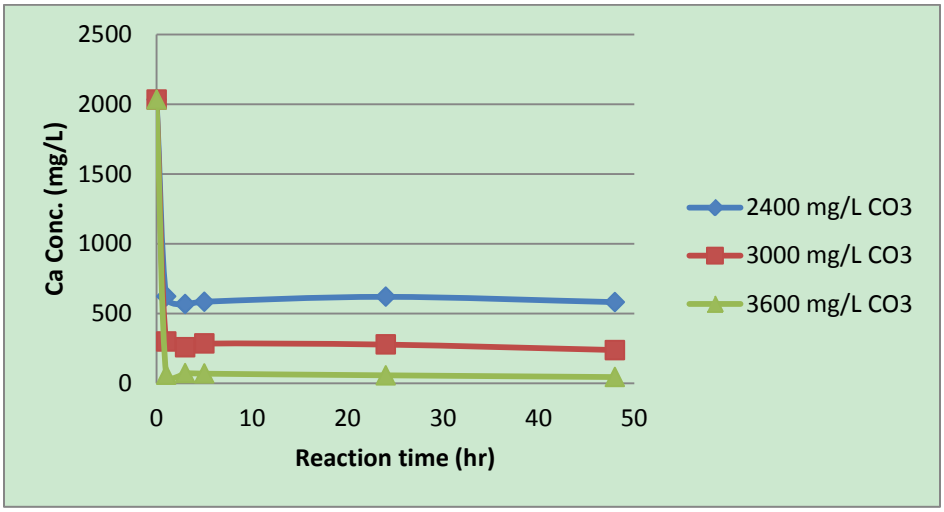

Figure 50. Ca concentration profiles for various CO_3 concentrations [synthetic Site A flowback water, 400 mg/L SO_4, pH 10].

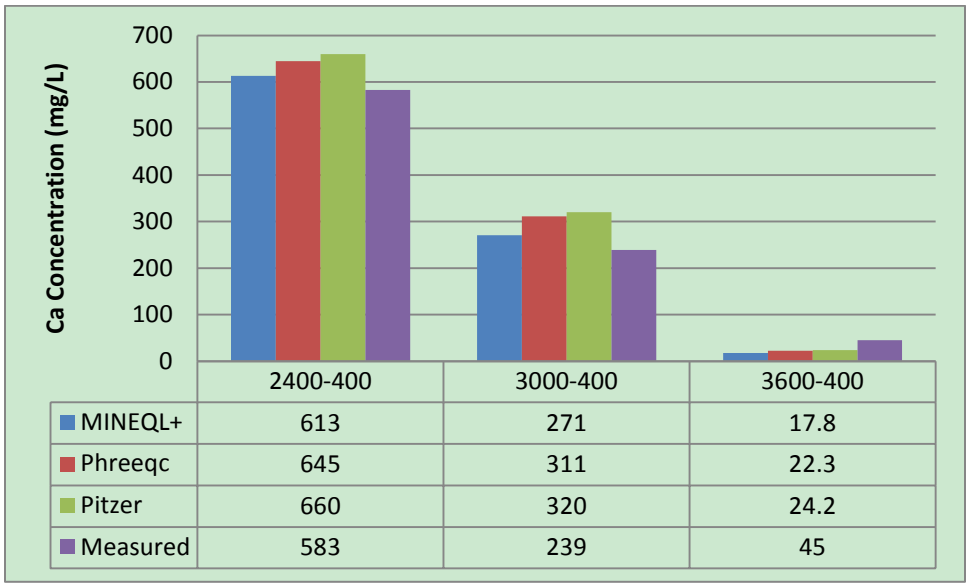

Figure 51. Measured and predicted Ca residual concentration at equilibrium for different carbonate doses [synthetic Site A flowback water, 400 mg/L SO_4, pH 10].

It has been shown in the literature that strontium coprecipitated in barite but that it could be ejected from the crystal during continuous and vigorous agitation (Gordon et al. 1954). It is possible that similar phenomenon can occur with Sr and Ba incorporated in the calcium carbonate. To verify this hypothesis, an experiment involving synthetic Site A flowback water with 400 mg/L SO_4^{2-} and 3000 mg/L CO_3^{2-} was conducted at pH 10 with 1 hour stirring followed by no stirring.

Compared with Figure 45 and 48, the profile of Ba in this experiment (Figure 52) reveals that Ba is still released into the solution but at a much lower rate; Ba concentration after 24 hours was only 86 mg/L compared to 141 mg/L on Figure 45. A chemical process by which Ba redissolves in solution is accelerated by mechanical action but not induced by it. Similar conclusion can be reached by comparing Sr profile in this experiment (Figure 53) with the one obtained with continuous mixing (Figure 48).

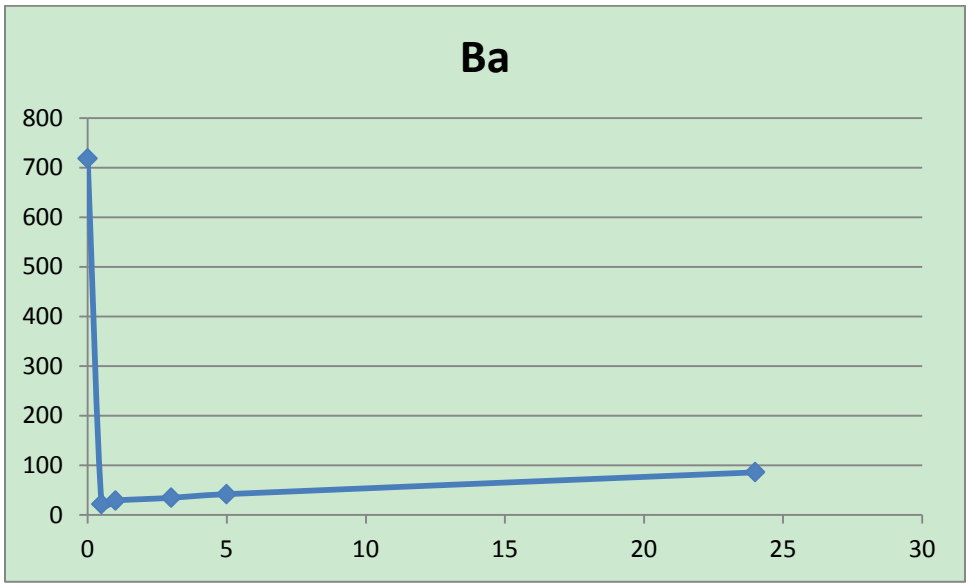

Figure 52. Ba concentration profiles in synthetic Site A flowback water with 400 mg/L SO_4 and 3000 mg/L CO_3.

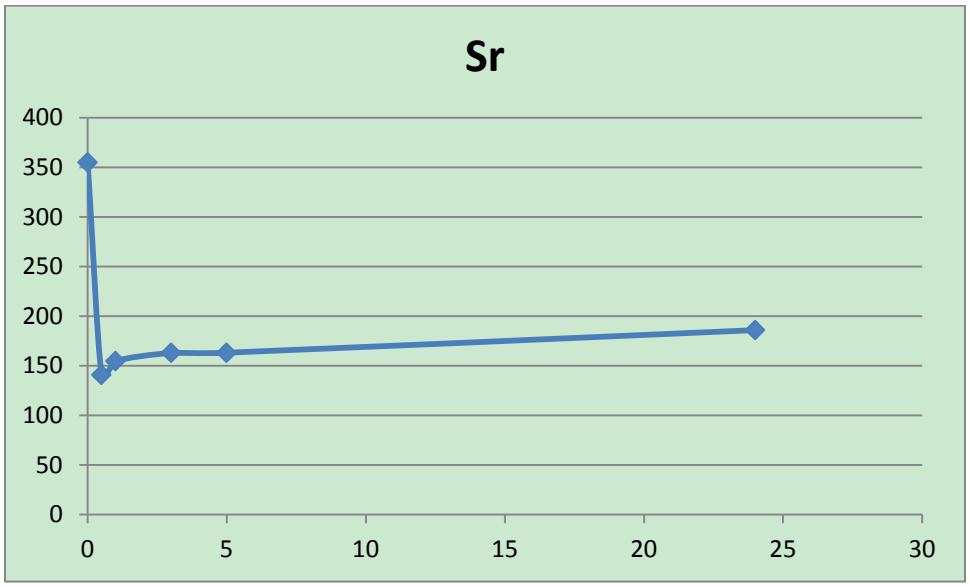

Figure 53. Sr concentration profiles in synthetic Site A flowback water with 400 mg/L SO_4 and 3000 mg/L CO_3.

Experimental results obtained for the bicarbonate and carbonate addition to the flowback water are summarized in Table 21. The addition of carbonate instead of bicarbonate and the resulting pH increase greatly improved the removal of Ba, Sr, and Ca. Further pH increase from 8 to 10 improves the removal of Ca by only 5-6%. The addition of carbonate enables the precipitation of barium and strontium and the removal efficiency increases with carbonate dosage. However, an increase in pH seems to have a negative impact on barium and particularly strontium precipitation. For 2400 ppm CO_3, the strontium precipitated at pH 10 is half of the amount precipitated at pH 8. This is because calcium is more sensitive to pH change than that of strontium. Thus more calcium removed makes the carbonate less available to precipitate strontium. Thereby, pH increase might not be necessary if only calcium, barium and strontium removal is at stake.

Table 21. Summary of experimental results obtained for bicarbonate and carbonate addition.

Doses	Ba removal	Sr removal	Ca removal	pH
2500ppm HCO3 + 400ppm SO4	75.2%	10.9%	32.7%	~6
3500ppm HCO3 + 400ppm SO4	75.9%	8.1%	43.4%	
4500ppm HCO3 + 400ppm SO4	74.4%	7.8%	49.0%	
2400ppm CO3 +400ppm SO4	82.0%	34.0%	68.1%	~8
3000ppm CO3 +400ppm SO4	90.3%	54.2%	82.1%	
3600ppm CO3 +400ppm SO4	93.9%	81.2%	93.0%	
2400ppm CO3 +400ppm SO4*	78.8%	16.8%	72.8%	~10
3000ppm CO3 +400ppm SO4*	81.7%	33.4%	88.9%	
3600ppm CO3 +400ppm SO4*	94.5%	75.8%	97.9%	

The three equilibrium models tested in this study failed to predict Ba and Sr equilibrium when carbonate is added. This is due to side reactions that include co-precipitation and adsorption. The prediction for Ca is fairly good when Pitzer model is utilized. Simultaneous precipitation of calcium, strontium and barium as sulfates and carbonates requires adding more parameters in Pitzer equation (e.g. for Ba^{2+}-Sr^{2+}-CO_3^{2-}) to accurately calculate concentrations at

equilibrium. In addition, operating conditions such as agitation may have a great impact on co-precipitation and is needed to be further examined.

4.5.4 Removal of target cations in actual flowback water at pH 6

This part of work focused on evaluating the impact of complexity of real flowback water on experimental and theoretical results. Actual flowback water not only contains a variety of inorganics, but also involves includes organic materials from either the rock formation or chemicals injected during hydraulic fracturing, which may impact precipitation kinetics, concentrations at equilibrium, crystal size and morphology. Therefore, the second set of experiments was performed on the actual Site A flowback water. The experimental method was the same as described previously. However, the differences in the initial ion concentrations between the synthetic and actual flowback water (Table 22) required new calculations of the equilibrium conditions.

Table 22. Analyses of major ions in the Site A flowback water.

Analyte	Synthetic water (mg/L)	Real Flowback water (mg/L)
Na	15385	
Ca	2224	1847
Mg	220	
Ba	781	656
Sr	367	348
Cl	29000	

The pH was measured each time after filtration. The experimental results with actual water revealed that the pH decreased with time and stabilized around 6.3 (Figure 54). This value is slightly higher than that in the synthetic water.

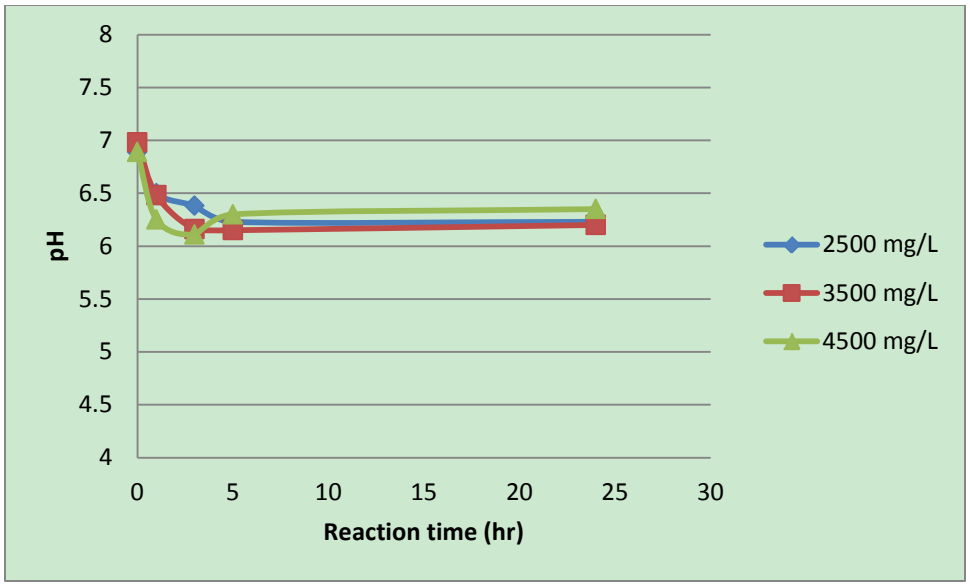

Figure 54. pH of actual Site A flowback water with 400 ppm SO4 and varing doses of bicarbonate.

Barium residual concentration profiles did not show any impact of bicarbonate even at a dosage as high as 4500 ppm (Figure 55). Experimental results after 24-hour run were compared with equilibrium predictions (Figure 56) using Davies equation (MINEQL+), "WATEQ" Debye-Hückel equation and Pitzer equation (PhreeqcI). Contrary to the data obtained with synthetic solution (Figure 37), measured Ba concentration in actual flowback water was lower compared to equilibrium predictions. Also, the discrepancies of Ba predictions are slightly lower compared with the synthetic flowback water.

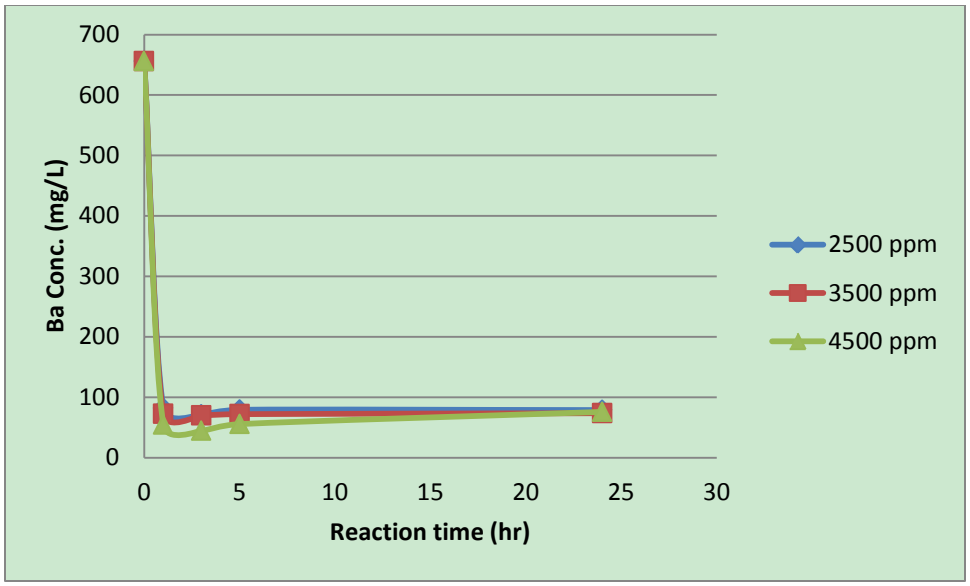

Figure 55. Barium residual profiles for different bicarbonate doses in actual Site A flowback water with 400 ppm SO_4.

	2500-400	3500-400	4500-400
MINEQL+	85.9	85.9	85.9
Phreeqc	84.6	84.6	84.6
Pitzer	84.6	84.6	84.6
Measurement	78.7	73.5	75.7

Figure 56. Barium residual concentration at equilibrium for different bicarbonate doses in actual Site A flowback water with 400 ppm SO_4.

In the case of Sr, the experimental results (Figure 57) showed the Sr removal in actual flowback water was improved compared with the results in synthetic flowback water (Figure 58).

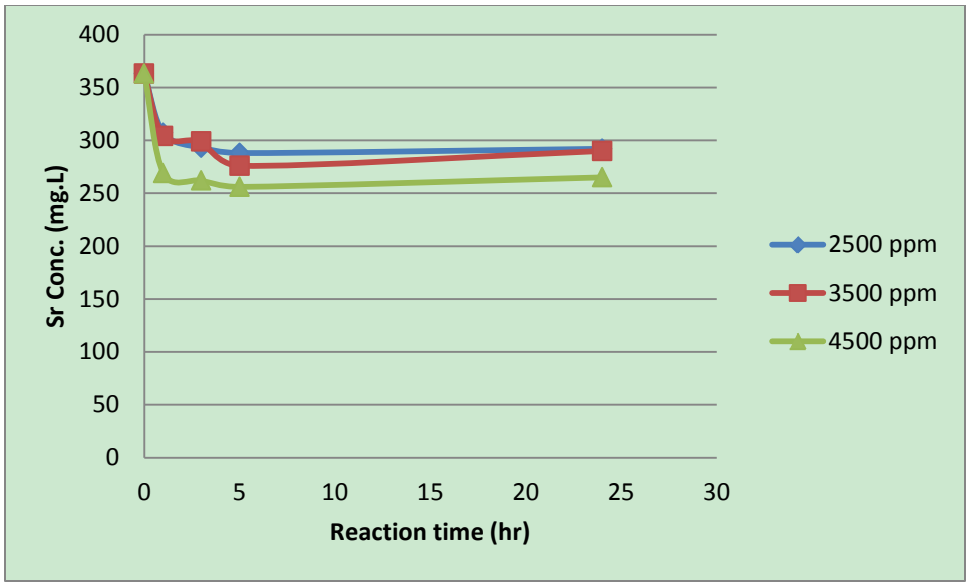

Figure 57. Strontium residual profiles for different bicarbonate doses in actual Site A flowback water with 400 ppm SO_4.

Such behavior can be explained by higher pH of the actual flowback water, which greatly impacts strontium carbonate precipitation. Compared with the data obtained in synthetic flowback water (Figure 38), Sr concentration measurements in actual flowback water also have better agreement with predictions by Pitzer model (Figure 59).

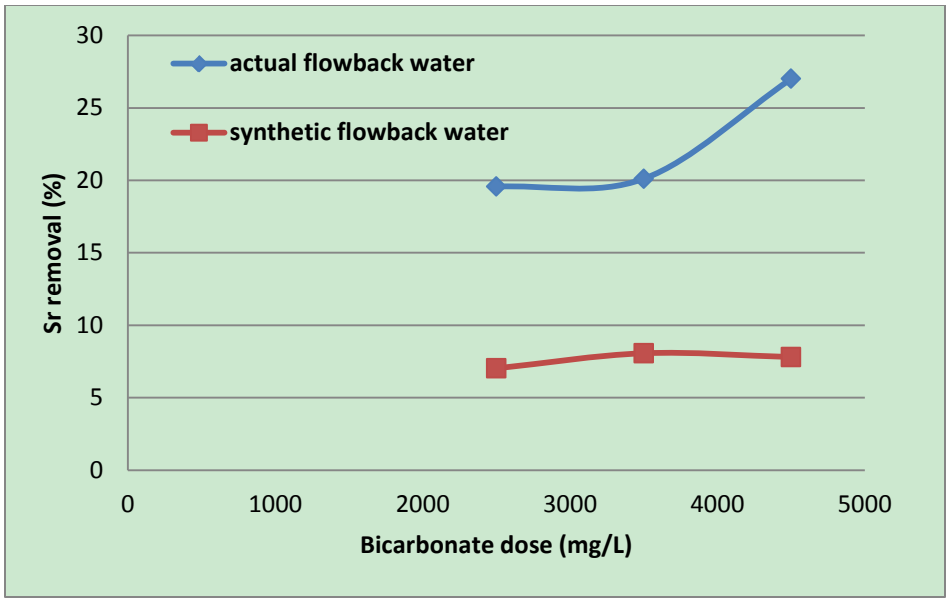

Figure 58. Variation of strontium removal through precipitation with bicarbonate in synthetic and actual Site A flowback waters.

	2500-400	3500-400	4500-400
MINEQL+	363	305	164
Phreeqc	348	347	270
Pitzer	348	323	254
Measurement	292	290	265

Figure 59. Strontium residual concentration at equilibrium for different bicarbonate doses in actual Site A flowback water with 400 ppm SO_4.

The calcium concentrations profiled on Figure 60 clearly show that the removal of Ca depends on the concentration of bicarbonate in the solution. Similarity with the data obtained in the synthetic flowback water (Figure 39), Ca predictions based on Pitzer equations shows better agreement with the measurements in actual flowback water (Figure 61) than the other two models.

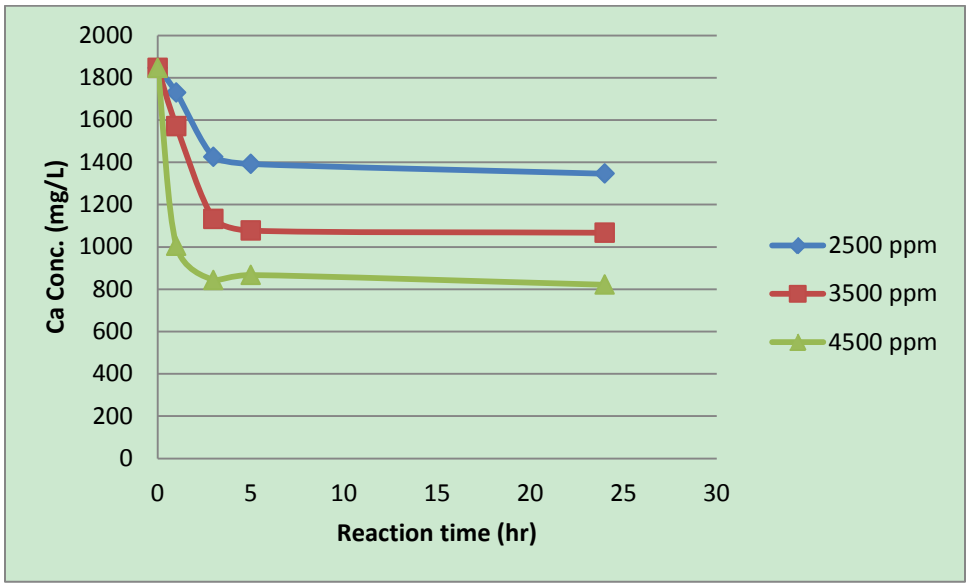

Figure 60. Strontium residual profiles for different bicarbonate doses in actual Site A flowback water with 400 ppm SO_4.

Figure 61. Strontium residual concentration at equilibrium for different bicarbonate doses in actual Site A flowback water with 400 ppm SO_4.

Contrary to strontium, similar percentage of calcium is removed either from the actual flowback water or from the synthetic flowback water (Figure 62). If the pH was the only factor, the higher pH in the actual flowback water would lead to an increase of calcium carbonate precipitation, which is not the case. It could be that the organic matter has a greater impact on calcium carbonate formation than on strontium carbonate. The organic matter effect offsets the pH effect on the calcium carbonate precipitation.

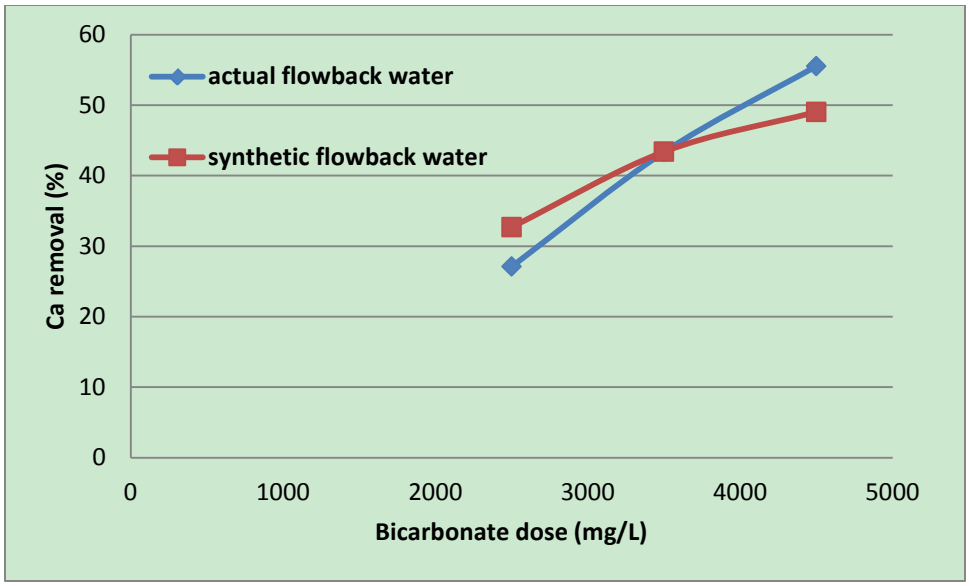

Figure 62. Variation of calcium removal through precipitation with bicarbonate in synthetic and actual Site A flowback waters.

5.0 SUMMARY AND CONCLUSIONS

Flowback water treatment is one of most challenging issues in Marcellus Shale gas production development. Preliminary studies showed that using Abandoned Mine Drainage (AMD) is a potential and sustainable way to solve this problem by introducing precipitating reagents (namely sulfate and carbonate) into the water body. It is thus interesting to investigate fundamental behavior of these mixtures.

This study focused on the use of sulfate and carbonate (caustic if necessary) to simulate the function of AMD water for reducing target ions (Ba, Sr, and Ca). Synthetic and actual flowback waters with a wide range of ionic strength (0.89 M ~ 3.41 M) were mixed with different precipitant doses and the results were compared with equilibrium models based on different equations and databases. The conclusions obtained in this study can be summarized as follows:

1. Many thermodynamic data and Pitzer parameters with respect to $BaSO_4$ do not exist in the original database of Pitzer model from PhreeqcI program, which made the calculations impossible. However, this problem has been successfully solved by adding the required reliable data from the literature.

2. Treatability studies with sulfate and synthetic flowback water showed that, strontium precipitation is a much slower process compared with barium precipitation. Degree of supersaturation has a positive impact on the precipitation kinetics while the salinity and present

of other divalent cations have negative impact. In addition, organics will increase the solubility of barite and celestite without significantly affecting the kinetics much.

3. Equilibrium calculations based on three different models have shown good agreement with experimental results for barium. Calculations based on the Pitzer model display a fairly good agreement with experimental data for strontium for a wide range of ionic strengths. Predictions based on Davis and WATEQ equations are only valid for low sulfate dose. The calculations based on MINEQL+ show a significant deviation when the removal of Sr exceeds 14%. The discrepancy between the measurements and calculations increases in the presence of organics due to numerous complexation reactions that are not accounted for in the models.

4. Sulfate is a very effective precipitating reagent for barium but fails to remove strontium and calcium. Results based on combined sulfate and carbonate experiments indicate that carbonate can be an excellent supplementary precipitation reagent for calcium and strontium removal and can reduce sulfate dose for barium removal (which means it can help sulfate control). Addition of carbonate without any pH adjustment (pH around 8) has shown even better performance for the removal of target ions than when the pH is increased to 10. For the mixtures of actual flowback water with combined precipitants, it is discovered that the removal of target ions is even better than that in synthetic flowback water at pH around 6.

5. The three models fail to predict barium and strontium equilibrium when carbonate is added. The prediction for calcium is fairly good when Pitzer model is utilized. One possible reason is that Pitzer model has not been fully parameterized for the system of Na-K-Ca-Mg-Ba-Sr-H-Cl-SO_4-OH-HCO_3-CO_3-CO_2-H_2O. The lack of parameters for Ba-Sr-HCO_3-CO_3 may account for such behavior. Another hypothesis for the discrepancies is the co-precipitation problem which needs to be investigated further.

6.0 FUTURE WORK

According to the results of this research, there are three issues that need to be investigated to achieve a better understanding of relevant chemistry and provide guidance for the practical work:

1. Pitzer model parameters for Ba-Sr-HCO_3-CO_3 should be collected from either literature or experimental results to augment PhreeqcI database for better model predictions.
2. According to Kolik, 2002, models based on law of mass-action could not predict solid solution well. Thus, for a better co-precipitation prediction, models based on Gibbs free energy minimization may be required.
3. For actual flowback water study, more data based on other higher ionic strength waters are required to better understand the behavior of precipitation kinetics and equilibria under relevant process conditions.

BIBLIOGRAPHY

Agilent Technologies, Inc., 2010. Flame Atomic Absorption Spectrometry Analytical Methods. Eighth Edition.

Ball JW, Nordstrom DK, 1991. User´s Manual for WATEQ4F -US Geological Survey Open-File Report pp 91-183

Bethke, C.M., 2008. Geochemical and Biogeochemical Reaction Modeling. Published by Cambridge University Press.

Burkin, A.R., 2001. Chemical hydrometallurgy: theory and principles. Imperial College, UK.

Blount,C.W., 1977. Barite Solubility and Thermodynamic Quantities Up to 300°C and 1400 bars. American Mineralogist, Volume 62, pages 942-957.

Bryant, J., Welton, T., Haggstrom, J., 2010. Will Flowback or Produced Water Do? Sand and Water Management.

Clegg, S., Whitefield, M., 1991. Activity Coefficients in Natural Waters. In: Pitzer, K. (Ed.), Activity Coefficients in Electrolyte Solutions, second ed. CRC, Boca Raton, FL, USA, pp. 279-434.

Church, T.M., and Wolgemuth, K., 1972. Marine barite saturation, Earth Planet. Sci. Lett., 15, 35-44.

Ciavatta, L., 1980. The specific interaction theory in the evaluating ionic equilibria. Ann. Chim. (Rome) 70: 551–562

Davies, CW, 1962. Ion Association, Butterwoths (London) pp 190.

Debye, P., Hückel, E., 1923. The theory of electrolytes. I. Lowering of freezing point and related phenomena. Phys.Z., 24, pp. 185-206.

de Witt, W., 1993. Principal Oil and Gas Plays in the Appalachian Basin (Province 131). U.S. Geological Survey Bulletin 1839-I, 37 p.

Dietzel, M., Gussone, N., Eisenhauer, A., 2004. Co-precipitation of Sr^{2+} and Ba^{2+} with aragonite by membrane diffusion of CO_2 between 10 and 50oC. Chemical Geology, 203, 139-151.

Economides, M.J., Watters, L.T. and Dunn-Norman, S., 1998. Petroleum Well Construction, John Wiley & Sons Ltd, West Sussex, England, 1998, p. 473.

Elizalde, M.P., Aparicio, J.L., 1995. Current theories in the calculation of activity coefficients—II. Specific interaction theories applied to some equilibria studies in solution chemistry [J]. Talanta Volume 42, Issue 3, Pages 395-400.

Engelder, T. and Lash, G., 2008. Unconventional Natural Gas Reservoir Could Boost U.S. Supply. Penn State Live.

Fan,C., Kan,A.T., Zhang, P., Tomson, M.B., 2010. Barite Nucleation and Inhibition at 0 to 200°C with and without Thermodynamic Hydrate Inhibitors. SPE Journal, 1-11.

Gildseth W, Habenschuss A, Spedding FH, 1972. Precision Measurements of Densities and Thermal Dilation of Water between 5 deg. and 80 deg., J. Chem. Eng. Data, 17 (4) 402-409.

Greenbergh, J.P., Moller, N., 1989. The Prediction of Mineral Solubilities in Natural Water: A Chemical equilibrium model for the Na-K-SO4-H2O system from zero to high concentrations at 25°C. geochim. Cosmochim. Acta 44, pp.981-997.

Güntelberg E., Untersuchungen über Ioneninteraktion, Phys. Chem., 123 (1926) 199-247.

Hamdona, S.K., and Hamza, S.M., 2009. Influence of polyphosphonates on the precipitation of strontium sulfate (Celestite) from aqueous solutions J. Taibah University for Science, 2, pp36-43

Harper, J.A., 2008. The Marcellus Shale - An Old "New" Gas Reservoir in Pennsylvania. Pennsylvania Geology, Volume 38, Number 1. Pennsylvania Bureau of Topographic and Geologic Survey.

Harvie, C.E., Moller, N., Weare, J.H. 1984. The Prediction of Mineral Solubilities in Natural Waters: the Na-K-Mg-Ca-H-Cl-SO4-OH-HCO3-CO3-CO2-H2O System to High Ionic Strength at 25^{o}C. Geochim. Cosmochim. Acta, 48, pp.723-751.

He, S., Oddo, J.E., Tomson, M.B., 1995. The Nucleation Kinetics of Barium Sulfate in NaCl Solutions up to 6 m and 90°C. Journal of Colloid and Interface Science 174, 319-326.

He, S., Oddo, J.E., Tomson, M.B., 1995. The Nucleation Kinetics of Strontium Sulfate in NaCl Solutions up to 6 m and 90°C with or without In hibitiors. Journal of Colloid and Interface Science 174, 327-335

Hennesy,A.J.B., Graham,G.M., 2002. The Effect of Additives on the Co-crystallisation of Calcium with Barium Sulfate. Journal of Crystal Growth 237-239 2153-2159.

Hill, D.G., Lombardi, T.E. and Martin, J.P., 2004. Fractured Shale Gas Potential in New York. Northeastern Geology And Environmental Sciences. Vol. 26. p. 8.

Holmes, H.F., Baes, C.F.B. Jr., Mesmer, R.E., 1987. The Enthalpy of Dilution of HCl(aq) to 648 K and 40 MPa: Thermodynamic Properties. J. Chem. Thermodyn. 19, pp.863-890.

Hückel E Zur, 1925. Theorie konzentrierterer wässeriger Lösungen starker Elektrolyte. Physikalische Zeitschrift, 26, 93-149.

Jones,F., Oliviera, A., Parkinson,G.M., Rohl, A.L., Stanley, A., Upson, T.,2004. The effect of calcium ions on the precipitation of barium sulfate 1: calcium ions in the absence of organic additives. Journal of crystal growth 262 572-580.

Jones, F., Piana, S., Gale, J.D., 2008. Understanding the Kinetics of Barium Sulfate Precipitation from water and water-methanol solutions. Crystal growth & Design vol.8, no.3, 817-822.

Kolik, D.A., 2002. Gibbs Energy Minimization Approach to Modeling Sorption Equilibria at the Mineral-Water Interface: Thermodynamic Relations for Multi-Site-Surface Complexation. American Journal of Science, Vol. 302, pp.227-279.

Kühn, M., Bartels, J., Pape, H., Schneider, W., Clauser, C., 2002. Modeling Chemical Brine-Rock Interaction in Geothermal Reservoirs.

Merkel,B.J., Planer-Friedrich, B., 2008. Groundwater Geochemistry: A Practical Guide to Modeling of Natural and Contaminated Aquatic Systems. 2nd Edition, Springer-Verlag Berlin Heidelberg.

Milleroa, F.J. Milne, P.J., Thurmond, V.L., 1984. The solubilitynext term of calcite, strontianite and witherite in NaCl solutions at 25°C. Geochimica et Cosmochimica Acta. Vol. 48, Issue 5, Pages 1141-1143

Milici, R.C.; Swezey, C.S., 2006. Assessment of Appalachian Basin Oil and Gas Resources: Devonian Shale–Middle and Upper Paleozoic Total Petroleum System. Open-File Report Series 2006-1237. United States Geological Survey.

Monnin, Chr. And Galinier, C., 1988. The Solubility of Celestite and Barite in Electrolyte Solutions and Natural Waters at 25°C: A Thermodynamic Study. Chem. Geol., 71: 283-296

Monnin, Chr., 1999. A Thermodynamic Model for the solubility of barite and celestite in electrolyte solutions and seawater to 200°C and to to 1 Kbar. Chemical Geology. 127, pp.141-159.

Nordstrom D.K., Plummer L.N., Langmuir D., Busenberg E., May H.M., Jones B.F., Parkhurst D.L., 1990. Revised chemical equilibrium data for major water-mineral reactions and their limitations.- In: Melchior DC, Bassett RL (eds), Chemical modeling of aqueous systems II. Columbus, OH, Am Chem Soc., pp.398-413.

O'Dowd, C., Lowe, J.A., Clegg, N., Smith, M., Clegg, S., 2000. Modeling Heterogeneous Sulphate Production in Maritime Stratiform Clouds. Journal of Geophysical Research, Vol. 105, No. D6, pp. 7143-7160.

Pabalan, R.T., and Pitzer, K. S., 1987a. Thermodynamics of concentrated electrolyte mixtures and the prediction of mineral solubilities to high temperatures for mixtures in the system Na-K-Mg-Cl-SO_4-OH-H_2O. Geochim. Cosmochim. Acta, 51, pp.2429-2443.

Parkhurst, D.L., Appelo, C.A.J., 1999. User's Guide To Phreeqc (Version 2) — A Computer Program For Speciation, Batch-Reaction, One-Dimensional Transport, And Inverse Geochemical Calculations. U.s. Geological Survey.

Pearson, F.J.Jr., Berner, U., 1991. Technical Report 91-17: Nagra Thermochemical Data Base I. Core Data. National Cooperative for the Disposal Radioactive Waste.

Pingitore, N.E. Jr., Eastman, M.P., 1974. The Experimental Partitioning of Ba2+ into Calcite. J. Chem. Geo., Vol. 45, Issues 1-2, pp113-120.

Pitzer K.S., 1973. Thermodynamics of electrolytes. I Theoretical basis and general equations, J. Phys. Chem., 77, 268-277.

Pitzer, K., and Mayorga G., 1973. Thermodynamics of electrolytes. II. Activity and Osmotic Coefficients for Strong Electrolytes with One or Both Ions Univalent. The Journal of physical Chemistry, Vol.77, No. 19.

Pitzer K.S., and Kim J., 1974. Thermodynamics of Electrolytes. IV. Activity and Osmosis Coefficients for Mixed Electrolytes. Phys. Chem.

Pitzer K.S., 1975. Thermodynamics of Electrolytes. V. Effects of Higher-Order Electrostatic Terms. Journal of Solution Chemistry, Vol. 4, No.3.

Pitzer, K., 1991 Activity Coefficients in Electrolyte Solutions, second ed. CRC, Boca Raton, FL, USA

Pletcher, J., 2008. "Drillers access mile-deep gas deposits in what may be new 'gold rush'." Herald Standard, May 19.

Plummer, L., Parkhurst, D., Fleming, G., Dunkle, S., 1988. A Computer Program Incorporating Pitzer's Equations for Calculation of Geochemical Reactions in Brines. U.S. Geological Survey, Reston, VA.

Prieto, M., 2009. Thermodynamics of Solid Solution-Aqueous Solution Systems. Mineralogy & Geochemistry, Vol. 70 pp. 47-85.

Risthaus, P., Bosbach, D., Becker, U., Putnis, A. 2001. Barite scale formation and dissolution at high ionic strength studied with atomic force microscopy. Colloids and Surface, 201-214

Reardon, E.J.; Armstrong, D.K. 1987. Celestite ($SrSO_4$(s)) Solubility in Water, Seawater and NaCl Solution. Geochimica et Cosmochimica Acta, Vol. 51, Issue 1, pp. 63-72.

Rogers, M., 2008. Marcellus Shale: What Local Government Officials Need to Know.

Sheikholeslami, R., Ong, H.W.K., 2003. Kinetics and thermodynamics of calcium carbonate and calcium sulfate at salinities up to 1.5 M. Desalination, 157, pp217-234.

Shen, D., Fu, G., AI-Saiari, H.A., Kan, A.T., Tomson, M.B., 2009. Barite Dissolution/Precipitation Kinetics in Porous Media and in the Presence and Absence of a Common Scale Inhibitor. September SPE Journal, 462-471.

Shen, D., Fu, G., H.A., Kan, Tomson, M.B., 2008. Seawater Injection, Inhibitor Transport, Rock-Brine Interactions, and BaSO4 Scale Control During Seawater Injection. SPE International Oilfield Scale Conference, 28-29 May 2008.

Smith, E., Hamilton-Taylor, J., William, D., Fullwood, N.J., McGrath, M. 2004. The effect of humic substances on barite precipitation-dissolution behaviour in natural and synthetic lake waters. Chemical Geology, 207 (1-2). pp. 81-89.

Smith, W.R., and Missen, R.W., 1982. Chemical reaction equilibrium analysis: Theory and algorithms: NewYork, Wiley, 364 p.

Terakado, Y., Taniguchi, M., 2006. A new method for the study of traceelement partitioning between calcium carbonate and aqueous solution: A test for Sr and Ba incorporation into calcite. Geochemical Journal, Vol. 40, pp. 161 to 170.

Truesdell, A.H., Jones B.F., 1973. WATEQ, a computer program for calculating chemical equilibria of natural waters, US Geol. Survey J. Research 2, pp.233-48.

Westall, J.C., Zachary, J.L., Morel, F.M.M. 1976. MINEQL, A Computer Program for the Calculation of Chemical Equilibrium Composition of Aqueous System (Cilvil Engineering Technical Note 18). Cambridge, MA: Massachusetts Institute of Technology.

Wolery, T.J., 1992a. EQ 3/6, A software package for geochemical modeling of aqueous systems: Package overview and installation guide (Ver.7.0).-UCRL - MA - 110662 Pt I Lawrence; Livermore Natl. Lab

Wolery, T.J., 1992b. EQBNR, A computer program for geochemical aqueous speciationsolubility calculations: Theoretical manual, user´s guide, and related documentation (Ver.7.0).-UCRL - MA - 110662 Pt I Lawrence; Livermore Natl. Lab

Yeboah, Y.D., Saeed, M.R., Lee, A.K.K., 1994. Kinetics of Strontium Sulfate Precipitation from Aqueous Electrolyte Solutions. Journal of Crystal Growth, Volume 135, Issues 1-2, Pages 323-330

Zhu, C., Anderson, C.,2003. Environmental Applications of Geochemical Modeling. Cambridge University press.